HYPERSPECTRAL REMOTE SENSING IN MINERAL EXPLORATION:

AMMONIUM-ILLITE AS A PATHFINDER FOR GOLD

A Thesis

Presented in Partial Fulfillment of the Requirements for the

Degree of Master of Science

with a

Major in Geology

in the

College of Graduate Studies

University of Idaho

by

David A. Browning

May 2014

Major Professor: Peter Isaacson, Ph.D.

Authorization to Submit Thesis

This thesis of David Browning, submitted for the degree of Master of Science with a Major in Geology and titled "Hyperspectral Remote Sensing in Mineral Exploration: Ammonium-Illite as a Pathfinder for Gold," has been reviewed in final form. Permission, as indicated by the signatures and dates below, is now granted to submit final copies to the College of Graduate Studies for approval.

Major Professor: _____ Date: _____
Peter Isaacson, Ph.D.

Committee Members: _____ Date: _____
Mickey Gunter, Ph.D.

_____ Date: _____
Melissa Mateer, Ph.D.

Department Chair: _____ Date: _____
Mickey Gunter, Ph.D.

Discipline's College Dean: _____ Date: _____
Paul Joyce, Ph.D.

Final Approval and Acceptance

Dean of the College Of Graduate Studies: _____ Date: _____
Jie Chen, Ph.D.

Abstract

The presence of ammonium-illite on the Earth's surface has been correlated to known deposits via structures at Carlin-type gold deposits, suggesting its importance as a vector for gold ore. Additionally, ammonium-illite has often been proposed as a geochemical exploration tool due to its formation in hydrothermal systems. Very little work has focused on ammonium-illite as an exploration tool due to the costly, time-consuming, and often inaccurate methods of ammonium detection, such as wet chemical methods or X-Ray Diffraction. Short-wave infrared reflectance spectroscopy has the ability to detect even trace amounts of ammonium quickly and effectively.

Two hyperspectral surveys were performed in Elko County, Nevada, USA. The hyperspectral images were processed to identify several clay anomalies, including ammonium-illite, on a regional exploration scale, while field truthing of an existing claim block showed a spatial relationship between ammonium-illite and gold soil anomalies on a project scale.

Acknowledgements

I would like to thank Peter Isaacson for sticking with me and providing me the opportunity to earn my degree at the University of Idaho, Melissa Mateer and Brian Cellura for their inspiration and guidance in creating and completing this project, and Mickey Gunter for his patience throughout the completion of this thesis. I would also like to thank the Alexander Goetz Instrument Support Program, a scholarship program run by ASD Inc., for providing me with a TerraSpec4 spectrometer for this study, and Miranda Gold Corp. for providing the hyperspectral and assay data. This project would not have been completed without the tremendous support I received from my family, specifically my wife Sasha, and for that I am grateful.

Table of Contents

List of Tables

List of Figures

Introduction

Since its inception in the 1960s, remote sensing has proved to be a quick and effective method for the identification of minerals. Remote sensing measures the reflectance and absorption of electromagnetic radiance at different wavelengths to identify different surfaces. Specific minerals can be identified based on the positioning of these absorption features. As seen in recent history, spectroscopy has become an effective tool in exploration efforts to quickly determine the presence and extent of alteration minerals related to a hydrothermal system (Bradford, 2008; Canet, C. et al., 2010; Crosta et al., 2009; De Almeida, 2009; Duke, 1994; Mateer, 2010; Soechting et al., 2009; Taranik et al., 2009; Thompson et al., 1999; Zamudio, 2009).

Spatial and spectral abilities vary between different sensors and data acquisition methods. The LandSat Thematic Mapper, a multispectral spaceborne instrument, has 7 spectral bands covering the Visible, SWIR, and Thermal IR regions (450-2350 nm and 10500-12500 nm) with a spatial resolution of 30 m in the Visible and SWIR regions and 120 m in the thermal IR region (Sabins, 1999). Alternatively, the HyMap sensor, an airborne hyperspectral instrument, offers 126 spectral bands across the visible and SWIR regions (450-2500 nm) with a spatial resolution of 3-5 meters depending on the flight elevation (Hussey, 2010). The increased coverage of the SWIR region, combined with a finer spatial resolution, creates a higher signal to noise ratio. This ratio is important as it allows for the detection of minerals even in areas, such as Nevada, where vegetation can cause mixed pixels in a hyperspectral image (Sabins, 1999; Bedell, 2004).

Carlin-type gold deposits are deposited hydrothermally creating geochemical and alteration footprints, or halos, around the ore body. By definition, Carlin-type deposits are sediment hosted, with the host rock ranging in age from Paleozoic, which is the most common, to Triassic. Some host rocks are also igneous, but these are less common than sedimentary hosts. The deposits are generally structurally controlled and usually contain high-angle normal or reverse faults, as well as

folding. Hydrothermal alteration associated with these deposits varies between decarbonatization, silicification, and argillization, although all three types can be present in the same deposit. Decarbonatization is often stratigraphically controlled and can be extremely variable even within a deposit. The amount of decarbonatization that occurs is often related to the porosity of the host rock, which in turn affects the size of the deposit. The strength of silicification can change from total replacement of silica, resulting in the production of jasperoids, to weak cementation and box-work veining. Argillization is the creation of phyllosilicates through alteration of feldspars caused by acidic hydrothermal fluids, and can occur at the center of the hydrothermal system, or at its boundaries (Arehart, 1996; Cline et al., 2005). Identification of alteration is crucial in mineral exploration as it often represents the footprint of the deposit, creating a natural exploration boundary.

Ammonium forms when ammonia (NH_3) is released through the decay of buried organic material and interacts with hydrogen ions to form ammonium (NH_4^+) (Williams et al., 1992). This chemical process is especially relevant to the Great Basin due to the carbonaceous muds and shale, which provide organic material for the generation of ammonium. The ammonium is then transported via hydrothermal fluid to a suitable host mineral. Ammonium replaces potassium (K^+) in silicate minerals, such as illite, and most often becomes emplaced in clays with a high negative layer charge, but rarely in positively charged clays, such as smectite (Williams et al., 1992). As the fluid passes various lithologies, different elements may be deposited if a suitable host exists. This may result in the deposition of gold in a porous, sub-surface rock, while ammonium may not be deposited until it comes in contact with a potassium-rich host rock (Mateer, 2010). The presence of ammonium-illite and other ammonium bearing minerals has been noted in hydrothermal theaters where an organic lithology is emplaced at depth (Baugh et al., 1998; Soechting et al., 2009).

Ammonium has been shown to have a consistent presence among Carlin-type deposits, producing a halo around the deposit in the same fashion as traditional geochemical pathfinders

(Kydd and Levinson, 1986; Mateer, 2010; Ridgway et al., 1991; Wilson et al., 1992). More specifically, the correlation of ammonium-illite on the surface to known structures at Carlin-type deposits suggest its importance as a vector for gold ore (Mateer, 2010). Very little work has focused on ammonium-illite as a vector for gold deposits due to the costly, time-consuming, and often inaccurate methods of ammonium detection, such as wet chemical methods or X-Ray Diffraction. Short-wave infrared (SWIR) reflectance spectroscopy, however, has the ability to detect even trace amounts of ammonium quickly and effectively (Baugh et al., 1998; Kruse and Hauff, 1991; Mateer, 2010). The SWIR range is particularly sensitive to clay minerals due to its ability to detect slight variations in crystal composition and element substitution (Thompson et al., 1999). The presence of argillic alteration and organic-rich lithologies makes ammonium a potentially effective exploration tool for the identification of hydrothermal fluid conduits in Northern Nevada.

This study uses airborne hyperspectral data to identify areas containing ammonium-bearing minerals in two main field areas: a large, under-explored area with potential to host Carlin-type mineralization, and a smaller, project scale claim block with anomalous soil samples present. Based on the theory that ammonium-illite can be used as a vector for gold deposits, it is hypothesized that identifying ammonium over large exploration areas can significantly reduce the size of exploration targets on a regional scale, while helping to identify drill targets on a project scale.

Chapter 1: Regional Geology

Northeastern Nevada is characterized by carbonate and siliciclastic rocks of the Paleozoic era, and represents a passive margin during the Lower Paleozoic which transitioned into a more active continental margin in the mid-Paleozoic. The ocean retreated from Nevada during the Early Triassic, resulting in deposition of continental rocks during the Triassic, Jurassic, and Cretaceous (Coats, 1987; Price, 2003).

The Antler Orogeny, locally known as the Roberts Mountain Thrust, occurred during the Late Devonian to Early Mississippian, and is considered the most significant tectonic feature in Northeastern Nevada (Coats, 1987). This orogeny thrust lower Paleozoic deep-water, siliciclastic and volcanic rocks (western assemblage), over a lower Paleozoic carbonate-rich rock package (eastern assemblage). Northeastern Nevada was further displaced by the Humboldt and Sonoma orogenies of the late Paleozoic, followed by the Nevadan, Elko, Sevier, and Laramide orogenies of the Mesozoic. This crustal thickening was followed by a period of extension associated with subduction-related calc-alkaline magmatism present in the Middle and Late Jurassic, Cretaceous, and into the Late Miocene. Since the Miocene, volcanism has transitioned to a bimodal basalt-rhyolite mixture due to rifting. Basin and Range extension began in the Late Eocene and this process is still affecting the area (figure 1) (John et al., 2003).

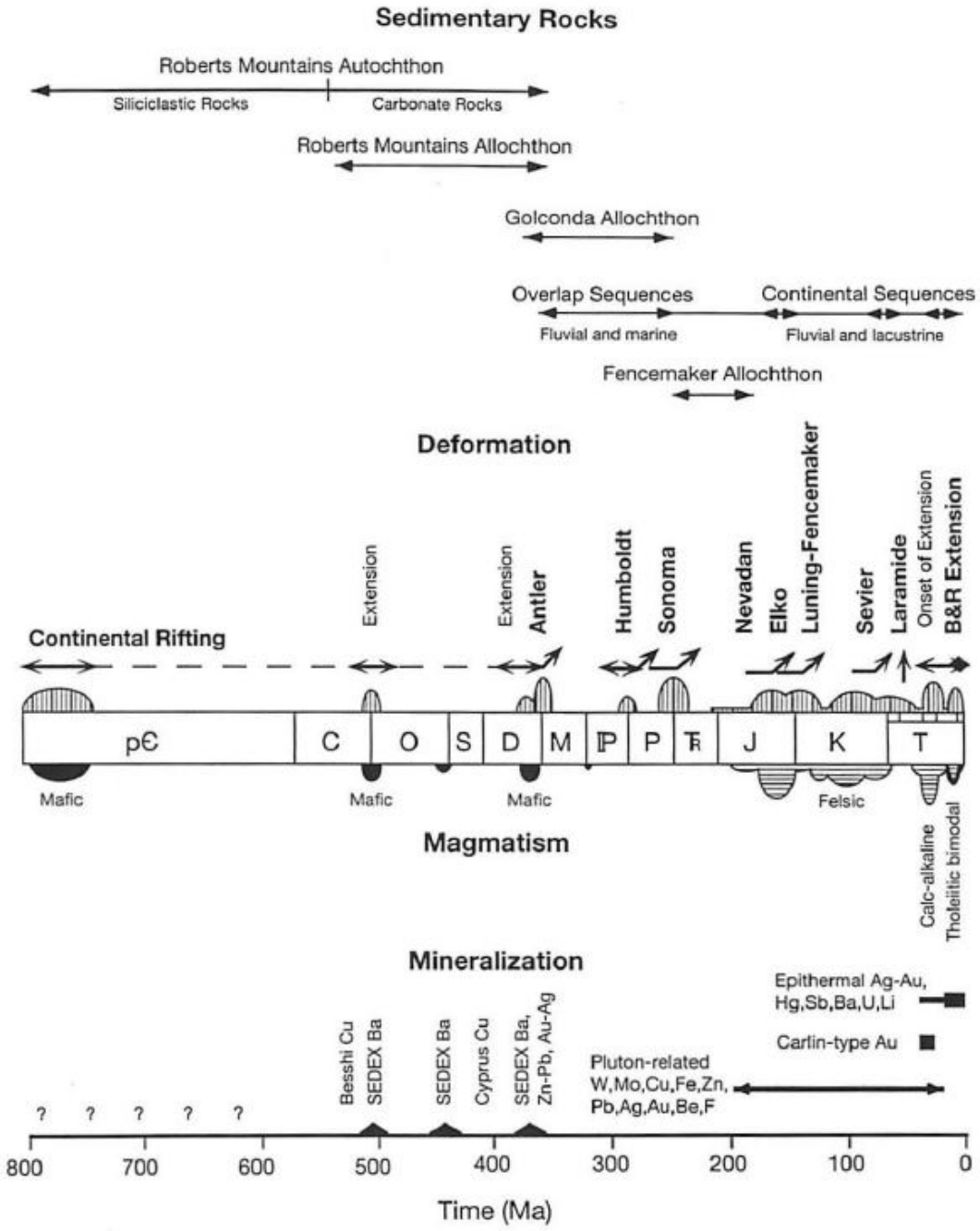

Figure 1 - Figure from John et al., 2003, illustrating facies types of the different allochthons, deformation of allochthons, and estimated times of varying mineralization types. This figure represents the tectonic history of Western North America, but is focused specifically on Northern Nevada.

Summer Camp Hills Geology

The geology described below is for the three subset areas from which samples were collected. Figure 2 provides an overview of the formations and structures present in the entire 117 square mile Summer Camp Hills survey area. For a complete geologic explanation of the Summer Camp Hills survey area, please refer to the references cited below.

The Summer Camp Hills area consists largely of eastern assemblage sedimentary rocks ranging in age from Devonian through Pennsylvanian. One transitional assemblage unit is present in Fink's Canyon (figure 3), and a western assemblage unit is present in the Windermere Hills area (figure 4). A number of unconformities exist in the area due to the structural setting described above.

The oldest unit is an unnamed collection of western assemblage rocks (DOs) containing mudstone, shale, chert, siltstone, quartzite, greenstone, and limestone. Of the three sub areas, this mixed unit is only present in the Windermere Hills area (figure 4), where it has been broken down into three formations, all believed to be Devonian in age; the basal unit is the Valder Formation, containing black argillite and tan siltite. The Agort Chert overlies this, consisting of dark chert and argillite in beds up to 50 feet thick. Platy quartz siltite of the Noh Formation is the upper most unit of the sequence. Brecciation is also common in the area as a result of thrusting (Coats, 1987).

The Devonian Simonson Dolomite (Dd), although described as part of a Devonian sequence along with the Sevy Dolomite and the Nevada Formation, is the only unit of this sequence present in the Summer Camp Hills subset areas. The Simonson Dolomite is described as coarsely crystalline, medium to dark gray laminated thick-bedded dolomite, with alternating light and dark layers. The basal unit is described as a sandy, cross-bedded dolomite. The upper most units in this area consist of a dolomite conglomerate (Coats, 1987; Mueller, 1993).

The unassigned Devonian unit (Dt) is a thrust plate believed to be a member of the transitional assemblage between the western and eastern assemblages. This unit consists of dark

carbonaceous limestone overlain by light-gray, siliceous, platy limestone. Of the three sub areas, this unit is only observed in the Fink's Canyon area (figure 3) (Coats, 1987).

The Middle to Late Devonian Guilmette and Devil's Gate Formations (Dgd) are mapped as light-gray, thick-bedded limestone (Mueller, 1993). Any dolomite present in the Guilmette and Devil's Gate Formations is believed to be recrystallization caused by hydrothermal fluids (Coats, 1987; Smith et al., 1990).

Unconformably overlying the Guilmette Formation in the study area is the Mississippian Tripon Pass Limestone (Mtp), a clastic-limestone consisting of calcisiltite, calcarenite, and calcirudite interbedded with black argillite, quartz siltite, and quartz-chert arenite. Clasts range in size from two inches up to one foot. Sole marks and rough grading of the beds indicate possible turbidity currents. The Tripon Pass Limestone is the age equivalent of the Joana Limestone, although it differs lithologically (Coats, 1987). Conodont fossils indicate Early Mississippian age (Smith et al., 1990).

The Mississippian Chainman Shale (Mc) is believed to be temporally correlative with the Mountain City Formation based on its stratigraphic relation and lithology (Coats, 1987). In the Summer Camp area the Chainman Shale is described as a mixture of shale, siltstone, sandstone, and conglomerate (Mueller, 1993). Lateral variation is common, ranging from the above description to black, fissile shale, to light-brown quartzite, sandstone, and silty cherty limestone. Of the three sub areas, this unit is only present in the Windermere Hills Area (Coats, 1987).

The Diamond Peak Formation (IPMdp), although it intertongues, with the Chainman Shale, is distinctive in the Summer Camp area. The Diamond Peak Formation is described in this area as a grouping of chert-pebble conglomerate, sandstone, siltstone, and fine-grained limestone (Coats, 1987).

The Carlin Sequence (PIPcs) in the Summer Camp Hills subset areas contains the Strathearn Formation, the Buckskin Formation, and the Carlin Canyon Formation. The Strathearn Formation is

unconformable to the underlying Western Assemblage. It consists of dark gray, medium-bedded, bioclastic calcarenite and calcirudite limestone beds commonly one to ten feet thick alternating with ten foot thick beds of quartz siltite. Lenses up to 80 feet thick of graded quartz-chert arenite and rudite, and quartz siltite beds also occur (Coats, 1987). The Buckskin Formation conformably overlies the Strathearn Formation and consists of a brown-gray, platy, calcareous quartz siltite containing medium-bedded quartz-chert arenite lenses as thick as 80 feet and brown, black, tan, and green subangular to sub-rounded chert clasts. Interbedded bioclastic, calcisiltite and calcarenite beds as thick as ten feet are also common. Many features of the Buckskin Formation are similar to the Strathearn Formation (Coats, 1987). The Carlin Canyon Formation conformably overlies the Buckskin Formation, despite the absence of the Beacon Flat Formation. The Carlin Canyon Formation is a buff, calcareous, locally dolomitic and cherty, quartz siltite containing medium-bedded calcilutite, calcisiltite, and calcarenite laterally grading into dark-brown to black, medium-bedded, blocky chert. Lenses of quartz-chert arenite and rudite up to 100 feet thick are present. The upper portion of the formation grades into bedded purplish chert. Alluvium (Qa) cover is present throughout the study area as a result of fluvial erosion, although it is largely only present in low-lying areas and drainages (Coats, 1987).

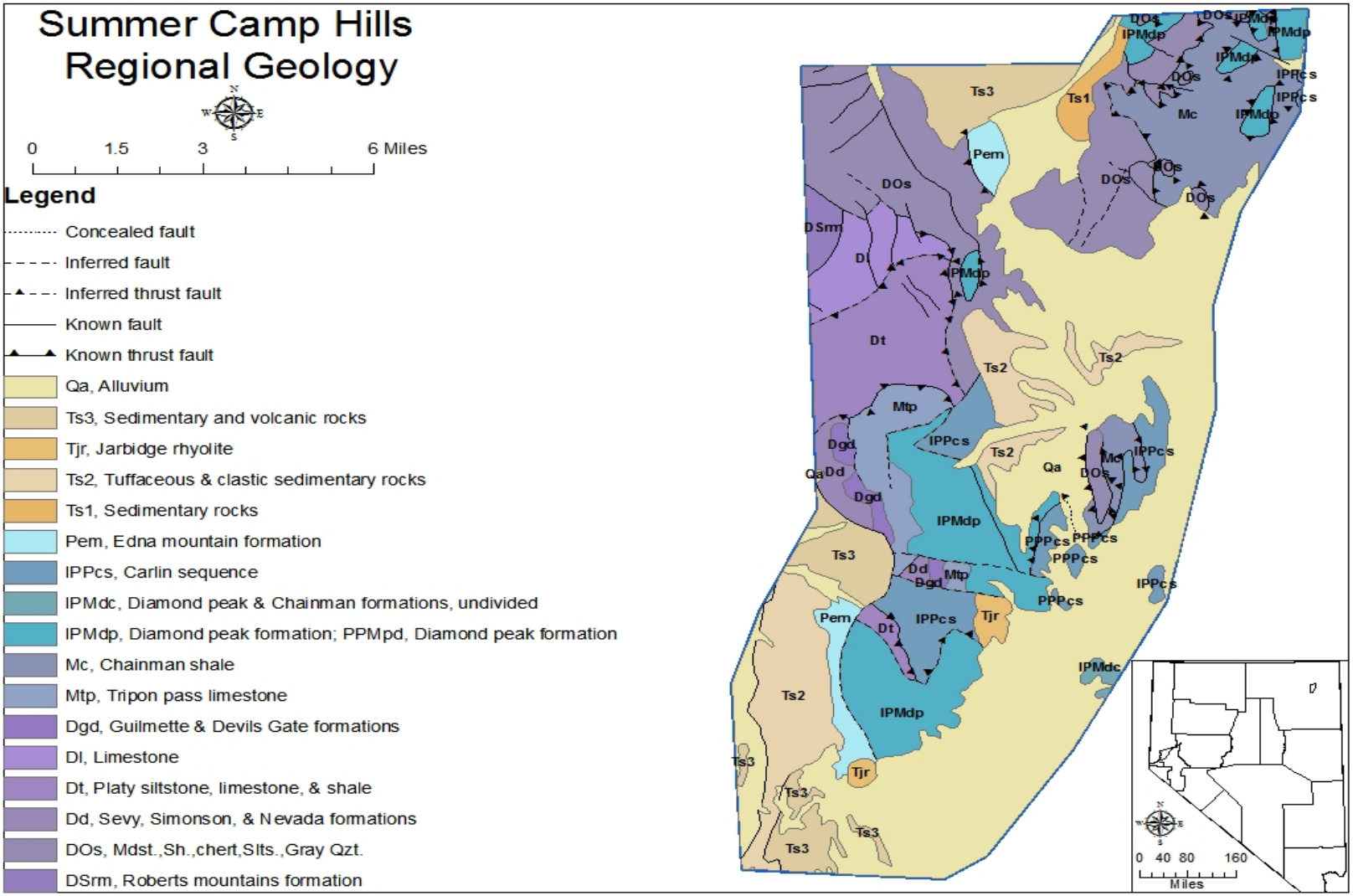

Figure 2 - Regional geology of the Summer Camp Hills area (modified from Coats, 1987)

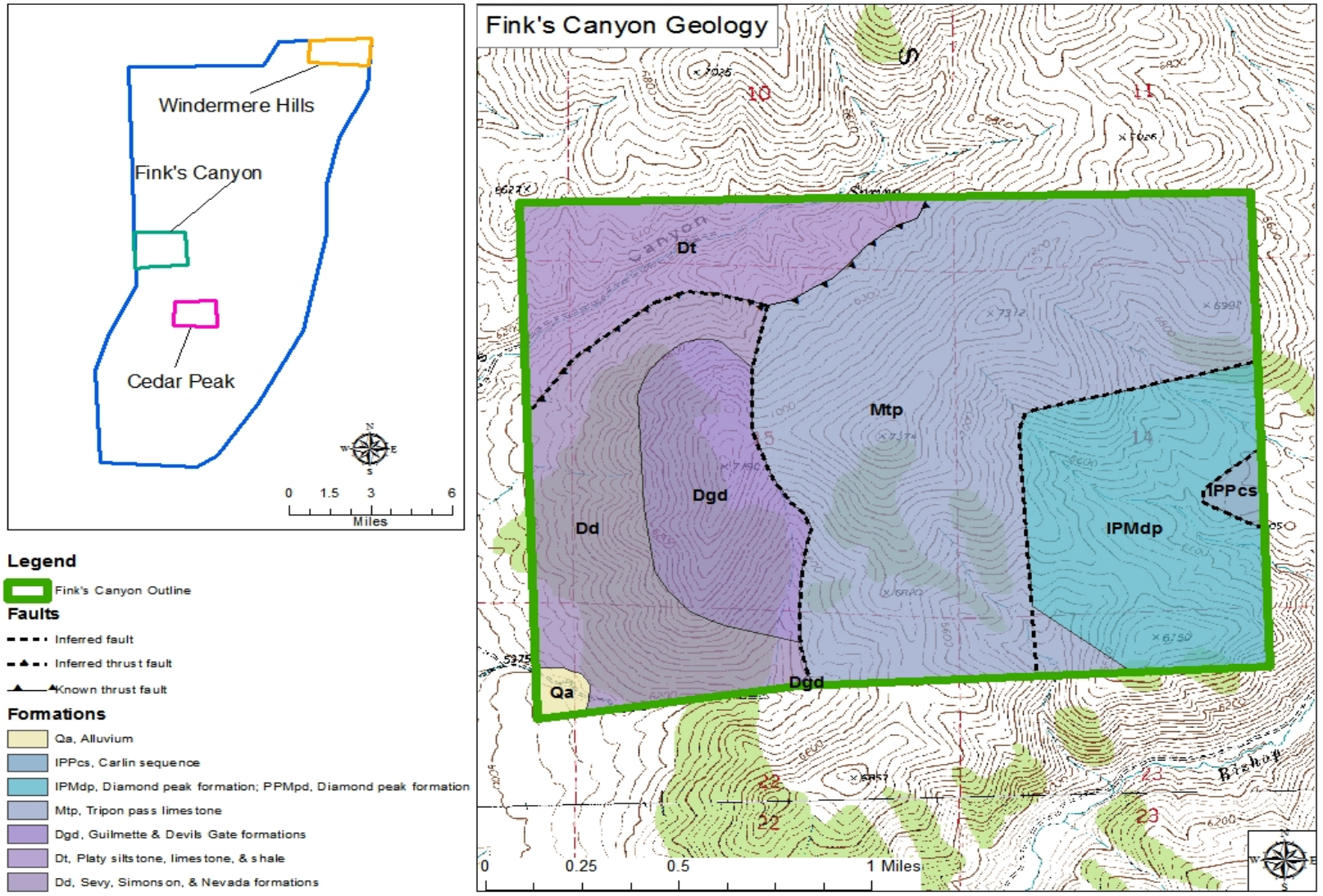

Figure 3 - Zoomed in view of the geology at Fink's Canyon (modified from Coats, 1987).

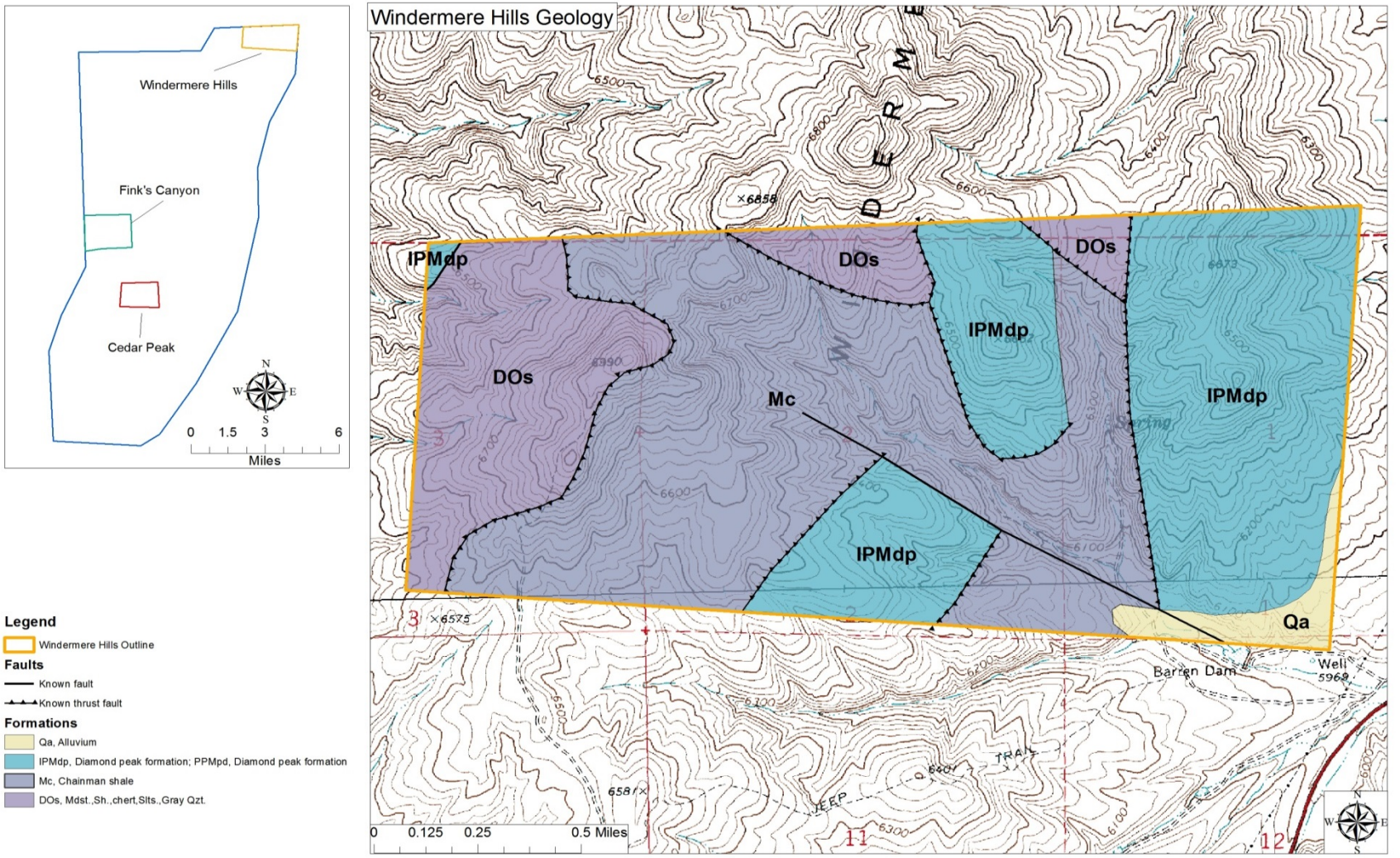

Figure 4 - Zoomed in view of the geology at Windermere Hills (modified from Coats, 1987).

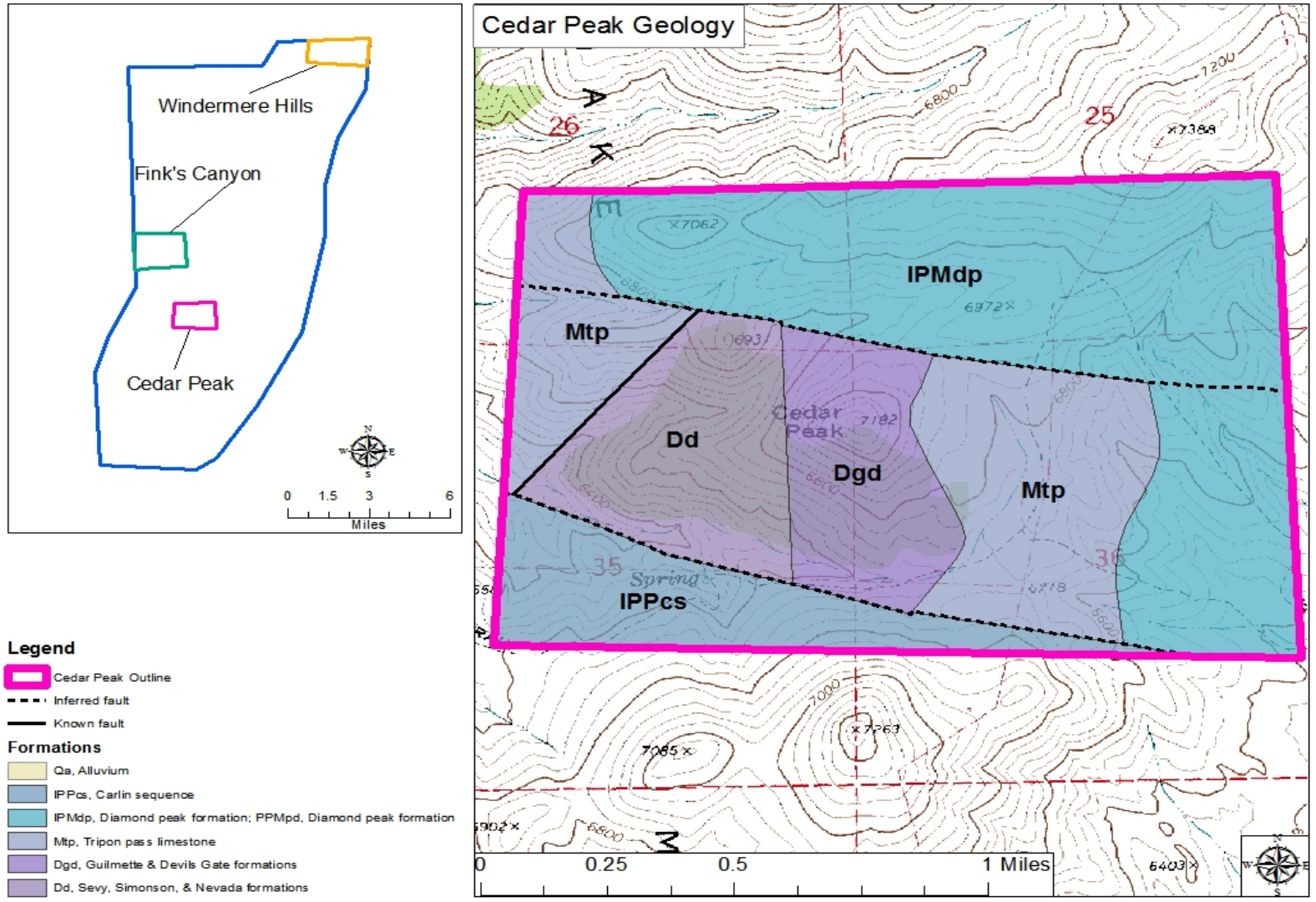

Figure 5 - Zoomed in view of the geology at Cedar Peak (modified from Coats, 1987).

Spruce Mountain Geology

The geology described for the Spruce Mountain area is restricted to the claim block held by Miranda Gold Corp. and surrounding areas where samples were collected (figure 7). An overview of the entire Spruce Mountain survey area is provided in figure 6, but for a complete description of the geology at Spruce Mountain, please refer to references cited below. The Spruce Mountain sampling area consists of Pennsylvanian and Permian carbonaceous rocks covered by Quaternary and Tertiary units. Many faults are present in the area resulting in a favorable Carlin-type setting (figure 7).

The Early and Middle Pennsylvanian Ely Limestone (IPe) is divided into two units at Spruce Mountain. The lower member of the Ely Limestone is a thick-bedded to massive, medium-gray, fine-grained limestone with abundant concentrically layered chert nodules. The upper member is the same thin-to thick-bedded, medium-gray, fine-grained limestone, but contains small spheroidal black chert nodules (Hope, 1968; Coats, 1987).

The undivided Pennsylvanian/Permian Limestone and Dolomite (IPPl) group represents the Riepe Spring Limestone and the Rib Hill Formation. The Riepe Spring Limestone consists of thick-bedded to massive, medium-gray, fine-grained limestone with nodular chert common in the lower part but sparse in the upper part. Chert-pebble conglomerate is present in the area but highly variable. The Rib Hill Formation in this area consists of tan-weathering platy siltstone and thin-bedded limestone. Fusulinids are present in both formations (Hope, 1968; Coats, 1987).

The Permian Pequop Formation (Pp) overlies the Ferguson Springs Formation. In the Spruce Mountain area it is broken down into a lower and an upper member. The lower member has medium-to thick-bedded, medium gray, fine-grained limestone with platy interbedded siltstones. Chert nodules, fusulinids, and echinoderm columnals are common (Hope, 1968; Coats, 1987). The upper member of the Pequop Formation consists of thick-bedded to massive, medium-to fine-

grained limestone. Echinoderm columnals are also common in this member, as are gastropods. Fusulinids, however, are rare in the upper member (Hope, 1968; Coats, 1987).

The Tertiary Phenorhyolitic to Phenodacitic Ignimbrite (Tt1) is the earliest widespread volcanic unit of the Tertiary and consists of two main rock types: a phenocryst-rich ignimbrite consisting of hornblende, augite, hypersthene, and plagioclase with black chert xenoliths, and a densely welded ignimbrite which is phenocryst-poor, but high in devitrified glass. Alluvium (Qa) cover is present as a result of fluvial erosion and is present in a large portion of the sampling area (Coats, 1987).

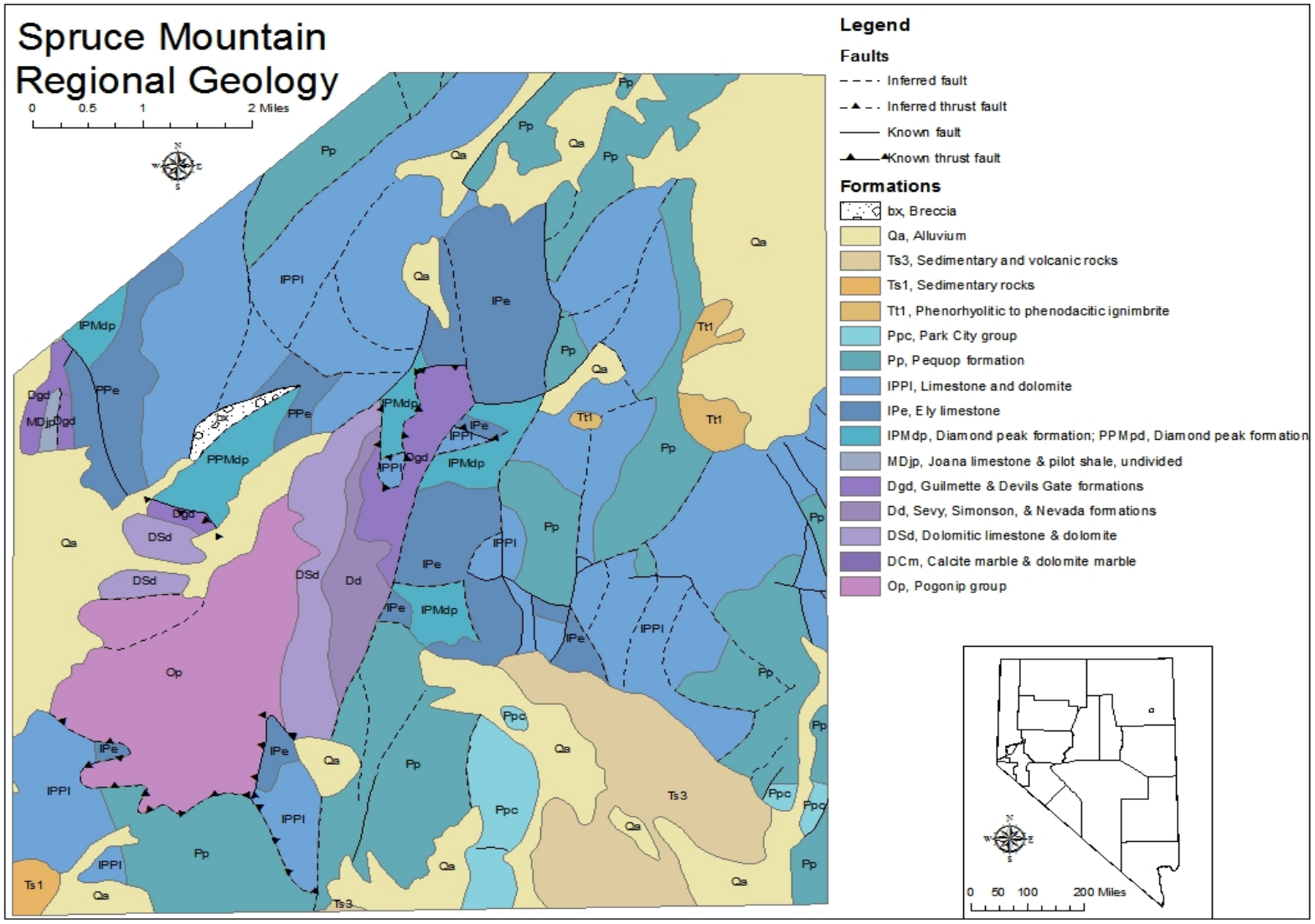

Figure 6 - Regional geology of the Spruce Mountain area (modified from Coats, 1987).

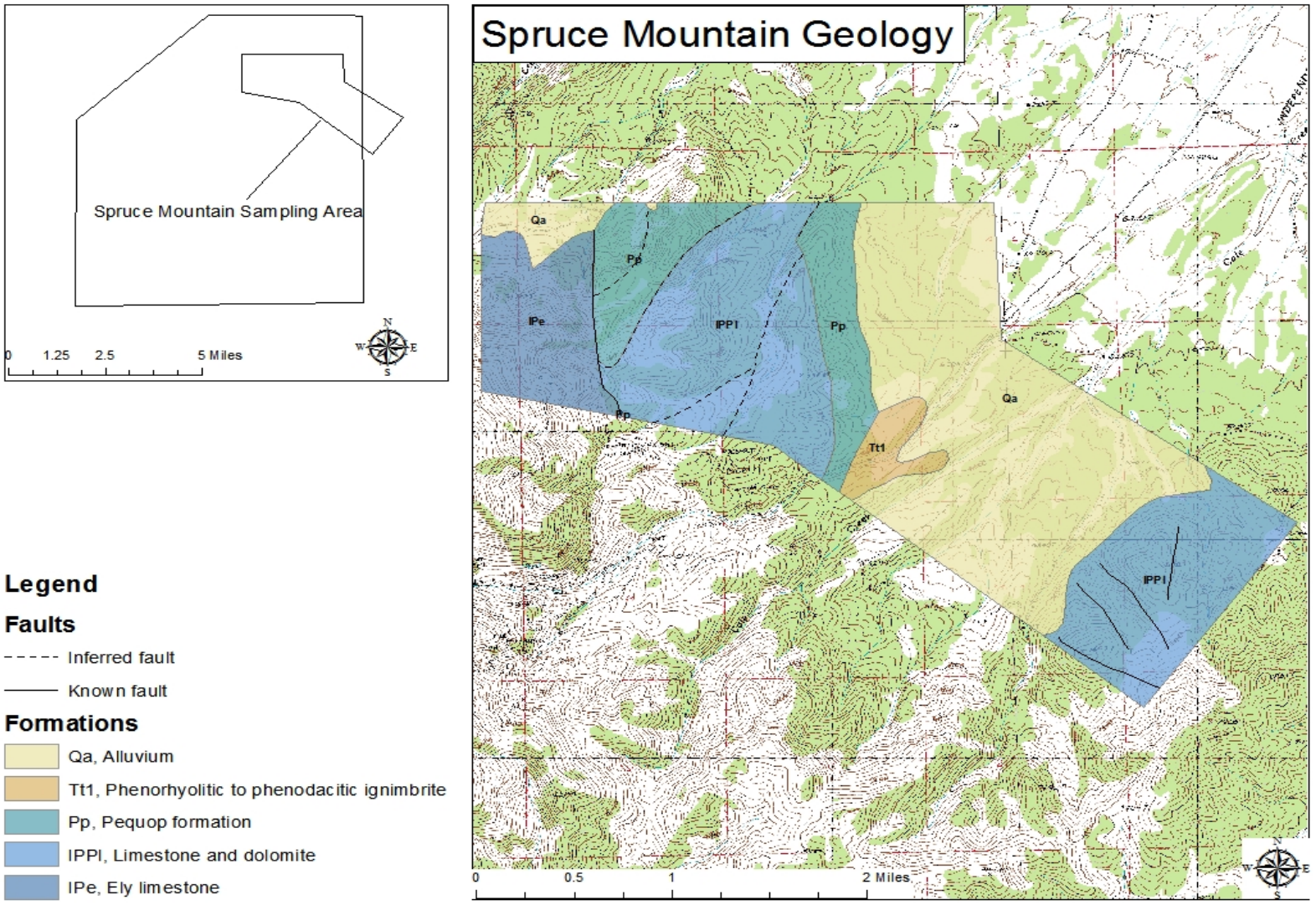

Figure 7 - Zoomed in view of the geology covering the sampling area at Spruce Mountain (modified from Coats, 1987).

Chapter 2: Methods

Remote Sensing

Three initial areas of Northeastern Nevada were chosen for the hyperspectral analysis (figure 8). The survey areas were chosen by staff geologists at Miranda Gold Corp. as areas of interest based on rock and soil geochemistry, emerging trends, proximity to recent gold discoveries, land status, and favorable stratigraphy. The three areas surveyed in Northeastern Nevada were the Summer Camp Hills, the Wood Hills, and Spruce Mountain (figure 8). The Summer Camp Hills area consists of 13 flight lines and covers approximately 117 square miles (303 square kilometers). The Woods Hill area contains 4 flight lines covering approximately 7 square miles (18 square kilometers). The Spruce Mountain area contains 9 flight lines and covers approximately 56.5 square miles (147 square kilometers). Only hyperspectral data for the Summer Camp Hills and Miranda Gold Corp.'s claim block in the Spruce Mountain area were used for this study.

Data acquisition for the three areas took place on September 14th and 15th, 2010, by HyVista Corp. using the HyMap scanner. The HyMap scanner, developed by Integrated Spectronics, consists of four whiskbroom sensors which deliver 126 spectral bands with a width of 15 - 20 nm per band, a spectral range of 450 nm to 2500 nm, and a spatial resolution of 3.8 meters for this survey (Hussey, 2010). The survey data collected by the HyMap scanner was subsequently delivered to Miranda Gold Corp. in October of 2010.

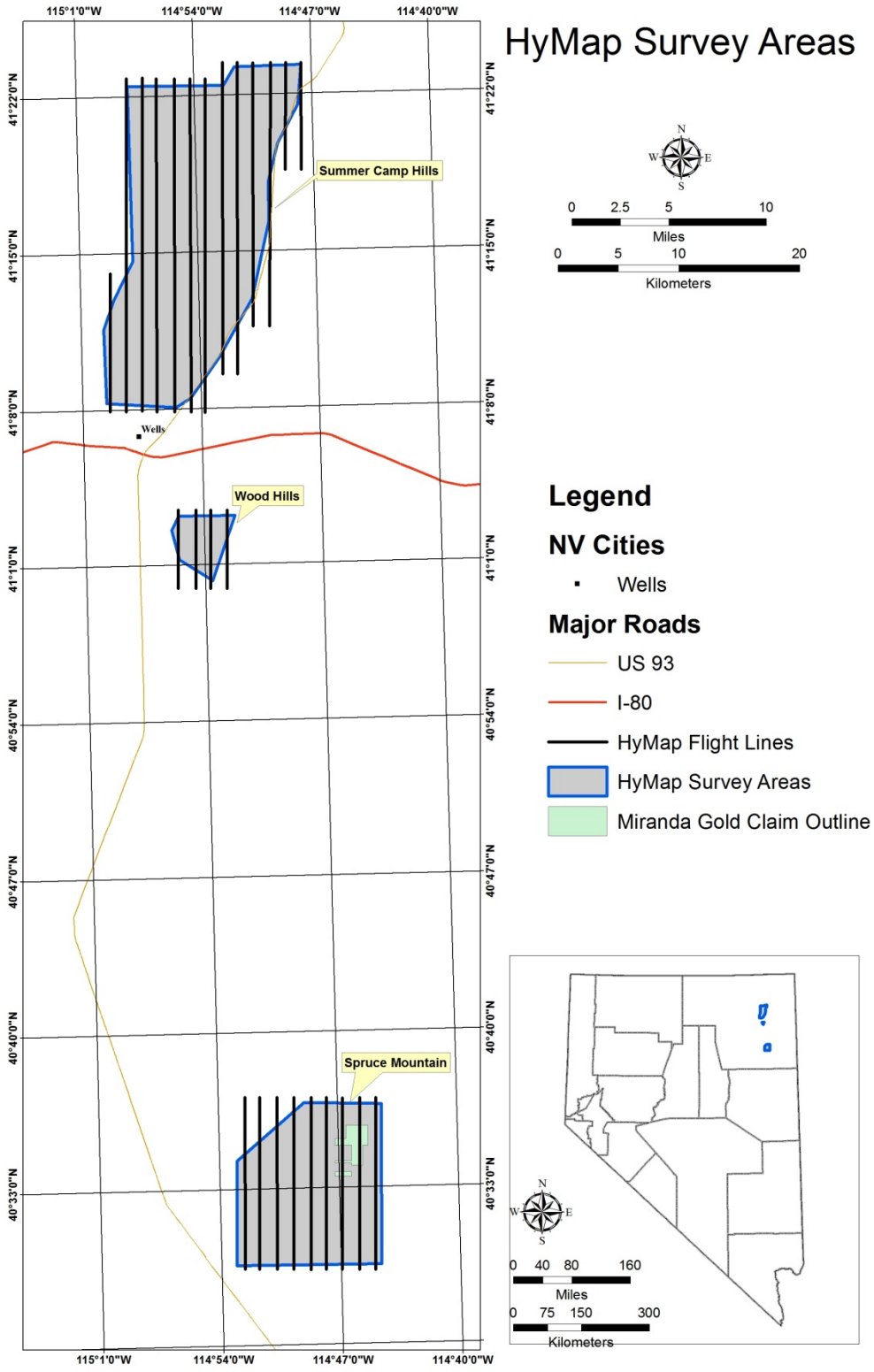

Figure 8 - Survey areas and flight lines flown by HyVista Corp. with the HyMap scanner in Elko County, Northeastern Nevada, USA.

Image Processing

Data processing was completed during the winter of 2011-2012. The individual flight lines for each area were georeferenced and mosaicked together in ENVI to create complete radiance images of the Summer Camp Hills and of Spruce Mountain. Only empirical methods were considered for the removal of atmospheric interference due to their ability to create spectra that are most comparable to reflectance data (Bedell and Coolbaugh, 2009; Gao, et al., 2009). Of the empirical methods, Empirical Line Correction was performed due to the success of this method in providing the best results for detecting ammonium illite in a previous study performed by Mateer (2010). For this correction method, field samples were collected at field sites represented by dark and light pixels in the image. The samples were analyzed with an ASD TerraSpec handheld spectrometer, which measures the reflectance spectra of the hand sample. The spectra of the hand samples were then paired with their corresponding pixels creating an empirical relationship between radiance and reflectance which the ENVI software then applied to the entire image.

The Spectral Hourglass Wizard was utilized in ENVI following image calibration. The Spectral Hourglass Wizard is a supervised workflow that isolates the most spectrally unique or spectrally pure pixels within a hyperspectral image. These pixels, known as end members, are then mapped to show the abundance of these minerals within the study area. Identification of the end member spectra using spectral analyst revealed that the Spectral Hourglass wizard isolated an abundance of noisy spectra and mixed spectra containing montmorillonite, calcite and vegetation. As these minerals were not pertinent to the study, a second method was employed which uses a spectral reference library to classify the image.

Spectral Angle Mapper (SAM) is a supervised classification tool within ENVI which treats spectra as vectors in n-dimensional space, where n equals the number of bands. This allows for the calculation of the angle between two spectra (Kruse et al., 1993). The user can input reference

spectra and assign a specific angle between the reference spectra and the spectra within the image. The program will then highlight all pixels within the image that contain spectra which fall within the assigned angle. The smaller the angle, the fewer pixels will be highlighted, and the purer these pixels will be with respect to the reference spectra. In this study, various angles were used in SAM for each mineral of interest, a method demonstrated by Dennison et al. (2004). This method served to identify pixel purity and abundance of these spectra over a very large area, making it the preferred analysis method for this study. The reference spectra used were two different ammonium-illite spectrum signatures, an illite spectrum signature, a kaolinite spectrum signature, and a dickite spectrum signature. All reference spectra were obtained from the USGS spectral library. Each result was then converted into a vector file within ENVI and subsequently exported to a shape file, which could then be displayed digitally in ArcGIS.

Sample Collection and Analysis

Initial sample collection was performed around anomalous pixel clusters of illite, kaolinite, dickite or ammonium illite. The location of each sample was recorded with a Trimble Juno GPS unit equipped with ArcPad, a mobile GIS program. The hand samples were then scanned at the office of Miranda Gold Corp. with a TerraSpec 4 Hi-Res Mineral Spectrometer, which can detect spectra within the visible and SWIR regions (350-2500 nm).

Every surface of each sample was scanned with the spectrometer and given a unique name. Once the scanning process was completed the spectra were loaded in The Spectral Geologist (TSG) software. TSG uses spectra from reference libraries to compare and interpret spectra provided by the user, in this case spectra of the hand samples. The software provides a built in library with fifty reference spectra. This library was limited for the purpose of this study, and an auxiliary library was loaded to help with the identification of ammonium. The auxiliary library contained spectra of common minerals in Northern Nevada, particularly those associated with hydrothermal alteration,

such as illite, dickite, and kaolinite, in addition to ammonium-illite. The software then uses the built in and auxiliary libraries to interpret what minerals are represented by the spectra. The user can also do their own interpretation using the available libraries.

Once interpreted, the spectra were sorted based on the software's interpretation of what mineral(s) was present as determined by the spectral signature. Secondary analysis by the author was performed in this order, rather than ordered by sample name, to prevent bias of an interpretation based on minerals present on other surfaces of the same sample. Using Microsoft Excel, each spectral signature was assigned a mineral classification(s) based on the author's interpretation of the spectra. Minerals were classified as Min1, Min2, and Min3 based on the importance of the minerals to this study and/or mineral abundance (table 1).

Once analysis of all spectra was completed, the interpretations were sorted by sample name. The individual spectra of each surface of the hand sample were then combined to create a Min1, Min2, and Min3 designation for the entire hand sample based on the abundance of minerals and the importance of the mineral to the study. Any ammonium-bearing mineral was automatically listed as Min1 for its importance to this study. Min 2 and Min 3 were then decided by which minerals appeared the most on all the surfaces combined (table 2). The location and analysis of each hand sample were combined into a single spreadsheet and imported into ArcGIS. A shape file was created to display the prominent minerals for each sample.

The methodology for collecting, analyzing and interpreting samples, as well as mapping their spatial relationships, was repeated in the Cedar Peak area and the Miranda Gold Corp. claim block in the Spruce Mountain area. These two areas were studied more extensively because of the presence of ammonium-illite at Cedar Peak and both the favorable soil geochemistry and land position at Spruce Mountain.

Classification of Ammonium

Hand samples containing ammonium were classified as ammonium-illite or weak ammonium-illite based on interpretation of the spectra. This distinction was made on an individual sample basis depending on the strength of the absorption features at 2006 nm and 2116 nm, which are associated with ammonium. Although some of the spectra exhibited weak ammonium absorption features, for the sake of this study it was deemed important to acknowledge even the slightest amounts of ammonium. A weak ammonium signature may not be negative, but alternately could indicate a lack of ammonium in the system or that the sample was on the distal regions of the ammonium geochemical halo.

Chapter 3: Results

Results for Summer Camp Hills

Due to the large project area in the Summer Camp Hills (figure 8), it became essential to identify smaller targets based on clay anomalies. Searches for illite, kaolinite, and dickite, three minerals indicative of hydrothermal alteration and of particular interest due to their relation to Carlin-type gold deposits, were performed with various angles of error using Spectral Angle Mapper. An arbitrary, yet reasonable, first angle threshold was processed for each mineral, with the angle threshold slowly lowered so as to properly show large enough areas, yet also reduce false anomalies. The angle threshold is the maximum angle of error, in radians, allowed between the reference spectra and the image spectra. Illite was processed at .0825, .069, and .055 radians; Kaolinite was processed at thresholds of .255, .2125, and .17 radians; Dickite was processed at angles of .16, .12, and .08 radians. When plotted spatially, definite anomalous areas became apparent as false anomalies began to diminish. Ammonium-Illite was subsequently processed at .15 and .075 radians, with anomalous areas coinciding with those demonstrated by kaolinite, dickite, and illite (figure 9).

Shape files outlining the new areas of interest were created in ArcGIS and imported into ENVI. Spectral Angle Mapper was performed again on these smaller areas to reduce the interference of less pure pixels, resulting in better identification of pure pixels. In the Summer Camp Hills, a 117 square mile area was reduced to three zones of interest: Fink's Canyon (2.7 sq. miles; 7 sq. kilometers), Windermere Hills (5 sq. miles; 13 sq. kilometers), and Cedar Peak (1.5 sq. miles; 4 sq. kilometers).

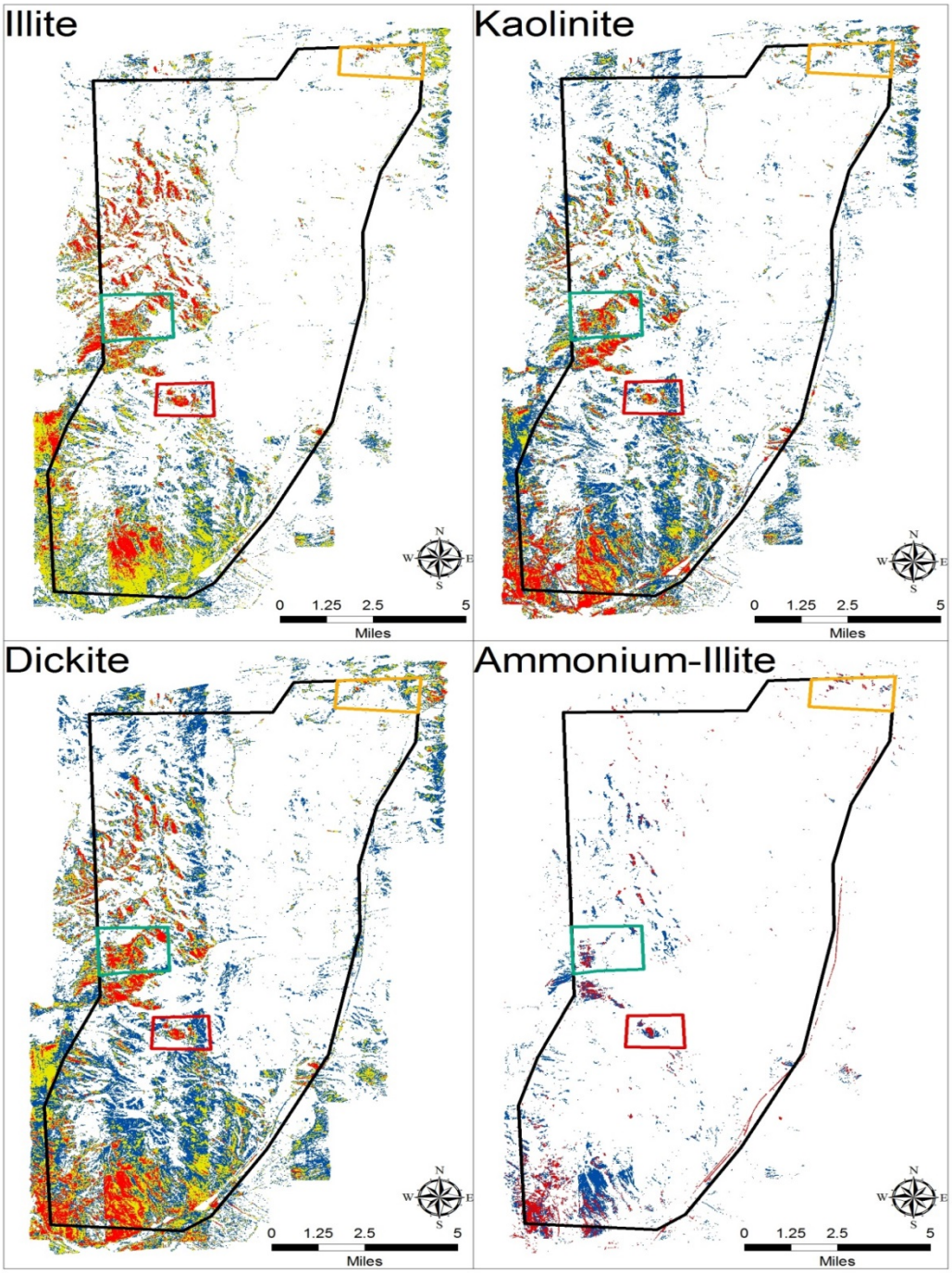

Figure 9 - Pixels in the Summer Camp Hills area representing the different angle thresholds performed in Spectral Angle Mapper. Blue represents the largest error, yellow represents the middle threshold, and red represents the smallest error angle. Note the coincidence of the red pixels for all clays. For illite Blue is .0825 radians, yellow is .069 radians, and red is .055 radians. For kaolinite blue is .255 radians, yellow is .2125 radians, and red is .17 radians. For dickite blue is .16 radians, yellow is .12 radians, and red is .08 radians. For ammonium-illite blue is .15 radians and red is .075 radians. The three outlines represent the anomalous areas explored in this study: Fink's Canyon (green rectangle), Windermere Hills (orange rectangle), and Cedar Peak (red rectangle).

Fink's Canyon

The Fink's Canyon area (figure 10) is a high relief ridge defined by two drainages, one of which is Fink's Canyon, the other contains a hot spring. The ridge consists of very thin-bedded or platy limestone. The area was identified through the initial image processing as described above, and was subsequently reprocessed. The final thresholds for this area were .04 radians for illite, dickite, kaolinite and ammonium-illite. The area was conspicuous for its high density of illite and ammonium-illite pixels along the ridge (figure 10). Of the eight samples collected several were interpreted as Illite, some with smectite or quartz mixtures, while one was interpreted as ammonium-illite (figure 10). The ammonium-illite sample was classified as weak due to the strength of the absorption features at 2006 nm and 2116 nm (figure 11). Follow up rock chip collection returned a max gold sample of 7 ppb Au, although barium in the area was elevated (up to 4260 ppb), along with mercury (up to 170 ppb) (table 4). Reclaimed drill pads in the area were also discovered, indicating previous exploration efforts.

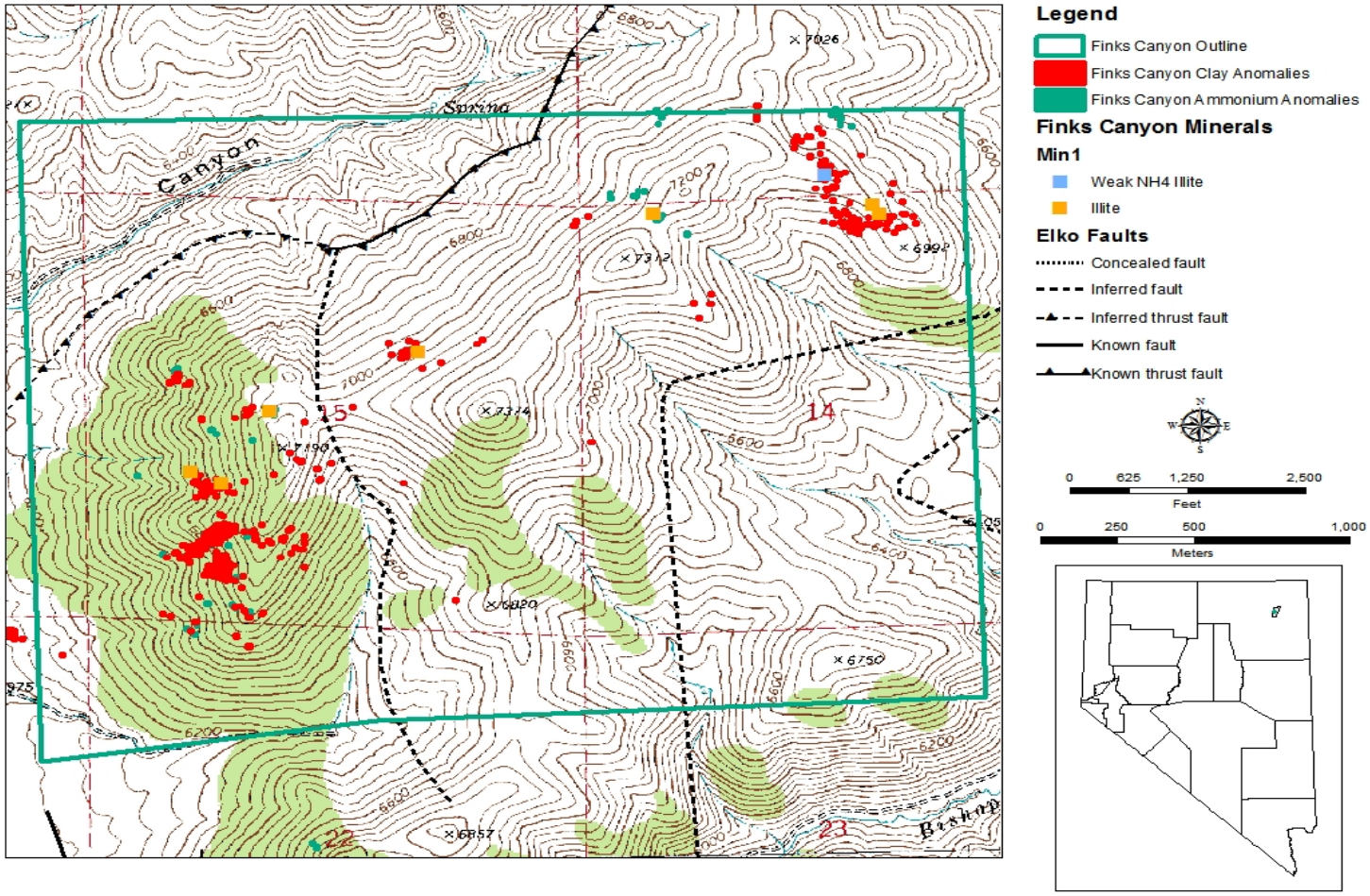

Figure 10 - Map showing the locations of illite, dickite, kaolinite, and ammonium pixels, sample locations, and interpretation of those hand samples (colored squares) at Fink's Canyon. Black lines are faults from Coats (1987). Illite, dickite, and kaolinite pixels were combined and labeled as clay anomalies (red circles), while the ammonium pixels are shown by the green circles. Any pixels that turned out to be float were ignored in the field to ensure sampling occurred at outcrop.

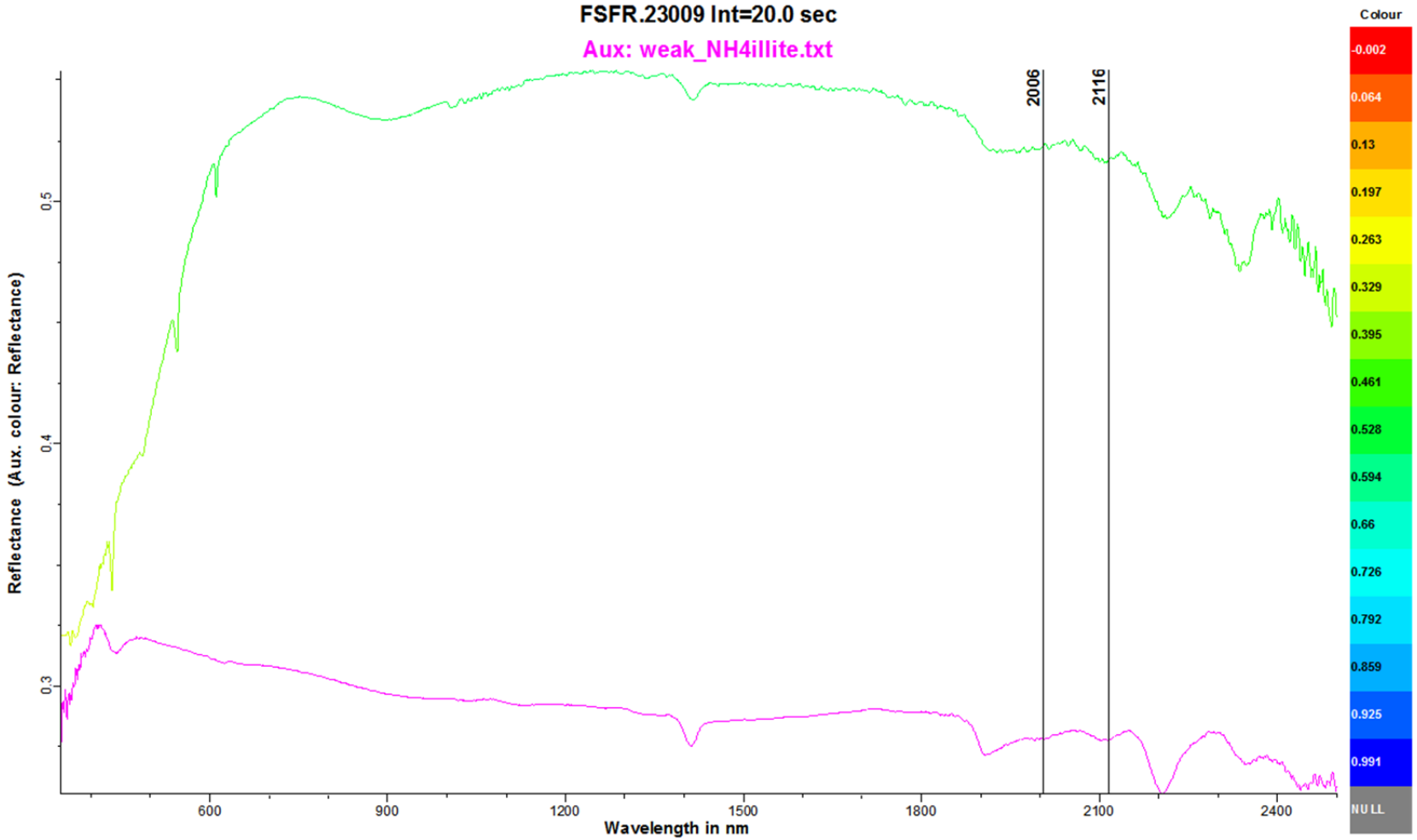

Figure 11 – Sample HS_SM_023 collected at Fink's Canyon. The green line represents the sample spectrum. The reference spectrum of a weak ammonium-illite is in magenta. Although weak, absorption features are present at 2006 nm and 2116 nm.

Windermere Hills

The Windermere Hills (figure 13) is an area of high relief consisting of limestone and sandstone with secondary silicification events evident (figure 12). Signs of previous exploration efforts such as abandoned mine adits and test pits are in the area. After being identified by the first pass of image processing, the subset area surrounding the anomalous pixels was processed a second time. Kaolinite was disregarded for this re-run as the dominant anomalies in this area were illite, dickite, and ammonium-illite. Examination of the spectra represented by kaolinite pixels in this area showed false anomalies, as the pixels were actually illite.

The final thresholds used were .055 radians for dickite, .042 radians for illite, and .057 radians for ammonium-illite. The secondary SAM processing produced a much smaller number of pixels than what was originally used to identify the area as a target. As such, only three samples were taken in the area nearest the pixels containing the purest spectra. The three samples were analyzed as two ammonium-illite samples and one illite-quartz mixture sample (figure 13). One ammonium-illite sample was classified as weak and one as normal ammonium-illite due to the strong absorption features at 2006 nm and 2116 nm (figure 14). Follow-up rock chip sampling returned gold values which were all below detection limit, although high silver (up to 140 ppb), barium (up to 2230 ppm), and zinc (up to 3390 ppm) values were observed (Table 5).

Figure 12 – Float hand sample collected in the Windermere Hills area. This sample was not assayed or analyzed with spectroscopy, but was collected for the secondary silicification evident by the quartz vein.

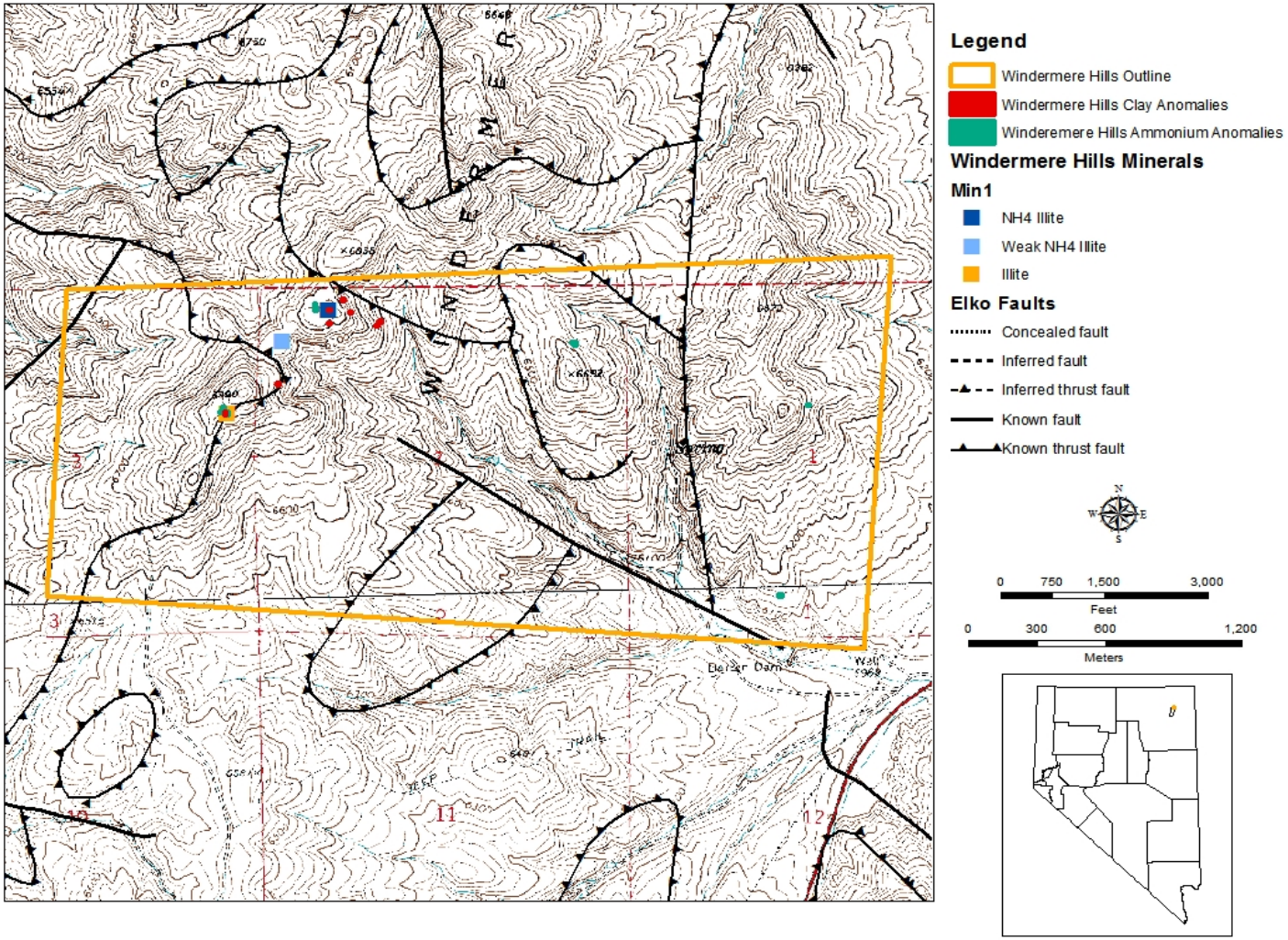

Figure 13 – Map showing the locations of illite, dickite, and ammonium pixels, sample locations, and interpretation of those hand samples (colored squares) in the Windermere Hills. Black lines are faults from Coats (1987). Illite and dickite pixels were combined and labeled as clay anomalies (red circles), while the ammonium pixels are shown by the green circles. Any pixels that turned out to be float were ignored in the field to ensure sampling occurred at outcrop.

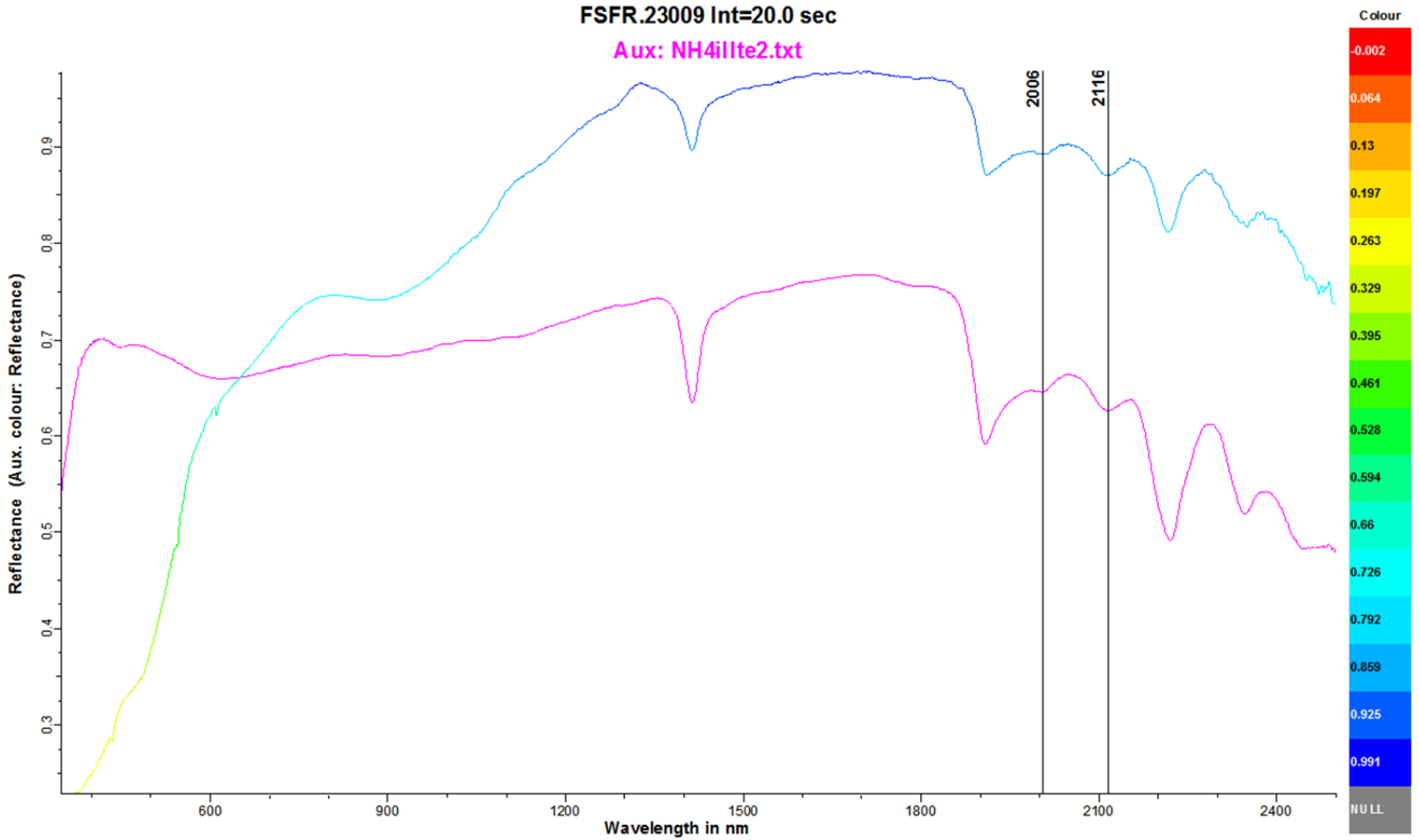

Figure 14 – Sample HS_SM_039 collected in the Windermere Hills. The sample spectrum is in blue. The ammonium-illite reference spectrum is in magenta. Note the definition of the absorption features at 2006 nm and 2116 nm.

Cedar Peak

Cedar Peak (figure 17) was sampled multiple times, and is the most promising of the three areas. This area was first identified as anomalous by the first pass of thresholds applied to the Summer Camp Hills area. It was then processed a second time with thresholds of .038 radians for illite, .04 radians for kaolinite, .042 radians for dickite, and .045 radians for ammonium-illite. The area was treated as a test site and was the first area sampled to determine if the narrowing down of a large area was effective. Twelve samples were collected based on pixel locations, and were subsequently analyzed using the TerraSpec spectrometer (figure 17). One strong ammonium-illite sample was among the samples collected (figure 18). In addition to the ammonium-illite sample, several faults in the area were noted, in addition to a large network of silicification which included silica coating on limestone and bedded silica up to 20 feet thick (figures 15, 16).

The presence of ammonium-illite, in addition to its spatial relation to extensive faulting and silicification, led to a second round of sampling. In an attempt to understand alteration patterns and structural control on the alteration, three samples lines were created by the author with 300 meters between each sample location. Sampling was performed by a field assistant, instructed to collect samples at outcrop or subcrop. Due to this method, some sample sites were passed or moved, creating an irregular sampling pattern. Seventeen samples were collected in this manner and analyzed with the TerraSpec spectrometer. Eight samples were interpreted as containing ammonium-illite, with three of these samples having a strong ammonium signature (figure 19).

Follow up rock chip sampling in the area returned higher numbers of gold than the previous area, although these samples were still not considered anomalous (13 and 10 ppb Au). Assay values of elevated barium (up to 2730 ppm), mercury (up to 490 ppb), magnesium (up to 7.19%), and zinc (up to 128 ppm) were recorded in the area (table 6).

Figure 15 – Bedded silica at Cedar Peak.

Figure 16 – Scabby silica on Devil's Gate Limestone at Cedar Peak.

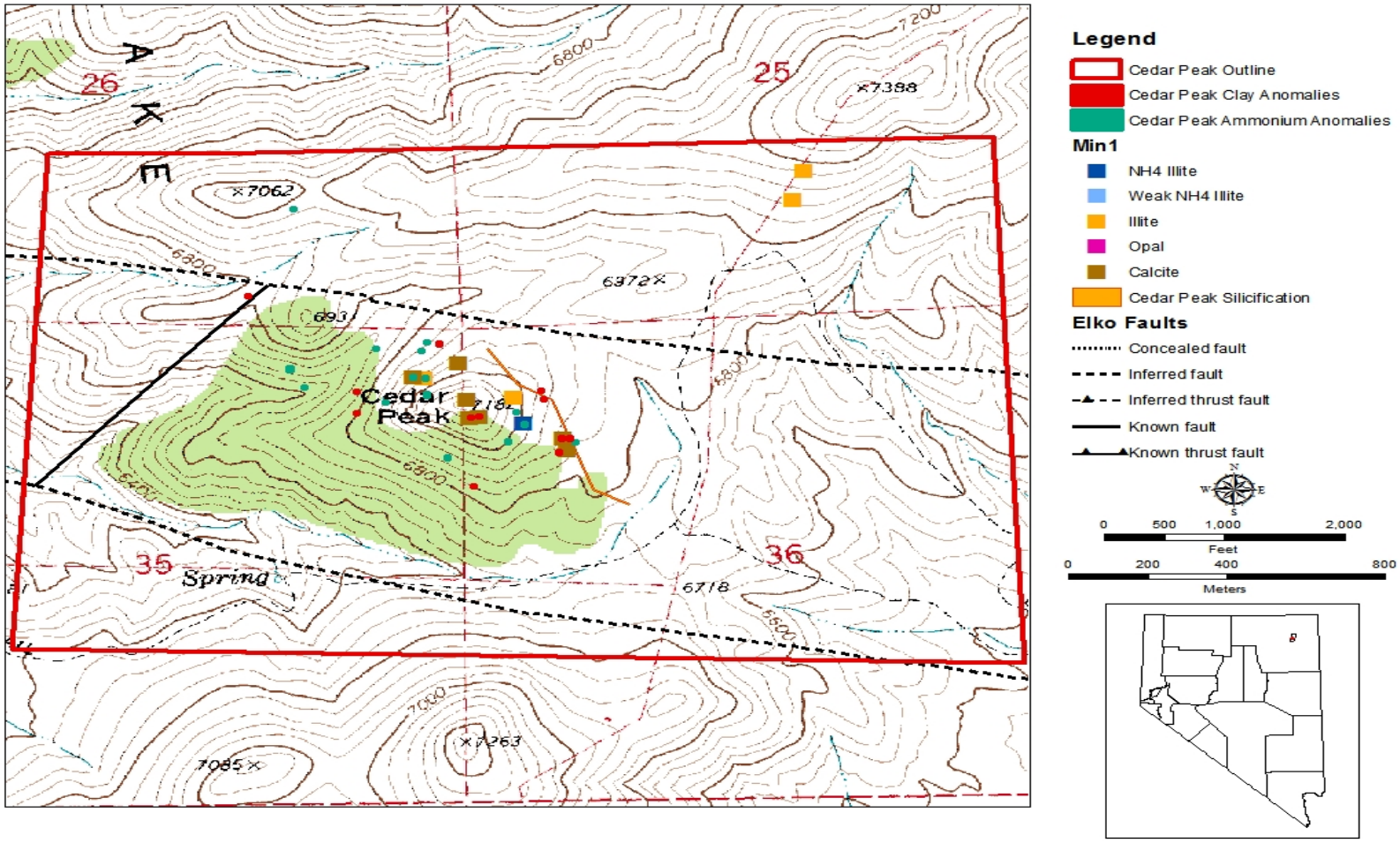

Figure 17 – Map showing the locations of illite, dickite, kaolinite, and ammonium pixels, locations of the initial sampling effort, and interpretation of those hand samples (colored squares) at Cedar Peak. Black lines are faults from Coats (1987). Illite, dickite, and kaolinite pixels were combined and labeled as clay anomalies (red circles), while the ammonium pixels are shown by the green circles. Any pixels that turned out to be float were ignored in the field to ensure sampling occurred at outcrop. The silicification network is represented by the orange line oriented NW-SE. Note the proximity of the ammonium-illite sample to the silicification, as well as the location of the ammonium and silicification between two inferred faults.

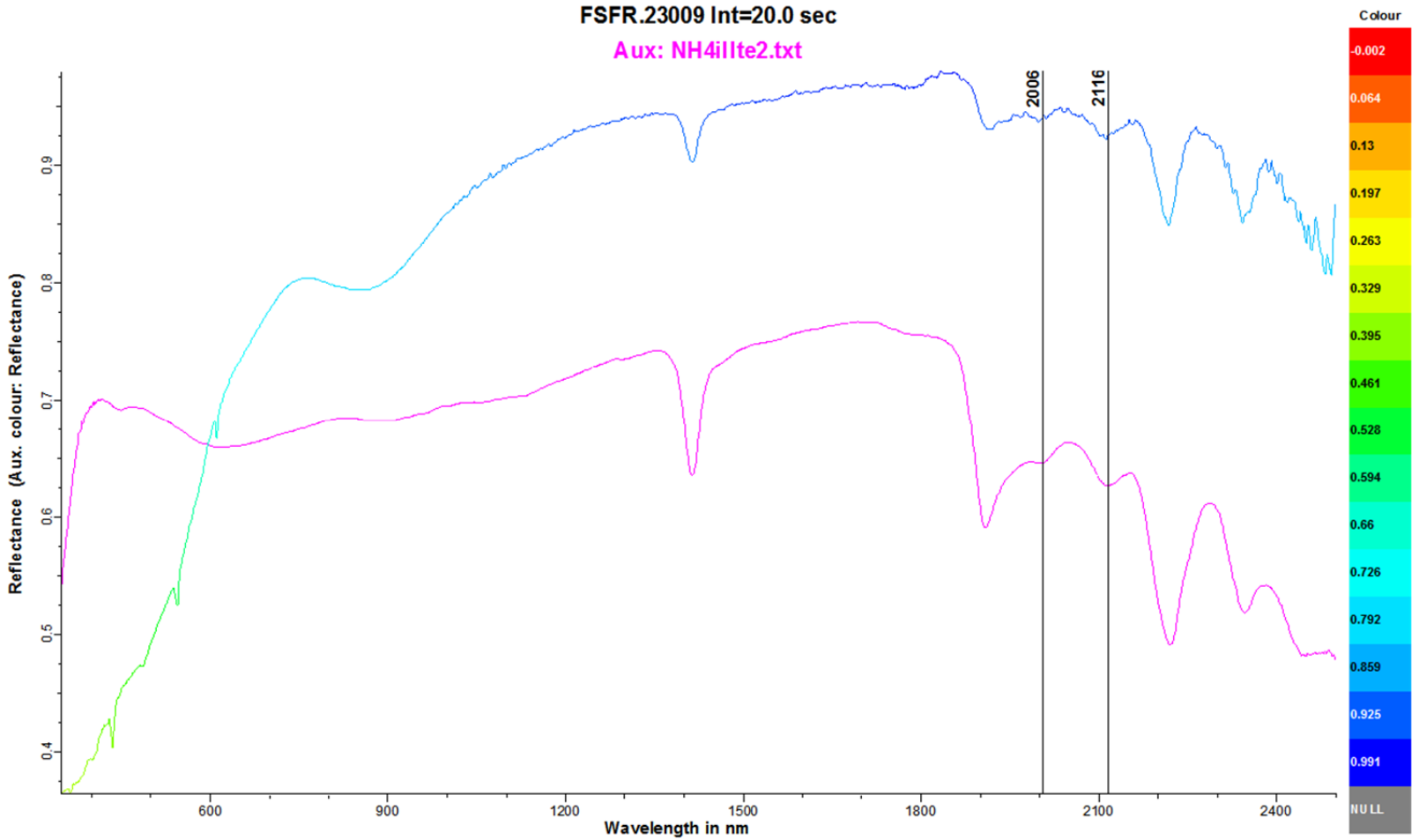

Figure 18 – Sample CP_2 collected in the initial sampling at Cedar Peak. The blue line represents the sample spectrum. The magenta line represents the reference spectrum of ammonium-illite.

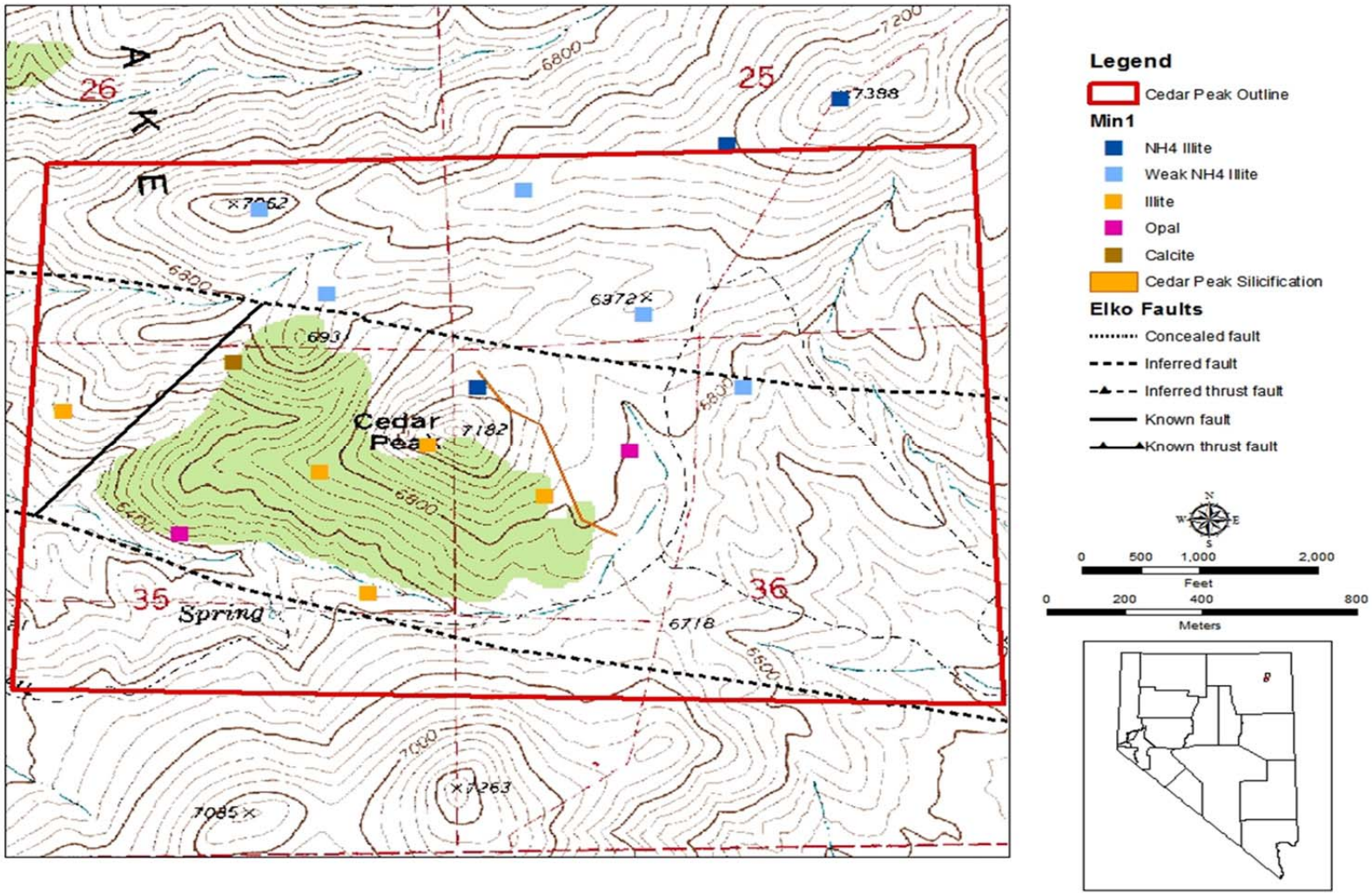

Figure 19 – Map showing the results of the secondary sampling grid with spectral interpretation (colored squares) with faults (black lines) from Coats (1987). The grid was widely spaced in an effort to sample both outside of the possible system as well as inside the system. The strong ammonium-illite samples to the northeast indicate that two hydrothermal ammonium conduits could be present in the area.

Minimum Noise Fraction Transformation

Based on the results of the sampling at Cedar Peak, it is apparent that there are structural controls present in the area which were not showing up on the county geology report. In an effort to determine smaller-scale structures, a forward Minimum Noise Fraction (MNF) transformation was performed on the Cedar Peak area to remove noise from the image. A MNF transformation maximizes the signal to noise ratio of an image, with the outputs being a number of bands specified by the user; band 1 is what the software deems is the purest pixels from the image with the strongest signal to noise ratio. The last band of the MNF transformation is the noisiest, and contains the weakest signal to noise ratio. Displaying individual bands of a MNF transformation often makes certain features in an image stand out. Displaying three bands as red, green, and blue to create a false color composite can highlight various features of an image, such as trends, not normally identified through other processing and analysis techniques.

After performing the Minimum Noise Fraction transformation in ENVI, the data were displayed in RGB, which allows the user to select three bands represented by red, green and blue to create a false color image. Bands 9, 5 and 12 were represented by red, green and blue respectively (figure 20). The presentation of the hyperspectral data in this fashion highlighted a general NW-SE trend in the area which had previously gone unnoticed. On the east side of the Cedar Peak area, the drainages are trending NW-SE. The bedding of the Devil's Gate Limestone, which comprises Cedar Peak, are along this same trend. Furthermore, two NW-SE lineaments bound Cedar Peak on the east and west sides, one of which is in the same location as the silica network and two strong ammonium-illite samples (figure 21).

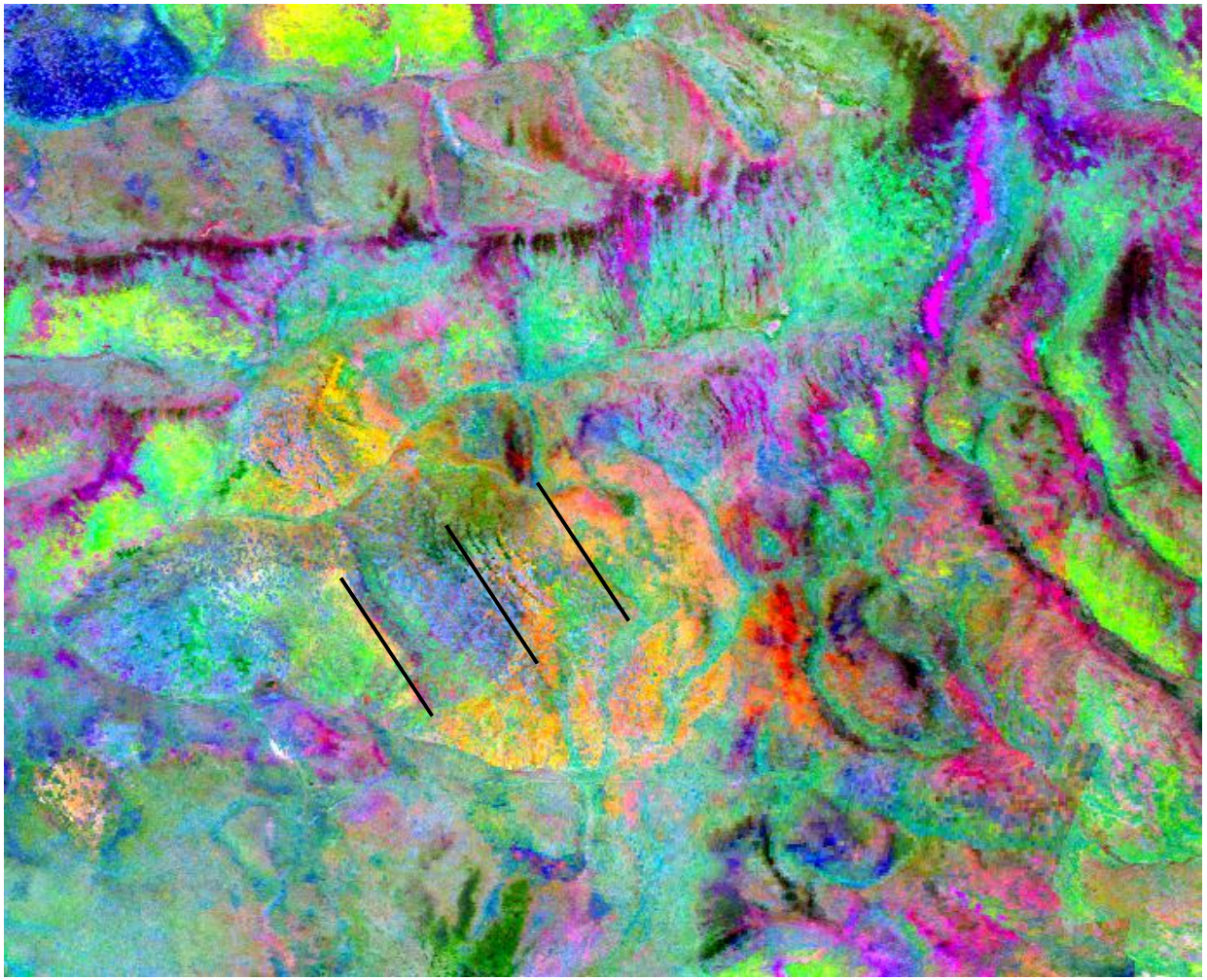

Figure 20 - MNF false color composite of the Cedar Peak area comprised of bands 9, 5 and 12 displayed as red, green and blue respectively. The black lines demonstrate the northwest trends not previously noticed in this study. The westernmost line shows a break between the Devil's Gate Limestone on the right and the Simonson Dolomite on the left. The middle black line shows the northwest trend of the beds in the Devil's Gate Limestone. The easternmost black line demonstrates a northwest trend in the same location as the silicification observed in the field and two ammonium-illite samples. The pink on the eastern extent of the image are drainages, also trending along the same NW-SE direction.

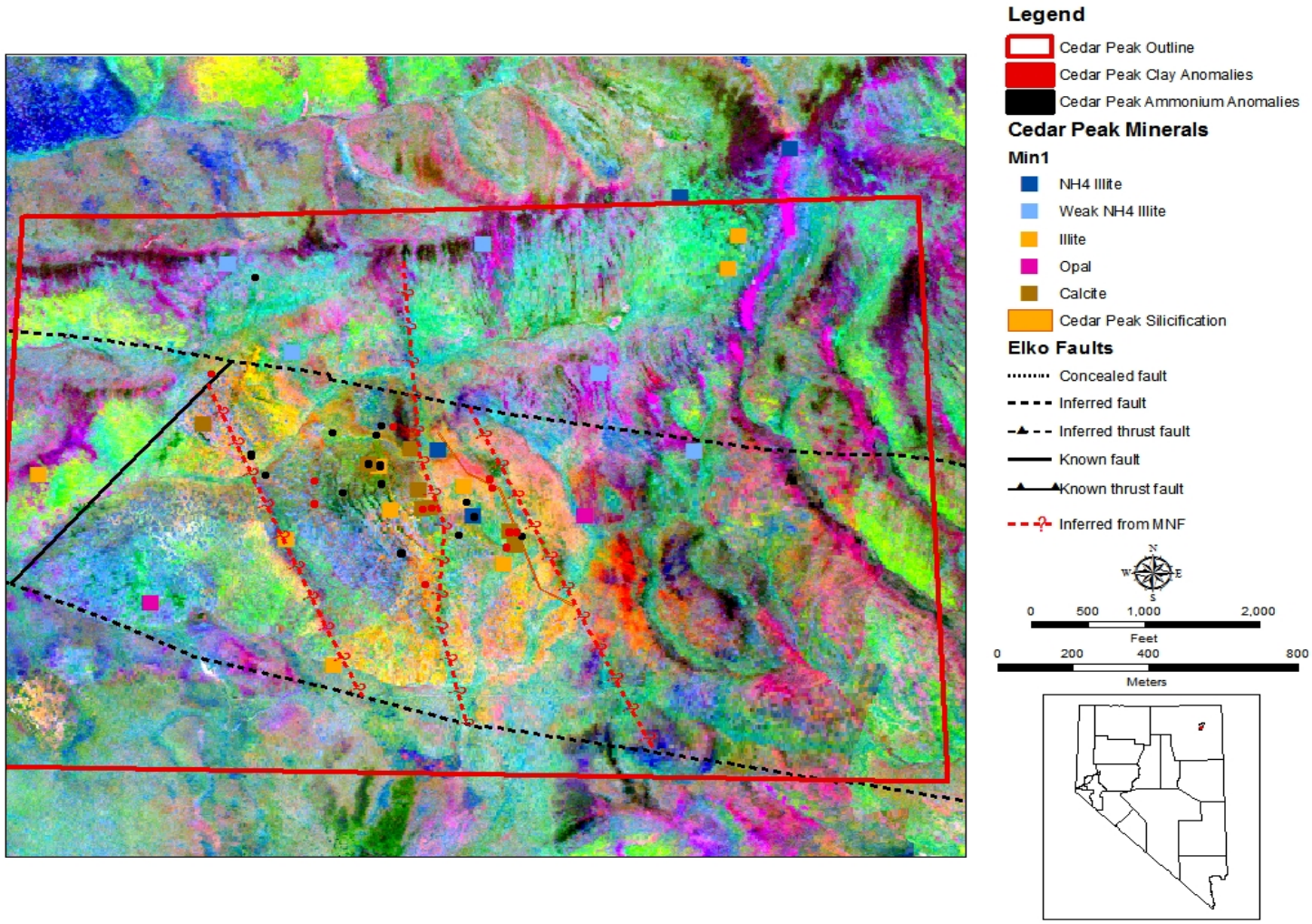

Figure 21 – Map of the Cedar Peak area showing county faults from Coats (1987) in black along with structures inferred from the base MNF image, ammonium-illite samples, clay and ammonium anomalies (red and black circles) and the silicification network observed in the field. The inferred faults, shown in red, are in the same location as the black trend lines in figure 20. The MNF was expanded beyond the Cedar Peak outline to include all samples collected.

Spruce Mountain

Spruce Mountain (figure 22) was included in this study to explore the possibility of using airborne remote sensing on a predefined exploration project area as opposed to a grass roots regional exploration area like the Summer Camp Hills. The study focused on Miranda Gold Corp.'s claim block on the east side of Spruce Mountain. Image processing for the Spruce Mountain area was performed with final thresholds of .087 radians for illite, .075 radians for kaolinite, .145 radians for dickite, and .13 radians for ammonium-illite. Structures believed to be controlling mineralization in the area are aligned in a northeast trend. As expected, pixels representing these spectra were aligned in the same northeast trend (figure 22). A grid was set up in a similar fashion to the grid used in the Cedar Peak area; the grid was designed to cross the northeast trending structures, as well as cross known jasperoids on the property. Several different clays were present on the property and surrounding areas, including eight samples interpreted as ammonium-illite (figure 22).

Shortly after the spectroscopy samples were collected, but before they were analyzed, Miranda Gold Corp. performed a soil sampling survey over the northern section of the claim block which tested a jasperoid and a northeast trending fault which were also covered by the spectral grid. Assays of samples associated with the jasperoid showed the highest gold values (max of 385 ppb) (table 8). Some of the samples with high gold values were also spatially associated with hand samples interpreted as weak ammonium-illite.

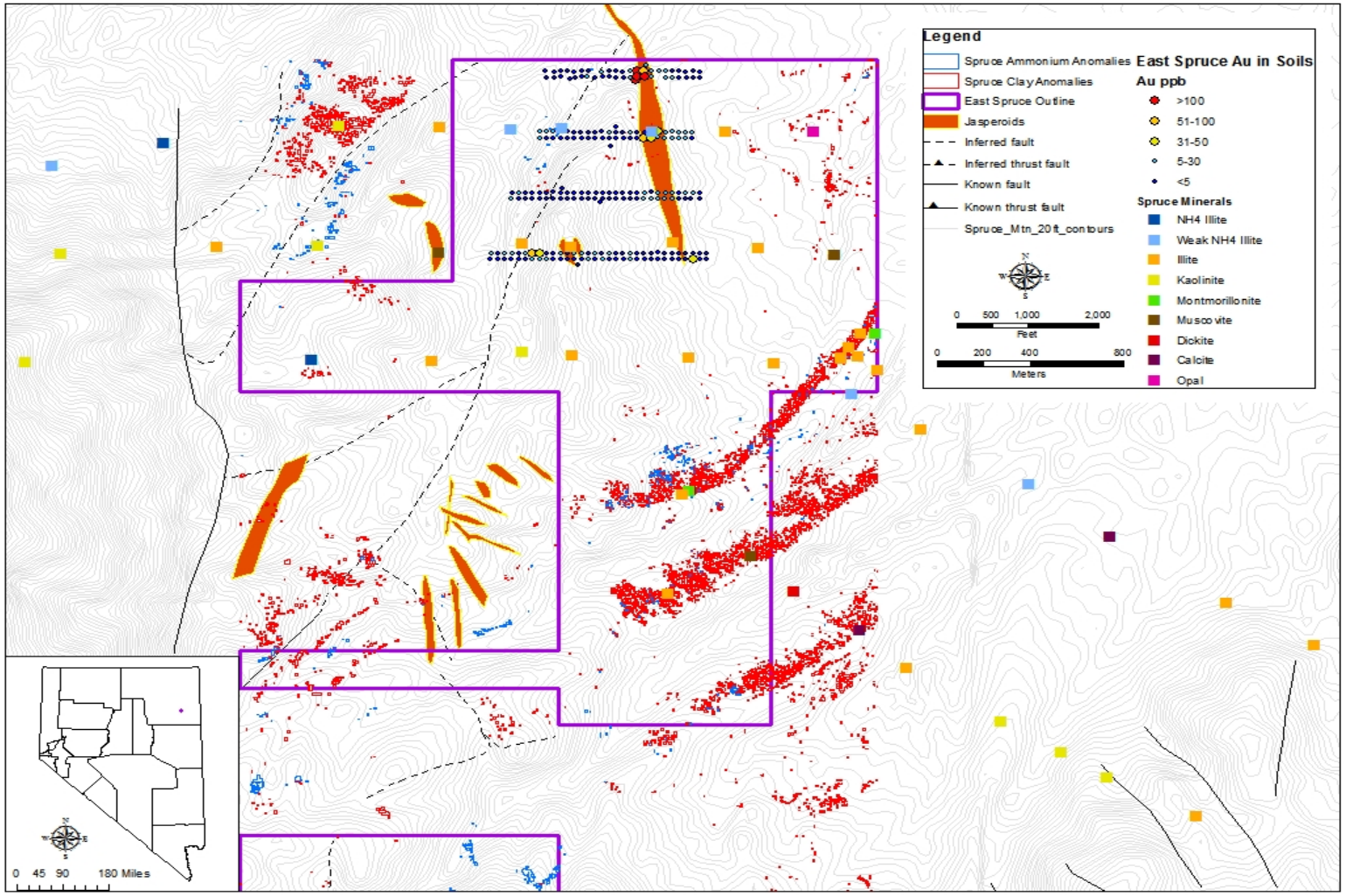

Figure 22 – Location of clay pixels (red outlines) and ammonium pixels (blue outlines), spectral hand sample grid with spectral interpretations (colored squares), faults (black lines) from Coats (1987), jasperoids (orange polygons), and soil survey with Au values (circles).

Chapter 4: Discussion

Although false anomalies occurred in all three of the Summer Camp Hills sub areas, ammonium-illite was still present in all three areas, proving that the presence of desired minerals can be determined through image processing. Additionally, all three sub-areas of the Summer Camp Hills proved to have value as an exploration target, further supporting the hypothesis that the presence of ammonium-illite in a hyperspectral image can provide exploration targets on a regional scale. Favorable geology, meaning stratigraphy that could host a Carlin-style gold deposit, was present in the Summer Camp Hills study areas. In all three areas the presence of hydrothermal clays, as identified by hyperspectral imagery, led to the discovery of hydrothermal effects not searched for in the imagery, such as secondary silica veins in the Windermere Hills or an extensive silica network at Cedar Peak. Additionally, through the Minimum Noise Fraction image features trending the same direction at Cedar Peak revealed possible structures which did not appear on published geology reports of the area. This type of evidence indicating hydrothermal alteration is a key tool in exploring for Carlin-type gold deposits.

While evidence of hydrothermal alteration was pervasive in the three areas, assay results of rock chip sampling in the area prevented the targets from evolving into actual exploration projects. Elevated numbers of several elements were, however, promising. These elements have a consistent role in defining the footprint of Carlin-type gold deposits, and therefore should not be entirely disregarded. The ability to narrow down areas with elevated elements and hydrothermal alteration without spending any time in the field could significantly reduce time and budget of exploration efforts. Although the Summer Camp Hills was narrowed down to three sub areas based on clay and ammonium anomalies, there were other anomalous areas that need to be followed up. The ease of identifying these areas through the identification of ammonium-illite from remote sensing data, as opposed to extensive field work, proved a useful tool and should be expanded upon.

The Spruce Mountain area was approached quite differently than the Summer Camp Hills area, and provided much different results. With the Spruce Mountain area having already been identified as an exploration project, the presence of hydrothermal clays, favorable stratigraphy, extensive faulting, and silicification was not the goal of surveying this area; rather it was the spatial relationship between elevated geochemistry and hydrothermal clays that was of interest. In the Spruce Mountain area there appeared to be a direct correlation between ammonium and faults, as the majority of hand samples interpreted as ammonium-illite were proximal to faults. Furthermore, the relationship between positive soil assays and ammonium-illite is interesting as this connection did not exist in the Summer Camp Hills area. This relation needs to be further explored, as an association between ammonium-illite and positive geochemistry could greatly increase the role of ammonium as a pathfinder for gold.

References Cited

Arehart, G.B., 1996. Characteristics and origin of sediment-hosted disseminated gold deposits: a review. Ore Geology Reviews, vol. 11, p. 383-403.

Baugh, W.M., Kruse, F.A., and Atkinson Jr., W.W., 1998. Quantitative Geochemical Mapping of Ammonium Minerals in the Southern Cedar Mountains, Nevada, Using the Airborne Visible/Infrared Imaging Spectrometer. Remote Sensing of Environment, 65: 292-308.

Bedell, R., 2004. Remote Sensing in Mineral Exploration. SEG Newsletter, No. 58, p.1, 8-14.

Bedell, R.L., and Coolbaugh, M.F., 2009. Appendix 2: Atmospheric Corrections. Reviews in Economic Geology, v.16, p.257-263.

Bradford, M., 2008. Mapping Clay Alteration Across The Northern Goldstrike Property Using Spectroscopy and Remote Sensing, Eureka County, Nevada. Master's Thesis. Bowling Green State University.

Canet, C. et al., 2010. A Statistics-based method for the short-wave infrared spectral analysis of altered rocks: An example from the Acoculco Caldera, Eastern Trans-Mexican Volcanic Belt. Journal of Geochemical Exploration, 105: 1-10.

Cline, J.S., Hofstra, A.H., Muntean, J.L., Tosdal, R.M., and Hickey, K.A., 2005. Carlin-Type Gold Deposits in Nevada: Critical Geologic Characteristics and Viable Models. Economic Geology 100th Anniversary Volume, p. 451-484.

Coats, R.R., 1987. Geology of Elko County, Nevada. Nevada Bureau of Mines and Geology, Bulletin 101.

Crosta, A.P., Ducart, F.D., de Souza Filho, C.R., Azevedo, F., and Brodie, C.G., 2009. Mineral Exploration for Epithermal Gold in Northern Patagonia, Argentina: From Regional- to Deposit-Scale Prospecting using Landsat TM and Terra ASTER. Reviews in Economic Geology, v.16, p.97-108.

De Almeida, T.I.R., De Souza Filho, C.R., Juliani, C., and Branco, F.C., 2009. Application of Remote Sensing to Geobotany to Detect Hydrothermal Alteration Facies in Epithermal High-Sulfidation Gold Deposits in the Amazon Region. Reviews in Economic Geology, v.16, p.135-142.

Dennison, P.E., Halligan, K.Q., and Roberts, D.A., 2004. A Comparison of error metrics and constraints for multiple endmember spectral mixture analysis and spectral angle mapper. Remote Sensing of Environment, V. 93, no. 3, P. 359-367

Duke, E.F., 1994, Near infrared spectra of muscovite, Tschermak substitution, and metamorphic reaction progress: Implication for remote sensing: Geology, v. 22, p. 621-624.

Gao, B., Montes, M.J., Davis, C.O., Goetz, A.F.H., 2009. Atmospheric Correction Algorithms for Hyperspectral Remote Sensing Data of Land and Ocean. Remote Sensing of Environment, Vol. 113, p. S17-S24.

Hope, R.A., 1968. Geologic Map of the Spruce Mountain Quadrangle, Elko County, Nevada. U.S. Geological Survey Geologic Quadrangle Map GQ-942.

Hussey, M.C., 2010. HyMap Survey and Processing Report. HyVista Corporation.

John, D.A., Hofstra, A.H., and Theodore, T.G., 2003. A Special Issue Devoted to Gold Deposits in Northern Nevada: Part 1. Regional Studies and Epithermal Deposits. Bulletin of the Society of Economic Geologists, vol. 98, no. 2, p. 225-234

Kydd, R.A., and Levinson, A.A., 1986. Ammonium halos in lithogeochemical exploration for gold at the Horse Canyon carbonate-hosted deposit, Nevada, U.S.A.: use and limitations. Applied Geochemistry, Vol. 1, p. 407-417.

Kruse, F.A., and Hauff, P.L., 1991. Identification of Illite Polytype Zoning in Disseminated Gold Deposits Using Reflectance Spectroscopy and X-Ray Diffraction – Potential for Mapping with Imaging Spectrometers. IEEE Transactions on Geoscience and Remote Sensing, vol. 29, no. 1, p. 101-104.

Kruse, F.A., Lefkoff, A.B., Boardman, J.W., Heidebrecht, K.B., Shapiro, A.T., Barloon, P.J., and Goetz, A.F.H., 1993. The Spectral image Processing System (SIPS) – Interactive Visualization and Analysis of Imaging Spectrometer Data. Remote Sensing of Environment, Vol. 44, p. 145-163.

Mateer, M., 2010. Ammonium Illite at the Jerritt Canyon District and Goldstrike Property, Nevada: Its Spatial Distribution and Significance in the Exploration of Carlin-Type Deposits. Thesis Dissertation. University of Wyoming.

Mueller, K. J., 1993. Geology of the Windermere Hills, Northeastern Nevada. Nevada Bureau of Mines and Geology Field Studies Map FS-4.

Price, J.G., 2003. Geology of Nevada. Proceedings of the 39th Forum on the Geology of Industrial Minerals, May 18-24, 2003. Nevada Bureau of Mines and Geology, Special Publication 33, p, 191-200.

Ridgway, J., Martiny, B., Gomez-Caballero, A., Macia-Romo, C., and Villasenor-Cabral, M.G., 1991. Ammonium geochemistry of some Mexican silver deposits. Journal of Geochemical Exploration, v. 40, p. 311-327.

Sabins, F.F., 1999. Remote Sensing for Mineral Exploration. Ore Geology Reviews, vol. 14, p. 157-183.

Smith Jr., F.J., Ketner, K.B., Hernandez, G.X., Harris, A.G., Stamm, R.G., and Smith, M.C., 1990. Geologic Map of the Summer Camp Quadrangle and Part of the Black Butte Quadrangle, Elko County, Nevada. U.S. Geological Survey Miscellaneous Investigations Series Map I-2097, scale 1:24,000.

Soechting, W., Rubinstein, N., and Godeas, M., 2009. Identification of Ammonium-Bearing Minerals by Shortwave Infrared Reflectance Spectroscopy at the Esquel Gold Deposit, Argentina. Economic Geology, v. 103, P. 865-869.

Taranik, J.V., and Aslett, Z.L., 2009. Development of Hyperspectral Imaging for Mineral Exploration. Reviews in Economic Geology, v.16, p. 83-95.

Thompson, A.J.B., Hauff, P.L., and Robitaille, A.J., 1999. Alteration Mapping in Exploration Application of Short-Wave Infrared (SWIR) Spectroscopy. SEG Newsletter No. 39, p.1, 16-27.

Williams, L.B., Wilcoxon, B.R., Ferrell, R.E., and Sassen, R., 1992. Diagenesis of ammonium during hydrocarbon maturation and migration, Wilcox Group, Louisiana, USA. Applied Geochemistry, Vol. 7, p. 123-134.

Zamudio, J.A., 2009. Focusing Field Exploration Efforts, Using Results from Hyperspectral Data Analysis of the El Capitan Gold-Platinum Group Metals-Iron Deposit, New Mexico. Reviews in Economic Geology, v.16, p.169-176.

Appendix A

Results of Spectroscopy Analysis

Table 1 – Spectra sorted alphabetically by the mineral suggested by The Spectral Geologist standard library. The Comp_Aux_Min column is the mineral suggested by the program based on the auxiliary library; Comp_Min_1 is the primary mineral suggested by the program based on its internal library; Comp_Min_2 is the secondary mineral suggested by the program based on its internal library. Min1, Min2, and Min3 are the minerals present as interpreted by the author based on 1) presence of ammonium and 2) strength of mineral's spectral signature, here interpreted as mineral abundance.

Sample	Comp_Aux_Min	Comp_Min_1	Comp_Min_2	Min_1	Min_2	Min_3
SC_HS_MM_015e	IS.txt	Ankerite	Dickite	Illite	Smectite	
CP_HS_MM_009b	DoloCO5f.000.txt	Ankerite	Palygorskite	Illite	Kaolinite	Calcite
CP_HS_MM_009c	IS.txt	Ankerite	Muscovite	Illite	Kaolinite	Calcite
CP_HS_MM_005c	MontNV6f.000.txt	Ankerite	Muscovite	Illite	Kaolinite	
HS_SM_00033c.asd	biotite_dickite.txt	Ankerite	NULL	Calcite	Illite	
HS_SM_00023b.asd	IS.txt	Ankerite	Montmorillonite	Illite	Smectite	
HS_SM_00042.asd	IS.txt	Ankerite	Dry Vegetation	Illite	Calcite	Smectite
CP_HS_MM_008b	mont.txt	Ankerite	Muscovite	Illite		
SC_HS_MM_003a	kailinite_nh4illite2.txt	Aspectral	NULL	Kaolinite	Weak NH4 Illite	
SC_HS_MM_005	BuddNV1f.002.txt	Aspectral	NULL	Illite	Smectite	
SC_HS_MM_006c	opaline_silica_illite.txt	Aspectral	NULL	Illite	Opaline Silica	
SC_HS_MM_007b	IS.txt	Aspectral	NULL	Quartz	Illite	
SC_HS_MM_008	Illite_quartz2.txt	Aspectral	NULL	Illite	Quartz	
SC_HS_MM_036	quartz_illite_TG.txt	Aspectral	NULL	Illite	Quartz	
HS_SM_00026.asd	MontNV6f.000.txt	Aspectral	NULL	Illite		
HS_SM_00013.asd	Quartz_Illite_DRC.txt	Aspectral	NULL	Illite	Quartz	
HS_SM_00023c.asd	IS.txt	Aspectral	NULL	Illite	Quartz	
CP_HS_MM_016d	OpalNVf.000.txt	Aspectral	NULL	Opal		
HS_SM_00002a.asd	phengitic_NH4illitexls.txt	Aspectral	NULL	NH4 Illite		
HS_SM_00017.asd	Quartz_Illite_DRC.txt	Aspectral	NULL	Illite	Quartz	
HS_SM_00024.asd	Quartz_Illite_DRC.txt	Aspectral	NULL	Illite	Quartz	
HS_SM_00019.asd	Quartz_Illite_DRC.txt	Aspectral	NULL	Illite	Quartz	

CP_HS_MM_017a	PalyAK1f.002.txt	Aspectral	NULL	Palygorskite	Opal	
HS_SM_00023.asd	IS.txt	Aspectral	NULL	Illite		
HS_SM_00029.asd	mont.txt	Aspectral	NULL	Illite		
CP_HS_MM_012b	Quartz_Illite_DRC.txt	Aspectral	NULL	Illite	Quartz	
HS_SM_00010.asd	Quartz_Illite_DRC.txt	Aspectral	NULL	Illite	Quartz	
HS_SM_00030.asd	mont.txt	Aspectral	NULL	Illite		
SC_HS_MM_003b	kailinite_nh4illite2.txt	Calcite	NULL	Kaolinite	Illite	
SC_HS_MM_003c	Illite_quartz2.txt	Calcite	Kaolinite PX	Kaolinite	Calcite	
SC_HS_MM_004c	DoloCO4f.000.txt	Calcite	NULL	Calcite		
SC_HS_MM_009b	kailinite_nh4illite2.txt	Calcite	NULL	Kaolinite	Weak NH4 Illite	
SC_HS_MM_009c	paragonite_ill.sco.txt	Calcite	Muscovite	Illite	Calcite	
SC_HS_MM_010a	Illite_kaolinite2.txt	Calcite	Muscovite	Illite	Kaolinite	
SC_HS_MM_012b	paragonite_ill.sco.txt	Calcite	NULL	Calcite		
SC_HS_MM_012c	DoloCO5f.000.txt	Calcite	NULL	Kaolinite	Calcite	
SC_HS_MM_012d	quartz_illite_TG.txt	Calcite	Kaolinite PX	Illite		
SC_HS_MM_013a	musc_quartz.txt	Calcite	Diaspore	Kaolinite	Weak NH4 Illite	Calcite
SC_HS_MM_013b	musc_quartz.txt	Calcite	NULL	Illite	Kaolinite	
SC_HS_MM_013c	DoloCO4f.000.txt	Calcite	NULL	Calcite		
SC_HS_MM_014b	quartz_illite_TG.txt	Calcite	NULL	Illite	Calcite	
SC_HS_MM_014c	quartz_illite_TG.txt	Calcite	NULL	Illite	Calcite	
SC_HS_MM_015a	musc_quartz.txt	Calcite	Kaolinite WX	Kaolinite	Calcite	
SC_HS_MM_015c	IS.txt	Calcite	Kaolinite WX	Kaolinite	Calcite	
SC_HS_MM_016a	BuddNV2f.004.txt	Calcite	Muscovite	Illite	Kaolinite	
SC_HS_MM_016b	DoloCO4f.000.txt	Calcite	Muscovite	Illite	Kaolinite	Calcite
SC_HS_MM_016c	musc_quartz.txt	Calcite	Muscovite	Illite	Kaolinite	Calcite
SC_HS_MM_016d	IS.txt	Calcite	NULL	Calcite		
SC_HS_MM_016e	Illite_quartz2.txt	Calcite	Muscovite	Illite	Kaolinite	Calcite
SC_HS_MM_017a	DoloCO4f.000.txt	Calcite	Kaolinite WX	Kaolinite	Calcite	
SC_HS_MM_017b	DoloCO5f.000.txt	Calcite	NULL	Calcite		

SC_HS_MM_017c	DoloCO4f.000.txt	Calcite	Muscovite	Kaolinite	Calcite	
SC_HS_MM_018a	musc_quartz.txt	Calcite	Muscovite	Muscovite	Calcite	
SC_HS_MM_018b	musc_quartz.txt	Calcite	Muscovite	Muscovite	Calcite	
SC_HS_MM_018d	musc_quartz.txt	Calcite	Muscovite	Muscovite	Calcite	
SC_HS_MM_019a	Illite_quartz2.txt	Calcite	Muscovite	Muscovite	Quartz	
SC_HS_MM_019b	DoloCO4f.000.txt	Calcite	Kaolinite WX	Kaolinite	Calcite	
SC_HS_MM_019c	Illite_kaolinite2.txt	Calcite	Kaolinite PX	Kaolinite	Illite	Calcite
SC_HS_MM_019e	Illite_quartz2.txt	Calcite	Kaolinite PX	Kaolinite	Calcite	
SC_HS_MM_020a	Kaolinite_Illite_Water.txt	Calcite	Kaolinite WX	Kaolinite	Calcite	
SC_HS_MM_020c	Kaolinite_Illite_Water.txt	Calcite	Kaolinite WX	Kaolinite	Calcite	
SC_HS_MM_021a	DoloCO4f.000.txt	Calcite	NULL	Kaolinite	Calcite	
SC_HS_MM_021b	DoloCO4f.000.txt	Calcite	NULL	Kaolinite	Calcite	
SC_HS_MM_022a	musc_quartz.txt	Calcite	Kaolinite PX	Muscovite	Quartz	
SC_HS_MM_023a	quartz_illite_TG.txt	Calcite	Muscovite	Illite	Calcite	
SC_HS_MM_023c	musc_quartz.txt	Calcite	Muscovite	Illite	Calcite	
SC_HS_MM_025a	quartz_illite_TG.txt	Calcite	Kaolinite PX	Illite	Kaolinite	Calcite
SC_HS_MM_025b	Al_illite2.txt	Calcite	Diaspore	Illite	Calcite	
SC_HS_MM_026a	DoloCO4f.000.txt	Calcite	Muscovite	Muscovite	Calcite	
SC_HS_MM_026c	musc_quartz.txt	Calcite	Kaolinite PX	Muscovite	Quartz	
SC_HS_MM_027a	DoloCO5f.000.txt	Calcite	NULL	Kaolinite	Calcite	
SC_HS_MM_027b	DoloCO4f.000.txt	Calcite	Muscovite	Kaolinite	Calcite	
SC_HS_MM_027c	DoloCO5f.000.txt	Calcite	Montmorillonite	Illite	Calcite	
SC_HS_MM_029	DoloCO5f.000.txt	Calcite	NULL	Calcite		
SC_HS_MM_030d	kailinite_nh4illite2.txt	Calcite	Montmorillonite	Kaolinite	Illite	
SC_HS_MM_031a	DoloCO5f.000.txt	Calcite	NULL	Calcite		
SC_HS_MM_033a	musc_quartz.txt	Calcite	Montmorillonite	Kaolinite	Calcite	
SC_HS_MM_033b	musc_quartz.txt	Calcite	Muscovite	Kaolinite	Calcite	
SC_HS_MM_034a	Illite_quartz2.txt	Calcite	Kaolinite PX	Kaolinite	Calcite	
SC_HS_MM_034b	Illite_kaolinite2.txt	Calcite	Kaolinite PX	Kaolinite	Calcite	

SC_HS_MM_034c	musc_quartz.txt	Calcite	Kaolinite PX	Kaolinite	Calcite	
SC_HS_MM_035a	Illite_quartz2.txt	Calcite	Muscovite	Illite	Calcite	
SC_HS_MM_035b	DoloCO4f.000.txt	Calcite	NULL	Illite	Kaolinite	Calcite
SC_HS_MM_035c	quartz_illite_TG.txt	Calcite	NULL	Illite	Calcite	
SC_HS_MM_037a	Illite_quartz2.txt	Calcite	Kaolinite WX	Illite	Kaolinite	
SC_HS_MM_037b	Illite_quartz2.txt	Calcite	Muscovite	Illite	Calcite	
SC_HS_MM_038a	opaline_silica_illite.txt	Calcite	Jarosite	Calcite		
SC_HS_MM_038b	DoloCO5f.000.txt	Calcite	Jarosite	Calcite		
SC_HS_MM_039a	Illite_quartz2.txt	Calcite	NULL	Calcite	Illite	
HS_SM_00044b.asd	biotite_dickite.txt	Calcite	NULL	Illite	Calcite	
HS_SM_00044a.asd	DoloCO5f.000.txt	Calcite	Dry Vegetation	Calcite		
HS_SM_00044.asd	calcite.txt	Calcite	Muscovite	Calcite		
HS_SM_00039a.asd	MontNV6f.000.txt	Calcite	NULL	Montmorillonite	Calcite	
HS_SM_00044c.asd	calcite2.txt	Calcite	Muscovite	Calcite		
HS_SM_CP1a.asd	calcite.txt	Calcite	NULL	Calcite	Illite	
HS_SM_00045.asd	calcite.txt	Calcite	Riebeckite	Calcite		
HS_SM_CP1c.asd	calcite.txt	Calcite	Muscovite	Calcite	Illite	
HS_SM_CP1b.asd	calcite.txt	Calcite	Montmorillonite	Calcite	Illite	
HS_SM_00033a.asd	calcite.txt	Calcite	NULL	Calcite		
HS_SM_00038b.asd	biotite_dickite.txt	Calcite	NULL	Calcite		
HS_SM_00036.asd	DoloCO4f.000.txt	Calcite	NULL	Calcite	Illite	
HS_SM_00024c.asd	biotite_dickite.txt	Calcite	NULL	Calcite	Quartz	
HS_SM_00034b.asd	calcite2.txt	Calcite	Riebeckite	Calcite		
HS_SM_00033d.asd	calcite.txt	Calcite	NULL	Calcite	Illite	
HS_SM_00038a.asd	DoloCO5f.000.txt	Calcite	NULL	Calcite		
HS_SM_00034c.asd	calcite.txt	Calcite	Wood	Calcite		
HS_SM_00035a.asd	calcite.txt	Calcite	NULL	Calcite	Illite	
HS_SM_00034d.asd	DoloCO5f.000.txt	Calcite	Wood	Calcite		
HS_SM_00035c.asd	calcite.txt	Calcite	NULL	Calcite	Illite	

HS_SM_00023d.asd	Weak_NH4illite_phengite.txt	Calcite	NULL	Weak Nh4 Illite		
HS_SM_00033b.asd	biotite_dickite.txt	Calcite	NULL	Illite	Calcite	
HS_SM_CP3.asd	biotite_dickite.txt	Calcite	Muscovite	Illite	Calcite	
CP_HS_MM_012c	calcite2.txt	Calcite	NULL	Calcite		
CP_HS_MM_010	calcite2.txt	Calcite	NULL	Calcite		
CP_HS_MM_007c	calcite2.txt	Calcite	NULL	Calcite	Illite	
CP_HS_MM_014a	calcite2.txt	Calcite	NULL	Calcite		
CP_HS_MM_015a	calcite2.txt	Calcite	Muscovite	Kaolinite	Calcite	
CP_HS_MM_014b	calcite2.txt	Calcite	NULL	Calcite		
CP_HS_MM_007b	calcite2.txt	Calcite	Montmorillonite	Illite	Calcite	
CP_HS_MM_007d	biotite_dickite.txt	Calcite	Muscovite	Illite	Calcite	
CP_HS_MM_017d	opaline_silica_illite.txt	Diaspore	Muscovite	Opaline Silica		
SC_HS_MM_022b	kailinite_nh4illite2.txt	Dickite	Calcite	Muscovite	Quartz	
SC_HS_MM_030c	musc_quartz.txt	Dickite	Calcite	Dickite	Kaolinite	
HS_SM_00041.asd	DoloCO4f.000.txt	Dolomite	NULL	Calcite	Illite	
HS_SM_00043.asd	quartz_illite_TG.txt	Dolomite	NULL	Calcite	Illite	
CP_HS_MM_009a	DoloCO5f.000.txt	Dolomite	Muscovite	Calcite	Illite	
HS_SM_00043a.asd	DoloCO4f.000.txt	Dolomite	NULL	Calcite	Illite	
CP_HS_MM_005e	MontNV6f.000.txt	Dolomite	Phengite	Calcite	Illite	
HS_SC_00004a.asd	DoloCO5f.000.txt	Dry Vegetation	Calcite	Dolomite		
HS_SC_00006b.asd	Illite_quartz2.txt	Dry Vegetation	NULL	Dolomite		
HS_SM_00002.asd	mont_kaol2.txt	Jarosite	NULL	Jarosite	Kaolinite	
SC_HS_MM_010c	Illite_quartz2.txt	Kaolinite PX	Calcite	Kaolinite	Illite	
SC_HS_MM_011	quartz_illite_TG.txt	Kaolinite PX	NULL	Illite	Kaolinite	
SC_HS_MM_012a	quartz_illite_TG.txt	Kaolinite PX	NULL	Kaolinite	Illite	
SC_HS_MM_014a	musc_quartz.txt	Kaolinite PX	Calcite	Kaolinite	Illite	
SC_HS_MM_014d	Illite_quartz2.txt	Kaolinite PX	NULL	Kaolinite	Illite	
SC_HS_MM_017d	quartz_illite_TG.txt	Kaolinite PX	Calcite	Kaolinite	Illite	Calcite
SC_HS_MM_017e	musc_quartz.txt	Kaolinite PX	Calcite	Kaolinite	Illite	

SC_HS_MM_024b	Quartz_Illite_DRC.txt	Kaolinite PX	NULL	Kaolinite	Illite	
SC_HS_MM_025c	musc_quartz.txt	Kaolinite PX	NULL	Kaolinite	Illite	
CP_HS_MM_003a	illite_kaolinite_NH4component.txt	Kaolinite PX	NULL	Kaolinite	NH4 Illite	
CP_HS_MM_011c	IS.txt	Kaolinite PX	NULL	Illite	Smectite	
CP_HS_MM_002a	illite_kaolinite_NH4component.txt	Kaolinite PX	Gypsum	Illite	Kaolinite	
CP_HS_MM_011d	Quartz_Illite_DRC.txt	Kaolinite PX	NULL	Illite	Quartz	
CP_HS_MM_001a	mont_kaol2.txt	Kaolinite PX	NULL	Kaolinite		
SC_HS_MM_015b	musc_quartz.txt	Kaolinite WX	Muscovite	Kaolinite	Illite	
SC_HS_MM_015d	Illite_quartz2.txt	Kaolinite WX	Calcite	Kaolinite	Calcite	
SC_HS_MM_019d	kailinite_nh4illite2.txt	Kaolinite WX	Calcite	Kaolinite	Weak NH4 Illite	
SC_HS_MM_020b	Illite_kaolinite2.txt	Kaolinite WX	Calcite	Kaolinite	Calcite	
HS_SM_00018a.asd	Illite_kaolinite2.txt	Kaolinite WX	Muscovite	Illite	Kaolinite	
CP_HS_MM_003b	illite_kaolinite_NH4component.txt	Kaolinite WX	Muscovitic Illite	Illite	Kaolinite	
CP_HS_MM_011a	Kaolinite_Mont.txt	Kaolinite WX	Muscovite	Illite	Kaolinite	
CP_HS_MM_004b	illite_kaolinite_NH4component.txt	Kaolinite WX	Muscovite	Kaolinite	Weak NH4 Illite	
CP_HS_MM_006a	kaolinite2.txt	Kaolinite WX	Muscovitic Illite	Kaolinite	Weak NH4 Illite	
CP_HS_MM_006b	IS_chlorite.txt	Kaolinite WX	Muscovite	Kaolinite	Weak NH4 Illite	
CP_HS_MM_001d	paragonite_mont.sco.txt	Kaolinite WX	NULL	Illite	Kaolinite	
HS_SM_00018c.asd	Kaolinite_Mont.txt	Kaolinite WX	Muscovite	Illite	Kaolinite	
CP_HS_MM_001c	mont_kaol2.txt	Kaolinite WX	NULL	Illite	Kaolinite	
HS_SM_00018b.asd	mont_kaol2.txt	Kaolinite WX	NULL	Kaolinite	Illite	
HS_SM_00005.asd	MontNV6f.000.txt	Magnesium Clays	Montmorillonite	Montmorillonite		
HS_SM_00007.asd	MontNV6f.000.txt	Magnesium Clays	Montmorillonite	Montmorillonite		
HS_SC_00001.asd	quartz_illite_TG.txt	Montmorillonite	DryVegetation	Montmorillonite		
HS_SC_00002.asd	quartz_illite_TG.txt	Montmorillonite	NULL	Illite		
HS_SC_00003.asd	quartz_illite_TG.txt	Montmorillonite	Wood	Illite		
HS_SC_00004.asd	quartz_illite_TG.txt	Montmorillonite	NULL	Illite		
HS_SC_00005.asd	quartz_illite_TG.txt	Montmorillonite	NULL	Illite		
HS_SC_00006.asd	quartz_illite_TG.txt	Montmorillonite	NULL	Illite	Quartz	

HS_SC_00006a.asd	Illite_quartz2.txt	Montmorillonite	Calcite	Illite	Quartz	
HS_SC_00007.asd	kailinite_nh4illite2.txt	Montmorillonite	Siderite	Illite	Quartz	
HS_SC_00008.asd	musc_quartz.txt	Montmorillonite	NULL	Montmorillonite		
HS_SC_00009.asd	quartz_illite_TG.txt	Montmorillonite	Kaolinite PX	Illite		
HS_SC_00009a.asd	OpalNV5f.000.txt	Montmorillonite	NULL	Montmorillonite		
SC_HS_MM_007a	OpalNVf.000.txt	Montmorillonite	Dolomite	Opal		
SC_HS_MM_028	Quartz_Illite_DRC.txt	Montmorillonite	Jarosite	Illite		
SC_HS_MM_032a	opaline_silica_illite.txt	Montmorillonite	NULL	Illite	Opaline Silica	
SC_HS_MM_032b	PalyAK1f.002.txt	Montmorillonite	NULL	Montmorillonite		
HS_SM_00004.asd	mont.txt	Montmorillonite	Dry Vegetation	Montmorillonite		
HS_SM_00002b.asd	mont_kaol2.txt	Montmorillonite	Wood	Montmorillonite		
HS_SM_00035.asd	mont.txt	Montmorillonite	Siderite	Montmorillonite		
HS_SM_00008.asd	quartz_illite_TG.txt	Montmorillonite	Dry Vegetation	Illite	Quartz	
HS_SM_00007a.asd	opaline_silica_illite.txt	Montmorillonite	NULL	Montmorillonite		
HS_SM_00009.asd	quartz_illite_TG.txt	Montmorillonite	Calcite	Illite	Quartz	Calcite
HS_SM_00006a.asd	opaline_silica_illite.txt	Montmorillonite	NULL	Opaline Silica	Montmorillonite	
HS_SM_00026a.asd	MontNV6f.000.txt	Montmorillonite	NULL	Montmorillonite		
HS_SM_00006.asd	quartz_illite_TG.txt	Montmorillonite	NULL	Montmorillonite		
CP_HS_MM_016c	mont.txt	Montmorillonite	Kaolinite PX	Montmorillonite		
CP_HS_MM_016b	mont_kaol.txt	Montmorillonite	NULL	Montmorillonite		
HS_SM_00003.asd	mont.txt	Montmorillonite	NULL	Montmorillonite		
HS_SM_00015.asd	quartz_illite_TG.txt	Montmorillonite	Dry Vegetation	Illite	Quartz	
HS_SM_00025a.asd	IS.txt	Montmorillonite	Ankerite	Illite	Smectite	
HS_SM_00001.asd	quartz_illite_TG.txt	Montmorillonite	NULL	Illite	Quartz	
SC_HS_MM_006a	IS.txt	Muscovite	NULL	Illite		
SC_HS_MM_006b	Illite_quartz2.txt	Muscovite	NULL	Illite	Quartz	
SC_HS_MM_018c	musc_quartz.txt	Muscovite	Calcite	NH4 Illite		
SC_HS_MM_023b	Quartz_Illite_DRC.txt	Muscovite	Calcite	Illite	Quartz	
SC_HS_MM_026b	musc_quartz.txt	Muscovite	Calcite	NH4 Illite		

SC_HS_MM_026d	quartz_illite_TG.txt	Muscovite	Kaolinite PX	Muscovite		
SC_HS_MM_030a	AL_NH4illite_fe.txt	Muscovite	Jarosite	Muscovite	Illite	
SC_HS_MM_030b	Illite_quartz2.txt	Muscovite	Jarosite	Illite	Quartz	
SC_HS_MM_031b	Muscovite.txt	Muscovite	Zoisite	Muscovite		
SC_HS_MM_031c	musc_quartz.txt	Muscovite	Zoisite	Muscovite		
SC_HS_MM_031d	paragonite_ill.sco.txt	Muscovite	Calcite	Illite	Quartz	
HS_SM_00039b.asd	noise4.txt	Muscovite	NULL	Illite		
CP_HS_MM_013b	IS.txt	Muscovite	NULL	Illite		
CP_HS_MM_013a	mont_kaol2.txt	Muscovite	NULL	Montmorillonite	Kaolinite	
CP_HS_MM_017c	IS.txt	Muscovite	Kaolinite WX	Muscovite		
CP_HS_MM_014c	OpalNVf.000.txt	Muscovite	Dolomite	Muscovite		
HS_SM_00020.asd	illite_kaolinite_NH4component.txt	Muscovite	Kaolinite WX	Muscovite		
CP_HS_MM_002b	Illite_quartz2.txt	Muscovite	Kaolinite WX	NH4 Illite	Kaolinite	
CP_HS_MM_007a	Quartz_Illite_DRC.txt	Muscovite	NULL	NH4 Illite	Kaolinite	
HS_SM_00011b.asd	mont.txt	Muscovite	NULL	Muscovite		
HS_SM_00011c.asd	Illite_quartz2.txt	Muscovite	Dickite	Muscovite		
HS_SM_00012.asd	IS.txt	Muscovite	Gypsum	Muscovite		
HS_SM_00011d.asd	Kaolinite_Mont.txt	Muscovite	NULL	Muscovite	Illite	
HS_SM_00025b.asd	Illite_kaolinite2.txt	Muscovite	NULL	Muscovite		
CP_HS_MM_017b	illite_kaolinite_NH4component.txt	Muscovitic Illite	Kaolinite WX	Kaolinite	Weak NH4 Illite	
HS_SM_00046.asd	normal_illite_quartz.txt	Muscovitic Illite	NULL	Illite	Muscovite	
CP_HS_MM_009d	musc_quartz.txt	Muscovitic Illite	Ankerite	Muscovite	Quartz	
HS_SM_00011.asd	IS_chlorite.txt	Muscovitic Illite	Dickite	Muscovite	Quartz	
CP_HS_MM_008a	mont.txt	Muscovitic Illite	Calcite	Montmorillonite		
HS_SM_00013b.asd	Illite_quartz2.txt	Muscovitic Illite	Kaolinite WX	Muscovite	Illite	
HS_SM_00037.asd	quartz_illite_TG.txt	Muscovitic Illite	Palygorskite	Illite	Muscovite	
CP_HS_MM_001b	illite_kaolinite_NH4component.txt	Muscovitic Illite	Kaolinite WX	Kaolinite	Weak NH4 Illite	
HS_SM_00013a.asd	Al_Illite3.txt	Muscovitic Illite	Kaolinite WX	Illite	Muscovite	
HS_SM_00025c.asd	illite3.txt	Muscovitic Illite	NULL	Illite		

CP_HS_MM_016a	kaolinite_muscovite_quartz.txt	Muscovitic Illite	NULL	Muscovite		
SC_HS_MM_001	quartz_illite_TG.txt	NULL	NULL	Illite	Quartz	
SC_HS_MM_002	quartz_illite_TG.txt	NULL	NULL	Illite	Quartz	
SC_HS_MM_004a	MontNV6f.000.txt	NULL	NULL	NULL		
SC_HS_MM_004b	Muscovite.txt	NULL	NULL	Muscovite		
SC_HS_MM_004d	opaline_silica_illite.txt	NULL	NULL	NULL		
SC_HS_MM_006d	musc_quartz.txt	NULL	NULL	Muscovite	Quartz	
SC_HS_MM_009a	DoloCO4f.000.txt	NULL	NULL	Dolomite		
SC_HS_MM_009d	kailinite_nh4illite2.txt	NULL	NULL	Kaolinite	Weak NH4 Illite	
SC_HS_MM_010b	kailinite_nh4illite2.txt	NULL	NULL	Kaolinite	Weak NH4 Illite	
SC_HS_MM_024a	BuddNV2f.004.txt	NULL	NULL	Illite	Kaolinite	
SC_HS_MM_039b	kailinite_nh4illite2.txt	NULL	NULL	Kaolinite	Weak NH4 Illite	
HS_SM_00034a.asd	DoloCO4f.000.txt	NULL	NULL	Calcite		
HS_SM_00024b.asd	SidCT2f.001.txt	NULL	NULL	Illite		
CP_HS_MM_013c	quartz_illite_TG.txt	NULL	NULL	Illite		
HS_SM_00024a.asd	Quartz_Illite_DRC.txt	NULL	NULL	Illite		
HS_SM_00023a.asd	biotite_dickite.txt	NULL	NULL	Illite		
HS_SM_00034f.asd	MontMgNVf.002.txt	NULL	NULL	Calcite		
HS_SM_00037a.asd	noise4.txt	NULL	NULL	NULL		
HS_SM_00022.asd	Quartz_Illite_DRC.txt	NULL	NULL	Illite		
HS_SM_CP2.asd	normal_illite_quartz.txt	NULL	NULL	NH4 Illite		
HS_SM_00014.asd	Quartz_Illite_DRC.txt	NULL	NULL	Illite		
HS_SM_00021.asd	mont_kaol.txt	NULL	NULL	Kaolinite	Montmorillonite	
HS_SM_00016.asd	Quartz_Illite_DRC.txt	NULL	NULL	Illite	Quartz	
CP_HS_MM_011b	Quartz_Illite_DRC.txt	NULL	NULL	Illite	Quartz	
HS_SM_00027.asd	mont.txt	NULL	NULL	Illite		
HS_SM_00032.asd	Quartz_Illite_DRC.txt	NULL	NULL	Illite		
HS_SM_00004a.asd	MontNV6f.000.txt	Palygorskite	Montmorillonite	Montmorillonite		
HS_SM_00031.asd	Illite_kaolinite2.txt	Phengite	Kaolinite WX	Illite	Kaolinite	

HS_SM_00037b.asd	Illite_quartz2.txt	Phengite	NH Alunite	Illite	Quartz	
HS_SM_00035b.asd	biotite_dickite.txt	Phengite	Calcite	Calcite		
HS_SM_00028.asd	Illite_kaolinite2.txt	Phengite	NULL	Illite	Kaolinite	
CP_HS_MM_005d	MontNV6f.000.txt	Phengite	Dolomite	Illite	Kaolinite	
HS_SM_00040.asd	Quartz_Illite_DRC.txt	Phengite	NULL	Weak Nh4 Illite		
CP_HS_MM_004a	illite_kaolinite_NH4component.txt	Phengite	Kaolinite WX	Illite	Kaolinite	
HS_SM_00039c.asd	Weak_NH4_Illite.txt	Phengite	NH Alunite	Nh4 Illite		
HS_SM_00039.asd	NH4illite.txt	Phengite	NULL	Nh4 Illite		
CP_HS_MM_005a	Illite_kaolinite2.txt	Phengite	Wood	Illite	Kaolinite	
CP_HS_MM_005b	Illite_phengite_NH4.txt	Phengitic Illite	NULL	Weak Nh4 Illite	Phengite	
HS_SM_00011a.asd	Illite_quartz2.txt	Phengitic Illite	Kaolinite PX	Illite	Quartz	
CP_HS_MM_015b	Illite_phengite.txt	Phengitic Illite	NULL	Illite	Phengite	
HS_SM_00034e.asd	MontNV6f.000.txt	Siderite	Montmorillonite	Montmorillonite		
CP_HS_MM_012a	OpalNV5f.000.txt	Siderite	Montmorillonite	Opal		
SC_HS_MM_040	quartz_illite_TG.txt	Zoisite	Jarosite	Illite	Quartz	

Table 2 – Final mineral interpretation sorted alphabetically by the sample name. Min1, Min2, and Min3 are the minerals present as interpreted by the author based on 1) presence of ammonium and 2) strength of mineral's spectral signature, here interpreted as mineral abundance. Samples containing "sc" in the Sample ID are from Spruce Mountain. Samples containing "cp" or "sm" in the sample ID are from the Summer Camp Hills.

Sample ID	Min1	Min2	Min3
HS_SC_001	Montmorillonite		
HS_SC_002	Illite		
HS_SC_003	Illite		
HS_SC_004	Illite	Dolomite	
HS_SC_005	Illite		
HS_SC_006	Illite	Quartz	Dolomite
HS_SC_007	Illite	Quartz	
HS_SC_008	Montmorillonite		
HS_SC_009	Illite	Montmorillonite	
sc_hs_mm_001	Illite	Quartz	
sc_hs_mm_002	Illite	Quartz	
sc_hs_mm_003	Weak Nh4 Illite	Kaolinite	Calcite
sc_hs_mm_004	Muscovite	Calcite	
sc_hs_mm_005	Illite	Smectite	
sc_hs_mm_006	Illite	Opaline Silica	Muscovite
sc_hs_mm_007	Opal	Illite	Quartz
sc_hs_mm_008	Illite	Quartz	
sc_hs_mm_009	Weak Nh4 Illite	Kaolinite	Dolomite
sc_hs_mm_010	Weak Nh4 Illite	Kaolinite	
sc_hs_mm_011	Illite	Kaolinite	
sc_hs_mm_012	Kaolinite	Illite	Calcite
sc_hs_mm_013	Weak Nh4 Illite	Kaolinite	Calcite
sc_hs_mm_014	Illite	Kaolinite	Calcite
sc_hs_mm_015	Kaolinite	Illite	Calcite
sc_hs_mm_016	Illite	Kaolinite	Calcite
sc_hs_mm_017	Kaolinite	Illite	Calcite
sc_hs_mm_018	Nh4 Illite	Muscovite	Calcite
sc_hs_mm_019	Weak Nh4 Illite	Kaolinite	Muscovite
sc_hs_mm_020	Kaolinite	Calcite	
sc_hs_mm_021	Kaolinite	Calcite	
sc_hs_mm_022	Muscovite	Quartz	
sc_hs_mm_023	Illite	Quartz	Calcite
sc_hs_mm_024	Illite	Kaolinite	
sc_hs_mm_025	Illite	Kaolinite	Calcite
sc_hs_mm_026	Nh4 Illite	Muscovite	Quartz

sc_hs_mm_027	Kaolinite	Calcite	Illite
sc_hs_mm_028	Illite		
sc_hs_mm_029	Calcite		
sc_hs_mm_030	Dickite	Illite	Muscovite
sc_hs_mm_031	Muscovite	Illite	Calcite
sc_hs_mm_032	Illite	Opaline Silica	Montmorillonite
sc_hs_mm_033	Kaolinite	Calcite	
sc_hs_mm_034	Kaolinite	Calcite	
sc_hs_mm_035	Illite	Calcite	Kaolinite
sc_hs_mm_036	Illite	Quartz	
sc_hs_mm_037	Illite	Kaolinite	Calcite
sc_hs_mm_038	Calcite		
sc_hs_mm_039	Weak Nh4 Illite	Kaolinite	Calcite
sc_hs_mm_040	Illite	Quartz	
cp_hs_mm_001	Weak NH4 Illite	Kaolinite	
cp_hs_mm_002	Nh4 Illite	Kaolinite	
cp_hs_mm_003	Nh4 Illite	Kaolinite	
cp_hs_mm_004	Weak NH4 Illite	Kaolinite	
cp_hs_mm_005	Weak Nh4 Illite	Kaolinite	Calcite
cp_hs_mm_006	Weak Nh4 Illite	Kaolinite	
cp_hs_mm_007	Nh4 Illite	Kaolinite	Calcite
cp_hs_mm_008	Illite	Montmorillonite	
cp_hs_mm_009	Illite	Kaolinite	Muscovite
cp_hs_mm_010	Calcite		
cp_hs_mm_011	Illite	Quartz	Kaolinite
cp_hs_mm_012	Opal	Illite	Calcite
cp_hs_mm_013	Illite	Montmorillonite	Kaolinite
cp_hs_mm_014	Muscovite	Calcite	
cp_hs_mm_015	Illite	Kaolinite	Phengite
cp_hs_mm_016	Opal	Montmorillonite	Muscovite
cp_hs_mm_017	Weak NH4 Illite	Opal	Muscovite
HS_SM_001	Illite	Quartz	
HS_SM_002	Nh4 Illite	Jarosite	Montmorillonite
HS_SM_003	Montmorillonite		
HS_SM_004	Montmorillonite		
HS_SM_005	Opal	Montmorillonite	
HS_SM_006	Montmorillonite		
HS_SM_007	Montmorillonite		
HS_SM_008	Illite	Quartz	
HS_SM_009	Illite	Quartz	
HS_SM_010	Illite	Quartz	

HS_SM_011	Muscovite	Illite	Quartz
HS_SM_013	Illite	Muscovite	Quartz
HS_SM_014	Illite		
HS_SM_015	Illite	Quartz	
HS_SM_016	Illite	Quartz	
HS_SM_017	Illite	Quartz	
HS_SM_018	Illite	Kaolinite	
HS_SM_019	Illite	Quartz	
HS_SM_020	Muscovite		
HS_SM_021	Kaolinite	Montmorillonite	
HS_SM_022	Illite		
HS_SM_023	Weak NH4 Illite	Quartz	Smectite
HS_SM_024	Illite	Quartz	Calcite
HS_SM_025	Illite	Muscovite	Smectite
HS_SM_026	Illite	Montmorillonite	
HS_SM_027	Illite		
HS_SM_028	Illite	Kaolinite	
HS_SM_029	Illite		
HS_SM_030	Illite		
HS_SM_031	Illite	Kaolinite	
HS_SM_032	Illite		
HS_SM_033	Calcite	Illite	
HS_SM_034	Calcite	Montmorillonite	
HS_SM_035	Calcite	Illite	Montmorillonite
HS_SM_036	Calcite	Illite	
HS_SM_037	Illite	Muscovite	Quartz
HS_SM_038	Calcite		
HS_SM_039	NH4 Illite	Montmorillonite	Calcite
HS_SM_040	Weak NH4 Illite		
HS_SM_041	Calcite	Illite	
HS_SM_042	Illite	Calcite	Smectite
HS_SM_043	Calcite	Illite	
HS_SM_044	Calcite	Illite	
HS_SM_045	Calcite		
HS_SM_046	Illite	Muscovite	

Appendix B

Results of Geochemical Analysis at Summer Camp Hills and Spruce Mountain

Table 3 – Method and detection limits for the geochemical analysis of rock chips in the Summer Camp Hills. Samples were analyzed by ALS Minerals using an acid digest with elements quantified by Inductively Coupled Plasma (ICP) with Mass Spectroscopy (MS). Gold was extracted through fire assay and quantified with Atomic Absorption Spectroscopy (AAS).

Analytes	Method	Unit	Range	Analytes	Method	Unit	Range
Au	FA-AAS	ppm	0.005-10	Mo	ICPMS	ppm	0.05-10,000
Ag	ICPMS	ppm	0.01-100	Na	ICPMS	percent	0.01-10
Al	ICPMS	percent	0.01-25	Nb	ICPMS	ppm	0.05-500
As	ICPMS	ppm	0.1-10,000	Ni	ICPMS	ppm	0.2-10,000
B	ICPMS	ppm	10-10,000	P	ICPMS	ppm	10-10,000
Ba	ICPMS	ppm	10-10,000	Pb	ICPMS	ppm	0.2-10,000
Be	ICPMS	ppm	0.05-1,000	Rb	ICPMS	ppm	0.1-10,00
Bi	ICPMS	ppm	0.01-10,000	Re	ICPMS	ppm	0.001-50
Ca	ICPMS	percent	0.01-25	S	ICPMS	percent	0.01-10
Cd	ICPMS	ppm	0.01-1,000	Sb	ICPMS	ppm	0.05-10,000
Ce	ICPMS	ppm	0.02-500	Sc	ICPMS	ppm	0.1-10,000
Co	ICPMS	ppm	0.1-10,000	Se	ICPMS	ppm	0.2-1,000
Cr	ICPMS	ppm	1-10,000	Sn	ICPMS	ppm	0.2-500
Cs	ICPMS	ppm	0.05-500	Sr	ICPMS	ppm	0.2-10,000
Cu	ICPMS	ppm	0.2-10,000	Ta	ICPMS	ppm	0.01-500
Fe	ICPMS	percent	0.01-50	Te	ICPMS	ppm	0.01-500
Ga	ICPMS	ppm	0.05-10,000	Th	ICPMS	ppm	0.2-10,000
Ge	ICPMS	ppm	0.05-500	Ti	ICPMS	percent	0.005-10
Hf	ICPMS	ppm	0.02-500	Tl	ICPMS	ppm	0.02-10,000
Hg	ICPMS	ppm	0.01-10,000	U	ICPMS	ppm	0.05-10,000
In	ICPMS	ppm	0.005-500	V	ICPMS	ppm	1-10,000
K	ICPMS	percent	0.01-10	W	ICPMS	ppm	0.05-10,000
La	ICPMS	ppm	0.2-10,000	Y	ICPMS	ppm	0.05-500
Li	ICPMS	ppm	0.1-10,000	Zn	ICPMS	ppm	2-10,000
Mg	ICPMS	percent	0.01-25	Zr	ICPMS	ppm	0.5-500
Mn	ICPMS	ppm	5-50,000				

Table 4 - Rock chip assay results for Fink's Canyon in the Summer Camp Hills. A negative number indicates that the sample was below detection level.

SampleID	Au_ppm	Ag_ppm	Al_%	As_ppm	B_ppm	Ba_ppm	Be_ppm	Bi_ppm	Ca_%	Cd_ppm	Ce_ppm	Co_ppm	Cr_ppm	Cs_ppm	Cu_ppm
FINKCD1	-0.005	0.02	0.07	6	-10	610	0.08	0.01	25	0.12	4.08	0.8	-1	0.16	4
FINKCD2	-0.005	0.02	0.05	6	-10	4260	0.11	0.01	25	0.36	4.27	0.5	-1	0.11	4.8
FINKCD3	-0.005	0.08	0.35	2	-10	90	0.31	0.04	16.75	0.3	10.45	3.8	4	0.34	9.3
FINKCD4	-0.005	0.09	0.36	28.3	-10	970	0.25	0.07	0.22	0.07	24.2	4.5	10	0.21	18.8
FINKCD5	0.005	0.04	0.06	24.4	-10	50	0.07	0.01	1.29	0.06	10.1	1.1	13	0.08	4.2
FINKCD6	-0.005	0.06	0.18	8.4	-10	80	0.12	0.02	0.26	0.05	9.09	1	13	0.18	5.4
FINKCD7	-0.005	0.13	0.27	4.4	-10	60	0.2	0.03	0.12	0.07	7.07	2.3	12	0.69	9.1
FINKCD8	0.007	0.05	0.13	75.6	-10	250	0.11	0.03	1.93	0.06	3.52	1.9	16	0.11	8.5
FINKCD9	0.005	0.07	0.33	35	-10	80	0.31	0.05	0.16	0.07	7.98	3	12	0.18	15.3
HS-SM-023	-0.005	0.05	0.7	4	10	1040	0.44	0.09	20.7	1.99	21.1	3.7	6	0.92	9.7
HS-SM-024	-0.005	0.07	0.72	5	10	1790	0.36	0.1	19.6	0.57	17.1	3.9	7	1.12	10.4
HS-SM-026	-0.005	0.05	0.63	3	10	200	0.42	0.09	21.5	0.48	20.6	3.2	7	0.79	8.9
HS-SM-028	-0.005	0.03	0.22	7.3	-10	3060	0.16	0.07	0.43	0.08	12.4	2.4	12	0.13	19.5
HS-SM-029	0.005	0.03	0.6	5	10	90	0.34	0.07	22.6	0.17	15.65	2.6	4	0.69	6.7
SampleID	**Fe_%**	**Ga_ppm**	**Ge_ppm**	**Hf_ppm**	**Hg_ppm**	**In_ppm**	**K_%**	**La_ppm**	**Li_ppm**	**Mg_%**	**Mn_ppm**	**Mo_ppm**	**Na_%**	**Nb_ppm**	**Ni_ppm**
FINKCD1	1.47	0.25	-0.1	0.02	0.03	-0.005	0.03	2.2	0.9	0.25	162	3.79	0.01	0.24	1.9
FINKCD2	1.66	0.25	-0.1	0.02	0.03	0.006	0.02	2.2	0.6	0.23	164	1.22	0.01	0.23	4
FINKCD3	1.46	1.11	-0.1	0.04	0.02	0.014	0.1	5.6	6.3	0.17	183	0.47	0.01	0.2	13.8
FINKCD4	1.43	1.57	0.05	0.05	0.16	0.009	0.17	14.8	1.2	0.04	136	0.78	0.01	0.12	25.4
FINKCD5	0.6	0.28	-0.1	0.02	0.01	0.005	0.03	5.6	0.9	0.01	59	1.32	-0.01	-0.05	3.5
FINKCD6	0.63	0.58	-0.1	0.04	0.02	-0.005	0.09	3.4	1	0.02	50	0.44	0.01	0.06	4.5
FINKCD7	1.02	0.82	-0.1	0.05	0.02	0.006	0.13	3.8	1.6	0.03	73	0.43	0.01	0.07	9.7
FINKCD8	1.32	0.45	-0.1	0.03	0.05	-0.005	0.07	1.7	0.9	0.03	69	2.4	0.01	0.06	8.8
FINKCD9	1.13	1.18	-0.1	0.05	0.02	0.012	0.18	10.2	1.8	0.03	48	1.36	-0.01	0.07	11.5
HS-SM-023	0.98	1.89	0.05	0.05	0.03	0.013	0.22	12	7.1	0.31	233	0.92	0.01	0.5	12.2
HS-SM-024	0.94	1.85	-0.1	0.1	0.03	0.011	0.2	9.7	8.7	0.45	337	0.47	0.02	0.45	10.2
HS-SM-026	1.1	1.65	-0.1	0.03	0.02	0.013	0.18	11.7	8.4	0.32	256	1.1	-0.01	0.33	11
HS-SM-028	0.98	1.07	-0.1	0.05	0.17	0.008	0.1	7.1	1	0.04	108	1.48	0.01	0.11	16.6
HS-SM-029	0.74	1.53	-0.1	0.06	0.03	0.009	0.14	9.1	5.9	2.9	275	0.26	0.01	0.53	6.5

SampleID	P_ppm	Pb_ppm	Rb_ppm	Re_ppm	S_%	Sb_ppm	Sc_ppm	Se_ppm	Sn_ppm	Sr_ppm	Ta_ppm	Te_ppm	Th_ppm	Ti_%	Tl_ppm
FINKCD1	90	0.9	1.5	0.001	0.02	0.26	0.6	0.4	-0.2	955	-0.01	0.04	0.3	-0.005	0.04
FINKCD2	180	1.2	1	-0.001	0.12	0.5	0.6	0.4	-0.2	1920	-0.01	0.04	0.2	-0.005	0.1
FINKCD3	290	5.2	5.5	0.001	0.01	0.21	3.2	0.7	0.2	632	-0.01	0.13	2	-0.005	0.05
FINKCD4	420	8.9	6.4	-0.001	0.03	2.9	1.1	0.5	0.2	93.1	-0.01	0.05	2.5	-0.005	0.09
FINKCD5	210	1.6	1.4	-0.001	0.01	0.53	0.5	0.5	-0.2	18.8	-0.01	0.03	0.3	-0.005	0.02
FINKCD6	220	2.4	4	-0.001	0.01	0.25	0.9	0.2	-0.2	9.3	-0.01	0.02	1.3	-0.005	0.02
FINKCD7	300	4.6	5.5	-0.001	-0.01	0.29	1.3	0.2	-0.2	8.4	-0.01	0.04	1.7	-0.005	0.04
FINKCD8	260	3.6	2.7	-0.001	0.04	1.11	0.7	1.2	-0.2	56.1	-0.01	0.04	0.7	-0.005	0.02
FINKCD9	120	4.6	6.9	-0.001	-0.01	0.55	1.7	0.3	0.2	6.8	-0.01	0.05	1.7	-0.005	0.04
HS-SM-023	360	6.1	11.6	-0.001	0.05	0.41	2.7	0.5	0.3	701	-0.01	0.09	2.3	0.017	0.1
HS-SM-024	500	6.3	11.6	-0.001	0.08	0.38	2.5	0.8	0.3	546	-0.01	0.06	2.3	0.022	0.1
HS-SM-026	430	5.8	9.6	0.001	0.02	0.24	2.7	0.9	0.2	936	-0.01	0.13	2.1	0.012	0.07
HS-SM-028	450	5.1	4.2	-0.001	0.08	4.17	0.8	0.6	-0.2	54.2	-0.01	0.03	1.5	-0.005	0.04
HS-SM-029	320	6.6	8.7	-0.001	0.02	0.36	1.8	0.9	0.2	178	-0.01	-0.01	1.8	0.018	0.09

SampleID	U_ppm	V_ppm	W_ppm	Y_ppm	Zn_ppm	Zr_ppm
FINKCD1	0.45	23	0.47	5.22	17	1.1
FINKCD2	0.41	27	0.54	4.98	33	0.7
FINKCD3	0.28	13	0.17	13.1	52	2.2
FINKCD4	0.32	21	0.84	4.52	57	2.4
FINKCD5	0.06	4	0.06	1.63	12	0.7
FINKCD6	0.13	6	0.08	2.06	15	1.5
FINKCD7	0.18	9	0.08	3.34	15	2.1
FINKCD8	0.12	12	0.23	1.38	11	1.1
FINKCD9	0.17	14	0.12	5.98	50	2.2
HS-SM-023	0.39	14	0.24	10.85	72	2.6
HS-SM-024	0.45	14	0.27	8.62	52	4.3
HS-SM-026	0.73	11	0.15	14.55	50	1.6
HS-SM-028	0.31	15	0.69	6.31	34	2.4
HS-SM-029	0.37	10	0.41	6.82	24	2.9

Table 5 – Rock chip assay results for Windermere Hills in the Summer Camp Hills. A negative number indicates that the sample was below detection level.

SampleID	Au_ppm	Ag_ppm	Al_%	As_ppm	B_ppm	Ba_ppm	Be_ppm	Bi_ppm	Ca_%	Cd_ppm	Ce_ppm	Co_ppm	Cr_ppm	Cs_ppm	Cu_ppm
HS-SM-038	-0.005	0.01	0.03	2	-10	130	0.06	-0.01	16.8	0.87	6.02	0.6	4	0.05	2.6
HS-SM-039	-0.005	0.09	0.58	9	10	320	0.62	0.11	10.65	2.62	20.9	5.5	9	0.53	16.4
WDCD1	-0.005	0.03	0.16	2.7	-10	1660	0.12	0.01	9.06	1.87	6.1	0.8	21	0.18	2.7
WDCD2	-0.005	0.04	0.38	6.5	-10	1150	0.22	0.03	7.83	0.19	15.8	2.1	17	0.54	4.6
WDCD3	-0.005	0.02	0.07	2.1	-10	2230	0.06	0.01	2.74	0.23	3.73	0.6	19	0.1	1.9
WDCD4	-0.005	0.07	0.66	9.1	10	190	0.34	0.07	5.22	0.14	21.3	4.5	20	1.25	10.8
WDCD5	-0.005	0.11	0.66	12.2	10	270	0.4	0.07	4.1	0.25	26.1	3.8	17	0.83	16.9
WDCD6	-0.005	0.01	0.03	0.7	-10	270	-0.05	0.01	0.57	0.07	0.87	0.4	16	0.06	2.3
WDCD7	0.009	1.65	0.25	141	10	130	0.15	0.21	0.32	4.59	12.2	1.3	19	0.37	53.1
WDCD8	-0.005	0.14	0.33	76.6	10	1890	2.1	0.05	0.34	8.78	6.3	135	6	0.99	27.4
WDCD9	-0.005	0.05	0.46	56.4	-10	350	0.24	0.02	0.13	0.09	6.99	0.8	105	0.23	3
SampleID	**Fe_%**	**Ga_ppm**	**Ge_ppm**	**Hf_ppm**	**Hg_ppm**	**In_ppm**	**K_%**	**La_ppm**	**Li_ppm**	**Mg_%**	**Mn_ppm**	**Mo_ppm**	**Na_%**	**Nb_ppm**	**Ni_ppm**
HS-SM-038	0.21	0.13	-0.1	0.02	0.02	-0.005	0.01	3	0.3	0.26	124	1.07	0.02	0.08	3
HS-SM-039	1.36	1.6	0.05	0.09	0.04	0.018	0.21	10.4	5.3	2.38	293	22.7	0.01	0.28	50.3
WDCD1	0.43	0.49	-0.1	0.07	0.02	-0.005	0.07	6.8	1.7	3.29	99	0.81	0.03	-99	8.7
WDCD2	0.77	1.07	0.05	0.06	0.03	0.009	0.12	9.4	4.2	0.2	318	0.64	0.02	-99	12.6
WDCD3	0.44	0.29	-0.1	0.05	0.03	-0.005	0.03	2.5	0.7	1.13	82	0.61	0.02	-99	5
WDCD4	1.42	2.05	0.11	0.19	0.08	0.013	0.25	10.4	6.5	1.28	207	0.75	0.02	-99	21.2
WDCD5	1.99	1.79	0.09	0.12	0.03	0.014	0.23	13.1	5.2	0.36	368	1.09	0.02	-99	29.6
WDCD6	0.48	0.2	-0.1	0.02	0.01	-0.005	0.02	0.4	0.3	0.04	58	0.38	-0.01	-99	2.7
WDCD7	15.1	3.82	0.34	0.13	0.66	0.037	0.55	10.7	7.4	0.09	283	26.7	0.15	0.32	38
WDCD8	34.7	1.8	0.75	0.06	0.08	0.008	0.13	3	1.3	0.06	10400	86.6	0.03	-99	1390
WDCD9	1.24	1.6	0.05	0.1	1.11	0.008	0.19	7	1.6	0.02	80	6.81	0.01	-99	5.4

SampleID	P_ppm	Pb_ppm	Rb_ppm	Re_ppm	S_%	Sb_ppm	Sc_ppm	Se_ppm	Sn_ppm	Sr_ppm	Ta_ppm	Te_ppm	Th_ppm	Ti_%	Tl_ppm
HS-SM-038	120	0.6	0.6	0.003	0.03	0.39	0.4	0.6	-0.2	548	-0.01	-0.01	0.3	-0.005	0.03
HS-SM-039	1570	7.3	10.2	0.001	0.03	3.37	4	4.8	0.3	174	-0.01	0.02	3.9	0.01	0.34
WDCD1	410	1.3	2.7	-0.001	0.15	0.74	1.2	0.6	-0.2	153.5	-0.01	-99	0.9	-0.005	0.06
WDCD2	1020	1.9	5.2	-0.001	0.05	0.7	2.1	0.6	-0.2	53.2	-0.01	-99	1.4	-0.005	0.1
WDCD3	300	1.3	1.2	0.001	0.08	0.26	1.2	0.5	-0.2	148	-0.01	-99	0.5	-0.005	0.04
WDCD4	600	4	12.4	-0.001	0.03	0.34	4.8	0.8	0.2	57	0.02	-99	2.9	-0.005	0.06
WDCD5	940	4	9	-0.001	0.04	0.49	3.1	1.3	0.2	58	-0.01	-99	2.8	-0.005	0.09
WDCD6	160	0.4	0.5	-0.001	-0.01	0.15	0.2	0.2	-0.2	13	-0.01	-99	0.2	-0.005	0.02
WDCD7	2170	632	14.4	0.001	1.43	15.8	2	15.2	0.5	160.5	<0.01	0.42	1.1	0.007	0.22
WDCD8	6170	4.4	4.8	0.001	0.01	14.3	2.5	0.6	-0.2	64.1	-0.01	-99	1.2	-0.005	1.66
WDCD9	1120	2	6.7	-0.001	0.25	4.27	1.3	1.8	0.2	52	-0.01	-99	1.1	-0.005	0.62

SampleID	U_ppm	V_ppm	W_ppm	Y_ppm	Zn_ppm	Zr_ppm
HS-SM-038	0.52	18	-0.1	7.12	26	0.7
HS-SM-039	2.42	80	0.27	15.9	198	5.7
WDCD1	0.46	8	0.19	6.89	40	3.1
WDCD2	0.67	21	0.45	8.41	44	3.4
WDCD3	0.37	3	0.13	4.35	17	1.8
WDCD4	0.63	17	0.26	9.45	55	7.2
WDCD5	0.73	25	0.45	13.95	141	6
WDCD6	0.31	2	-0.1	1.04	7	0.8
WDCD7	9.47	579	1.29	7.17	126	5.6
WDCD8	23.9	297	4.45	4.06	3390	1.5
WDCD9	0.73	35	0.16	6.3	42	3.2

Table 6 - Rock chip assay results for Cedar Peak in the Summer Camp Hills. A negative number indicates that the sample was below detection level.

SampleID	Au_ppm	Ag_ppm	Al_%	As_ppm	B_ppm	Ba_ppm	Be_ppm	Bi_ppm	Ca_%	Cd_ppm	Ce_ppm	Co_ppm	Cr_ppm	Cs_ppm	Cu_ppm
CPKCD1	0.005	0.05	0.13	21.1	-10	320	0.07	0.05	4.85	0.06	2.75	1.8	15	0.08	12.6
CPKCD2	0.01	0.05	0.22	20	-10	530	0.15	0.06	10.05	0.85	7.66	3.3	9	0.19	11.2
CPKCD3	0.006	0.06	0.43	11.8	-10	1060	0.25	0.07	0.49	0.09	6.22	3	8	0.3	7.6
CPKCD4	0.008	0.08	0.25	11.8	-10	100	0.19	0.06	0.38	0.06	7.66	2.5	14	0.17	15.1
CPKCD5	-0.005	0.02	0.28	11.5	-10	300	0.27	0.05	5.91	0.06	15.65	2.7	8	0.2	5.1
CPKCD6	-0.005	0.05	0.45	38.9	-10	1800	0.91	0.06	0.26	0.27	8.95	2.7	12	0.35	18.5
CPKCD7	-0.005	0.04	0.11	3.2	-10	2640	0.17	0.01	6.3	0.1	3.17	1.3	6	0.14	3.4
CPKCD8	0.005	0.03	0.2	19.4	-10	1540	0.38	0.03	5.49	0.15	10.75	2.1	7	0.2	6.4
CPKCD9	-0.005	0.05	0.2	12.2	-10	1420	0.31	0.04	9.29	0.09	10.45	2.7	6	0.2	5
CPKCD10	-0.005	0.04	0.17	29	-10	110	0.4	0.02	12.6	0.13	3.17	2.3	3	0.32	5.1
CPKCD11	-0.005	0.05	0.74	17	10	1010	0.4	0.04	14.3	0.28	14.1	12.3	29	1.05	50.8
CPKCD12	0.013	0.19	0.25	66.2	-10	1880	0.43	0.02	0.55	0.24	6.44	2.3	17	0.44	10.9
CPKCD13	-0.005	0.06	0.27	12.5	-10	2730	0.1	0.03	0.13	0.07	2.47	1.4	14	0.16	12
CPKCD14	0.006	0.02	0.15	10.4	-10	520	0.11	0.03	3.79	0.13	3.33	2.1	8	0.19	5.1
HS-SM-031	-0.005	0.08	0.16	4.8	-10	310	0.2	0.05	0.31	0.16	4.59	1.6	14	0.15	11.9
HS-SM-034	-0.005	0.02	0.03	-2	-10	20	0.09	0.01	25	0.03	1.92	0.6	1	-0.05	1.6
HS-SM-035	-0.005	0.01	0.64	-2	-10	90	0.33	0.05	25	0.17	14.15	2.4	5	0.84	4.8
HS-SM-042	0.005	-0.01	0.05	3	-10	300	0.08	-0.01	25	0.11	4.41	0.8	1	0.07	1.6
HS-SM-044	-0.005	-0.01	0.02	2	-10	20	-0.05	-0.01	25	0.05	2.07	0.7	-1	-0.05	0.9
HS-SM-046	0.007	0.07	0.22	18	-10	80	0.27	0.09	0.64	0.1	9.32	4.5	9	0.2	16.1

SampleID	Fe_%	Ga_ppm	Ge_ppm	Hf_ppm	Hg_ppm	In_ppm	K_%	La_ppm	Li_ppm	Mg_%	Mn_ppm	Mo_ppm	Na_%	Nb_ppm	Ni_ppm
CPKCD1	0.96	0.49	-0.1	0.03	0.06	0.007	0.06	1.7	0.5	0.06	92	0.61	0.01	0.09	9.3
CPKCD2	0.87	0.98	-0.1	0.06	0.1	0.01	0.09	3.6	1.6	0.78	246	0.82	0.01	0.22	13.3
CPKCD3	1.19	1.56	-0.1	0.13	0.11	0.007	0.11	3.6	3.3	0.07	205	1.02	0.01	0.18	13.8
CPKCD4	1.03	1.21	0.05	0.05	0.11	0.008	0.13	4.8	1	0.03	92	2.5	-0.01	0.09	16.9
CPKCD5	0.8	1.11	0.05	0.06	0.06	0.007	0.14	7	2.4	3.26	162	5	0.01	0.15	11.2
CPKCD6	3.28	1.66	0.07	0.13	0.49	0.012	0.1	6.2	3.7	0.07	124	66.5	0.01	0.19	38
CPKCD7	0.39	0.52	-0.1	0.03	0.2	-0.005	0.04	1.6	1.2	3.66	143	0.83	0.03	0.16	7.1
CPKCD8	0.97	0.97	0.1	0.03	0.36	0.006	0.09	5.8	1.8	2.13	149	4.09	0.02	0.21	15.1
CPKCD9	0.78	1.14	-0.1	0.04	0.11	0.007	0.09	4.5	1.5	4.3	177	5.12	0.03	0.27	10.7
CPKCD10	0.7	0.78	-0.1	0.02	0.47	-0.005	0.06	1.5	1	7.19	305	6.32	0.02	0.24	14.3
CPKCD11	5.7	2.18	0.14	0.06	0.06	0.032	0.21	5.9	6	0.26	1100	1.61	0.02	0.21	46
CPKCD12	3.99	0.84	0.08	0.06	0.08	0.005	0.08	6	0.8	0.05	360	3.57	0.01	0.2	26.1
CPKCD13	0.66	0.76	-0.1	0.04	0.02	0.009	0.08	0.9	1.4	0.04	53	0.58	0.01	0.05	8.1
CPKCD14	0.62	0.65	-0.1	0.03	0.44	0.005	0.07	1.4	1.6	0.59	144	2.67	0.01	0.14	10.2
HS-SM-031	1.1	0.56	-0.1	0.03	0.04	0.007	0.08	2.1	1	0.03	90	0.79	-0.01	0.06	15.1
HS-SM-034	0.07	0.08	-0.1	-0.02	0.01	-0.005	0.02	1.1	0.3	0.21	20	0.79	-0.01	-0.05	1.4
HS-SM-035	0.49	1.69	0.05	0.09	0.02	0.009	0.13	6.8	5.9	0.23	128	1.62	0.02	0.71	1.5
HS-SM-042	0.06	0.17	0.09	0.02	0.05	-0.005	0.02	2.2	1.2	0.74	50	0.29	0.03	0.18	0.3
HS-SM-044	0.06	0.11	0.11	-0.02	0.02	-0.005	0.01	0.9	0.3	0.17	25	0.31	0.02	0.16	4.1
HS-SM-046	1.2	1.15	-0.1	0.07	0.09	0.007	0.09	5.7	1.4	0.04	177	1.57	-0.01	0.09	21.2

SampleID	P_ppm	Pb_ppm	Rb_ppm	Re_ppm	S_%	Sb_ppm	Sc_ppm	Se_ppm	Sn_ppm	Sr_ppm	Ta_ppm	Te_ppm	Th_ppm	Ti_%	Tl_ppm
CPKCD1	500	6.5	1.9	-0.001	-0.01	1.96	1.1	0.4	-0.2	21.8	-0.01	0.03	0.6	-0.005	0.02
CPKCD2	1070	7.2	3.3	-0.001	0.03	2.63	1.9	0.5	0.2	50.9	-0.01	0.06	1	-0.005	0.04
CPKCD3	440	5.5	5.2	-0.001	0.02	1.45	2.6	0.2	0.2	11.5	-0.01	0.03	1.2	0.006	0.08
CPKCD4	650	7.7	4.4	-0.001	-0.01	2.2	2	0.5	-0.2	22.7	-0.01	0.03	1.3	-0.005	0.04
CPKCD5	460	4.3	4.8	0.001	0.01	0.7	2.6	0.8	-0.2	39.1	-0.01	0.01	1.6	-0.005	0.08
CPKCD6	750	30.7	4.9	-0.001	0.06	9.01	1.8	0.9	0.2	20.7	-0.01	0.05	1.2	0.006	0.35
CPKCD7	650	5.9	1.8	0.001	0.08	1.11	1.2	0.3	-0.2	32.9	-0.01	0.01	0.4	-0.005	0.03
CPKCD8	520	10.8	3.3	-0.001	0.04	2.83	1.4	17.2	-0.2	35.9	-0.01	0.02	1	-0.005	0.05
CPKCD9	320	5.7	3.7	-0.001	0.04	2.47	1.6	0.4	-0.2	49.8	-0.01	0.01	1.1	-0.005	0.06
CPKCD10	220	6.5	2.9	0.004	-0.01	4.34	0.8	0.6	-0.2	23.1	-0.01	0.02	0.5	-0.005	0.07
CPKCD11	900	3.8	8.9	0.001	0.03	0.81	8.5	1.2	0.2	440	0.01	0.1	1.1	0.005	0.32
CPKCD12	2050	5.3	3.7	-0.001	0.04	2.8	1.9	0.4	-0.2	26.4	-0.01	0.04	0.8	0.005	0.15
CPKCD13	310	4.4	4.1	-0.001	0.06	0.66	1.2	0.5	-0.2	77.3	-0.01	0.02	1.3	-0.005	0.02
CPKCD14	120	8.2	2.9	-0.001	0.04	1.5	1.3	0.2	-0.2	25.1	-0.01	0.02	0.6	-0.005	0.07
HS-SM-031	520	5.3	4	0.001	0.02	0.65	1.4	0.5	-0.2	22.2	-0.01	0.02	1.9	-0.005	0.02
HS-SM-034	30	1.1	0.7	0.001	0.02	0.14	0.3	0.8	-0.2	226	-0.01	-0.01	0.2	-0.005	-0.02
HS-SM-035	200	3.9	9	0.001	0.02	0.48	1.4	0.3	0.3	153	-0.01	0.01	1.6	0.018	0.06
HS-SM-042	110	1.2	0.8	-0.001	0.04	0.32	0.5	0.3	-0.2	343	-0.01	0.01	0.2	-0.005	-0.02
HS-SM-044	30	0.3	0.4	0.001	0.01	0.16	0.3	0.2	-0.2	218	-0.01	0.01	-0.2	-0.005	-0.02
HS-SM-046	680	7.4	3.8	-0.001	-0.01	2.19	1.9	0.7	0.2	8.7	-0.01	0.06	1.5	-0.005	0.09

SampleID	U_ppm	V_ppm	W_ppm	Y_ppm	Zn_ppm	Zr_ppm
CPKCD1	0.2	13	0.63	4.23	23	1.4
CPKCD2	0.91	16	0.7	7.64	89	2.6
CPKCD3	0.39	13	0.53	3.45	15	5.9
CPKCD4	0.34	19	0.34	4.86	17	2.1
CPKCD5	0.67	9	0.34	3.91	6	2.8
CPKCD6	1.35	34	0.68	13.8	103	5.3
CPKCD7	0.33	4	3.35	1.44	16	1.9
CPKCD8	1.12	10	6.83	2.01	70	1.9
CPKCD9	0.71	7	4.14	2.79	10	2.1
CPKCD10	1.44	10	11.3	1.95	54	1.1
CPKCD11	0.63	123	0.93	17.5	128	2
CPKCD12	3.8	40	0.85	9.72	87	1.9
CPKCD13	0.35	17	0.27	3.19	21	1.3
CPKCD14	0.54	6	0.41	.98	33	1.5
HS-SM-031	0.39	14	0.15	5.41	68	1.2
HS-SM-034	0.54	1	-0.1	0.7	2	-0.5
HS-SM-035	0.76	9	0.18	5.07	18	5.1
HS-SM-042	0.64	2	0.21	2.27	15	1.2
HS-SM-044	0.29	2	-0.1	0.63	2	-0.5
HS-SM-046	0.3	15	0.6	5.12	16	3.2

Table 7 - Method and detection limits for the geochemical analysis of soil samples collected at Spruce Mountain. Samples were analyzed by ALS Minerals using trace-level acid digest with elements quantified by Inductively Coupled Plasma (ICP) with Mass Spectroscopy (MS). Gold was extracted through acid digest and quantified with ICP-MS. Super trace and ore grade methods were used, and their ranges provide the low and high levels of detection.

Analytes	Method	Unit	Range	Analytes	Method	Unit	Range
Au	ICPMS	ppm	0.0001-100	Mo	ICPMS	ppm	0.01-10,000
Ag	ICPMS	ppm	0.01-100	Na	ICPMS	percent	0.001-10
Al	ICPMS	percent	0.01-25	Nb	ICPMS	ppm	0.002-500
As	ICPMS	ppm	0.1-10,000	Ni	ICPMS	ppm	0.04-10,000
B	ICPMS	ppm	10-10,000	P	ICPMS	percent	0.001-1
Ba	ICPMS	ppm	10-10,000	Pb	ICPMS	ppm	0.005-10,000
Be	ICPMS	ppm	0.05-1,000	Rb	ICPMS	ppm	0.005-1000
Bi	ICPMS	ppm	0.001-10,000	Re	ICPMS	ppm	0.001-50
Ca	ICPMS	percent	0.01-25	S	ICPMS	percent	0.01-10
Cd	ICPMS	ppm	0.001-1,000	Sb	ICPMS	ppm	0.005-10,000
Ce	ICPMS	ppm	0.003-500	Sc	ICPMS	ppm	0.005-10,001
Co	ICPMS	ppm	0.001-10,000	Se	ICPMS	ppm	0.1-1,000
Cr	ICPMS	ppm	0.001-10,000	Sn	ICPMS	ppm	0.01-500
Cs	ICPMS	ppm	0.005-500	Sr	ICPMS	ppm	0.01-10,000
Cu	ICPMS	ppm	0.01-10,000	Ta	ICPMS	ppm	0.005-500
Fe	ICPMS	percent	0.001-50	Te	ICPMS	ppm	0.01-500
Ga	ICPMS	ppm	0.004-10,000	Th	ICPMS	ppm	0.002-10,000
Ge	ICPMS	ppm	0.005-500	Ti	ICPMS	percent	0.001-10
Hf	ICPMS	ppm	0.002-500	Tl	ICPMS	ppm	0.002-10,000
Hg	ICPMS	ppm	0.004-10,000	U	ICPMS	ppm	0.005-10,000
In	ICPMS	ppm	0.005-500	V	ICPMS	ppm	0.1-10,000
K	ICPMS	percent	0.01-10	W	ICPMS	ppm	0.001-10,000
La	ICPMS	ppm	0.002-10,000	Y	ICPMS	ppm	0.003-500
Li	ICPMS	ppm	0.1-10,000	Zn	ICPMS	ppm	0.1-10,000
Mg	ICPMS	percent	0.01-25	Zr	ICPMS	ppm	0.01-500
Mn	ICPMS	ppm	0.1-50,000				

Table 8 – Geochemical analysis results for soil samples collected at Spruce Mountain. Highlighted rows indicate that the sample was within 200 feet of an ammonium-illite sample. A negative number indicates that the sample was below detection level.

Sample_ID	Au_ppb	Au_ppm	Ag_ppm	Al_%	As_ppm	B_ppm	Ba_ppm	Be_ppm	Bi_ppm	Ca_%	Cd_ppm	Ce_ppm	Cr_ppm	Cs_ppm	Cu_ppm
CSES4-001	15.7	0.0157	0.115	1.66	195.5	20	134.5	0.69	0.17	8.63	0.99	27.6	15.9	2.23	18.05
CSES4-002	2.8	0.0028	0.07	1.69	35.6	10	151.5	1.01	0.2	1.32	0.56	41.9	14.9	2.86	17.9
CSES4-003	2.7	0.0027	0.085	1.73	26.5	10	161	0.99	0.22	1.6	0.8	41.3	16.3	2.87	20
CSES4-004	4.6	0.0046	0.07	1.69	13.75	20	166.5	0.87	0.17	4.19	0.77	33.3	14.3	2.99	17.5
CSES4-005	1.5	0.0015	0.062	1.68	12.4	10	159.5	0.88	0.2	1	0.5	34.1	15.9	3.11	14.95
CSES4-006	2.3	0.0023	0.046	1.94	14.55	10	173	1.01	0.21	0.73	0.44	34.4	19.6	3.29	14
CSES4-007	1.4	0.0014	0.092	1.6	11.35	20	164	0.89	0.16	8.59	0.46	27.6	15.5	2.63	14.65
CSES4-008	0.6	0.0006	0.071	2.04	15	10	182.5	1	0.22	1.49	0.53	33.3	20.6	3.42	16.5
CSES4-009	2.1	0.0021	0.104	0.91	13	10	99.3	0.55	0.09	13.9	0.43	14.6	11	1.66	11.4
CSES4-010	0.6	0.0006	0.06	1.47	15.95	20	158	0.79	0.16	8.77	0.4	22.3	14.8	2.54	13.35
CSES4-011A	2.5	0.0025	0.052	1.26	27.1	10	116.5	0.67	0.13	6.09	0.42	19.7	14.9	2.09	11.95
CSES4-011B	2.6	0.0026	0.087	1.72	34.6	10	172	0.83	0.19	7.28	0.75	27.1	17.8	2.73	17.4
CSES4-012	1.1	0.0011	0.096	2.46	19.05	10	311	1.22	0.34	1.46	0.76	42.3	23.1	4.11	18.35
CSES4-013	1.6	0.0016	0.091	2.05	16.95	20	215	1.08	0.2	5.8	0.57	35.7	17.9	3.37	16.7
CSES6-001	19.5	0.0195	0.071	1.63	25.7	20	144	0.86	0.16	5.35	0.49	31.6	18.9	2.77	23.3
CSES6-002	2.1	0.0021	0.077	1.89	13.95	10	195.5	0.84	0.19	1.49	0.57	39.7	18.3	3.07	21.2
CSES6-003	1.7	0.0017	0.086	1.79	14	20	202	0.77	0.19	2.99	0.63	32	20.1	6.08	20.2
CSES6-004	1.5	0.0015	0.067	2.2	10.55	20	225	0.83	0.2	2.44	0.82	38.7	20.1	3.4	20.9
CSES6-005	1.6	0.0016	0.085	2.12	10.55	20	201	0.82	0.19	4.7	0.88	36.1	19.2	3.33	20.2
CSES6-006	3.6	0.0036	0.071	1.78	9.49	20	167.5	0.65	0.16	8.16	0.54	29.8	15.2	2.65	15.5
CSES6-007	3.4	0.0034	0.086	1.79	12.75	20	197	0.74	0.17	6.96	0.6	31.6	16	3.14	21.8
CSES6-008	1.1	0.0011	0.067	2.12	13.7	20	225	0.79	0.18	5.63	0.4	34.6	19.3	3.72	19.1
CSES6-009	1.3	0.0013	0.06	1.97	14.8	20	196.5	0.76	0.19	1.06	0.34	36.8	18.6	3.66	19.15
CSES6-010	0.7	0.0007	0.057	1.98	12.35	10	183.5	0.78	0.19	0.67	0.54	37.9	19.8	3.28	17.05
CSES6-011	0.9	0.0009	0.055	1.91	11.1	10	194	0.73	0.16	2.28	0.49	33.8	15.9	3.17	15.9
CSES6-012	1.3	0.0013	0.063	1.68	11.5	20	173.5	0.67	0.15	6.24	0.43	27.5	14.7	2.61	15.8
CSES6-013	2	0.002	0.071	1.82	11.35	10	172.5	0.77	0.17	6.39	0.42	31.4	16	2.68	16.7
CSES6-014A	2.5	0.0025	0.079	1.75	11.25	10	158	0.71	0.16	5.82	0.42	31	15.4	2.47	15.25

Sample_ID	Au_ppb	Au_ppm	Ag_ppm	Al_%	As_ppm	B_ppm	Ba_ppm	Be_ppm	Bi_ppm	Ca_%	Cd_ppm	Ce_ppm	Cr_ppm	Cs_ppm	Cu_ppm
CSES6-014B	1.2	0.0012	0.051	2.07	10.5	10	178	0.76	0.19	2.58	0.42	36.4	17.8	3.08	14.3
CSES6-015	2.9	0.0029	0.118	1.66	14	10	151	0.76	0.15	11.05	0.4	28.5	14.6	2.44	16.1
CSES6-016	3.2	0.0032	0.077	1.57	14	20	142	0.65	0.14	10.4	0.35	26.3	13.3	2.33	15.6
CSES6-017	2.4	0.0024	0.093	1.39	11	20	138	0.58	0.13	13.6	0.4	23.9	12	1.75	15.35
CSES6-018	3.2	0.0032	0.107	1.93	11.8	10	191.5	0.79	0.15	8.78	0.47	33.5	14.2	2.84	15.1
CSES6-019	2.6	0.0026	0.071	1.46	13	20	142	0.62	0.14	11	0.43	29.1	12.6	2.1	14.7
CSES6-020	10.1	0.0101	0.091	1.46	22	20	130	0.58	0.13	11.9	0.39	24.1	12.3	2.01	15.25
CSES6-021	7.9	0.0079	0.181	1.89	28.8	10	182.5	0.76	0.17	7.92	0.51	31.3	15.3	2.64	17.85
CSES6-022	7.3	0.0073	0.205	1.97	23.8	20	184	0.85	0.17	7.49	0.51	32.1	15.8	2.69	19.15
CSES6-023	28.9	0.0289	0.166	1.95	26.4	20	192.5	0.8	0.18	8.87	0.49	34	16.4	2.44	20.2
CSES6-024	6.1	0.0061	0.194	2.08	18.65	20	196.5	0.82	0.2	8.44	0.55	30.7	17.3	2.77	20
CSES6-025	2.1	0.0021	0.145	2.44	21	20	241	0.96	0.22	3.67	0.6	43.9	20	3.45	24.4
CSES6-026	2.3	0.0023	0.082	1.76	14.2	10	171	0.67	0.18	3.11	0.54	33.9	15.9	2.52	15.35
CSES6-027	2	0.002	0.074	1.77	12.9	10	179	0.7	0.17	3.67	0.55	34.1	15.1	2.6	17.25
CSES6-028	2.9	0.0029	0.074	1.76	14.65	10	175	0.67	0.17	2.38	0.56	33.4	16.3	2.45	15.65
CSES8-001	2.4	0.0024	0.105	1.96	13.9	10	194.5	1.02	0.24	2.25	0.55	37.3	20.8	2.75	19.95
CSES8-002	1.6	0.0016	0.1	2.06	12.85	10	174	1.13	0.24	0.51	0.53	39.7	21.1	2.62	18.75
CSES8-003	1.5	0.0015	0.101	1.62	12.25	10	135	1.02	0.27	0.29	0.49	43.6	19.5	2.88	18.6
CSES8-004	4.3	0.0043	0.174	2.29	15.95	10	181	1.38	0.25	0.61	0.6	38.5	25.1	3.2	22.7
CSES8-005	0.5	0.0005	0.114	1.2	15.95	10	112.5	0.72	0.17	1.48	0.79	27.8	21.4	1.9	15
CSES8-006	2.5	0.0025	0.11	1.68	14.2	20	176	0.88	0.19	3.53	0.64	32.3	21.1	3.88	18.25
CSES8-007	9.9	0.0099	0.122	1.25	14.55	20	131	0.69	0.15	8.95	0.58	24.6	17.8	4.13	15.95
CSES8-008	19.8	0.0198	0.097	1.48	21.3	20	153.5	0.86	0.16	6.26	0.64	26.3	19.1	3.71	17.5
CSES8-009	13.1	0.0131	0.071	0.82	38.5	10	85.2	0.54	0.1	8.95	0.59	17.6	14.3	1.83	13.35
CSES8-010	2.9	0.0029	0.08	2.05	17.55	20	180	1.03	0.21	4.36	0.74	31.1	22	4.87	20.2
CSES8-011	2.4	0.0024	0.065	1.82	17.6	10	147.5	1.1	0.21	1.1	1.54	34.1	26.7	3.73	16.3
CSES8-012	1	0.001	0.051	1.7	10.05	10	142.5	0.86	0.18	1.49	0.81	30.3	19	3.11	12.85
CSES8-013	0.4	0.0004	0.071	2.18	9.7	10	217	1.11	0.21	0.98	1.29	35.7	21.1	3.87	16.4
CSES8-014A	2	0.002	0.097	2.32	10.3	10	234	1.15	0.22	1	1.41	41.4	20.3	4.03	17.8

Sample_ID	Au_ppb	Au_ppm	Ag_ppm	Al_%	As_ppm	B_ppm	Ba_ppm	Be_ppm	Bi_ppm	Ca_%	Cd_ppm	Ce_ppm	Cr_ppm	Cs_ppm	Cu_ppm
CSES8-014B	1.2	0.0012	0.081	2.33	10.05	20	220	1.08	0.22	1.49	0.95	37.9	22	3.92	17.85
CSES8-015	5.7	0.0057	0.126	2.04	10.9	10	212	0.94	0.2	3.76	1.07	36.2	16.9	3.53	16.75
CSES8-016	3.7	0.0037	0.106	2.11	11.15	10	211	0.98	0.2	0.71	0.85	36.2	18.7	3.33	15.05
CSES8-017	5.8	0.0058	0.103	1.87	11	10	192	0.91	0.18	3.85	0.7	33.9	16.2	3.05	15.6
CSES8-018	3.5	0.0035	0.104	1.84	12.3	10	174.5	0.94	0.19	3.2	0.75	33.7	16.2	2.87	16.5
CSES8-019	2.3	0.0023	0.11	2.11	11.4	10	196.5	1.16	0.22	2.04	0.84	38.6	18.8	3.24	17.6
CSES8-020	3.9	0.0039	0.129	2.06	10.6	20	192	0.94	0.2	3.73	0.71	32.4	17.7	2.91	16.45
CSES8-021	5.4	0.0054	0.091	1.51	11.8	10	142	0.73	0.14	9.55	0.44	23.8	12.7	2.2	13.7
CSES8-022	1.7	0.0017	0.117	2.12	11.75	10	202	1.03	0.21	2.28	0.64	38.8	19.3	2.99	17.45
CSES8-023	-0.2	-0.0002	0.063	1.74	17.25	10	142	0.91	0.2	1.06	0.46	32.8	17.7	2.57	13.55
CSES8-024	2	0.002	0.073	1.48	19.45	10	123	0.81	0.15	7.33	0.47	24.6	13.9	2.34	12.7
CSES8-025	0.9	0.0009	0.058	1.67	16.6	10	125.5	0.7	0.18	6.29	0.46	28.2	14.7	2.41	13.8
CSES8-026	1.2	0.0012	0.054	1.36	16.65	10	122	0.65	0.14	7.6	0.5	27.3	12.5	2.36	12.3
CSES8-027	2.5	0.0025	0.039	0.71	19	-10	73.5	0.38	0.07	11.9	0.33	16.9	7.1	1.12	7.38
CSES8-028	4.5	0.0045	0.102	1.67	21.6	10	138.5	0.76	0.19	6.47	0.54	28.6	14	2.68	16.15
CSES8-029	3.6	0.0036	0.096	1.62	17.4	10	149	0.84	0.18	8.02	0.49	27.7	13.9	2.67	16.25
CSES8-030	31.4	0.0314	0.098	1.47	28.4	10	167.5	0.59	0.13	8.46	0.44	26.9	12.8	2.14	14.6
CSES8-031	3.8	0.0038	0.074	1.96	13.45	20	185.5	0.77	0.19	4.61	0.44	33	15.5	2.73	18.2
CSES8-032	3.9	0.0039	0.088	2.12	12.65	20	195.5	0.81	0.2	5.48	0.5	34.8	16.4	3.18	19.1
MMES3-001	5.4	0.0054	0.118	1.77	12.75	10	192	1	0.19	5.24	0.35	33	14.1	2.62	15.9
MMES3-002	10.8	0.0108	0.093	1.85	26.6	10	152	1.14	0.21	0.56	0.55	46.5	20.4	2.59	16.35
MMES3-003	8.7	0.0087	0.124	2.15	38.2	20	176	1.09	0.21	3.23	0.85	36.2	18.5	3.56	21.9
MMES3-004	4.6	0.0046	0.056	1.38	13.3	10	134.5	0.68	0.14	5.06	0.56	26.8	13.8	2.39	14.8
MMES3-005	2.2	0.0022	0.06	1.49	14.3	10	129	0.71	0.17	1.41	0.46	28.2	15	2.5	15.65
MMES3-006	2.4	0.0024	0.073	1.65	14.05	20	167	0.84	0.19	2.91	0.48	34	15.5	2.91	15.4
MMES3-007	1.5	0.0015	0.084	1.82	12	20	179.5	0.82	0.18	4.68	0.46	33.4	15.8	3.19	15.95
MMES3-008	0.8	0.0008	0.089	1.63	12.2	20	179	0.78	0.17	7.1	0.47	29.2	13.4	3.06	15.75
MMES3-009	2.5	0.0025	0.11	1.05	14	10	206	0.62	0.1	10.35	0.43	19.9	10.6	1.81	12.3
MMES3-010	1.5	0.0015	0.07	1.07	15	10	133.5	0.6	0.11	12.7	0.31	20.3	11	1.68	12.75

Sample_ID	Au_ppb	Au_ppm	Ag_ppm	Al_%	As_ppm	B_ppm	Ba_ppm	Be_ppm	Bi_ppm	Ca_%	Cd_ppm	Ce_ppm	Cr_ppm	Cs_ppm	Cu_ppm
MMES3-011	0.0054	0.052	1.14	42	20	231	0.63	0.13	10.45	0.49	18.25	13.3	2.33	14.45	
MMES3-012A	1.6	0.0016	0.096	1.88	20.8	10	267	0.92	0.26	1.95	0.57	36.6	17.7	2.99	16.8
MMES3-012B	1.2	0.0012	0.084	1.6	19	20	335	0.84	0.17	5.4	0.6	31.6	13.7	2.55	14.45
MMES3-013	3.7	0.0037	0.09	1.33	19	10	168.5	0.7	0.15	10.9	0.54	24.2	13.6	2.09	13.45
MMES3-014	10.7	0.0107	0.099	1.57	27.7	20	149.5	0.86	0.2	4	0.57	32.8	14.4	2.09	15.4
MMES3-015	3.3	0.0033	0.103	1.84	23.6	10	165.5	0.98	0.24	1.65	0.54	40	18.3	2.44	15.75
MMES3-016	4.3	0.0043	0.067	1.82	19.35	10	155	1.08	0.23	0.71	0.62	43.9	18.4	2.43	15.9
MMES3-017	29.4	0.0294	0.136	1.68	32.7	10	185.5	0.9	0.2	4.71	0.47	32.6	14.9	2.25	16.35
MMES3-018	30.6	0.0306	0.106	1.63	36.2	20	207	0.83	0.18	8.65	0.42	27.3	14.1	2.19	15.2
MMES3-019	16.1	0.0161	0.155	1.94	31.4	20	227	0.95	0.21	4.88	0.58	38.1	16.6	2.77	19.8
MMES3-020	24.5	0.0245	0.097	1.42	68.2	10	115	0.83	0.15	2.57	0.55	34.5	14	1.52	13.85
MMES3-021	15.7	0.0157	0.05	1.54	37.6	10	139.5	0.73	0.17	4.29	0.48	31.5	14	1.7	14.3
MMES3-022	8.7	0.0087	0.093	1.85	30.1	10	179.5	0.95	0.22	1.5	0.62	42.2	16.6	2.2	16.65
MMES3-023	7.9	0.0079	0.107	1.71	31.5	10	176.5	0.93	0.2	2.11	0.57	39.1	15.7	2.27	16.85
MMES4-014	3.7	0.0037	0.088	1.35	17.3	20	156	0.75	0.16	8.53	0.48	28.1	11.5	1.95	14
MMES4-015	4.4	0.0044	0.113	1.5	21.8	10	144.5	0.91	0.17	4.89	0.4	31.6	13.3	2.08	14.2
MMES4-016	74.3	0.0743	0.099	1.57	33.9	10	147	0.82	0.19	2.35	0.48	36.5	14.2	2.07	14.3
MMES4-017	33.6	0.0336	0.155	1.64	43	10	131.5	0.91	0.22	1.6	0.6	42.6	18.4	2.06	15
MMES4-018	26.4	0.0264	0.092	1.9	41.6	10	182.5	1.03	0.24	1.17	0.78	46.9	18.7	2.53	15.15
MMES4-019	7.7	0.0077	0.077	1.83	34.9	20	177.5	0.93	0.23	2.91	0.52	37.3	15.9	2.41	14.55
MMES4-020	23.2	0.0232	0.082	1.81	46.9	20	191	0.9	0.21	2.67	0.63	40.5	15.9	2.41	15.4
MMES4-021	24.3	0.0243	0.074	1.65	41.9	20	161.5	0.79	0.16	6.5	0.48	32.8	13.1	2.16	14.25
MMES4-022	7.8	0.0078	0.076	1.95	25.8	10	199.5	1.1	0.25	2.06	0.46	47.7	16.4	2.9	18.15
MMES4-023	2.6	0.0026	0.078	1.73	24.2	10	194	0.94	0.24	0.88	0.54	42.7	15.8	2.43	15.8
MMES5-001	1.4	0.0014	0.051	1.86	16.85	10	180.5	0.98	0.23	1.18	0.47	34.8	20.5	3.18	16.6
MMES5-002	10.5	0.0105	0.068	1.82	15.85	10	174.5	0.97	0.2	3.12	0.59	32.6	19.2	3.17	19.05
MMES5-003	1	0.001	0.125	1.18	20.3	10	111.5	0.68	0.17	1.7	0.81	30.3	23	2.04	17.2
MMES5-004	0.7	0.0007	0.061	1.91	10.05	20	193.5	0.82	0.19	2.53	1.02	32.9	17.6	3.36	18.8
MMES5-005	1.3	0.0013	0.076	2.04	11.45	20	206	0.94	0.21	4.31	0.89	32.9	18.2	3.66	17.85

Sample_ID	Au_ppb	Au_ppm	Ag_ppm	Al_%	As_ppm	B_ppm	Ba_ppm	Be_ppm	Bi_ppm	Ca_%	Cd_ppm	Ce_ppm	Cr_ppm	Cs_ppm	Cu_ppm
MMES5-006	1.2	0.0012	0.048	1.95	9.04	10	192	0.89	0.2	1.62	0.5	34.8	18.6	3.36	17.45
MMES5-007	0.4	0.0004	0.035	2.02	8.62	20	191.5	0.95	0.22	1.59	0.43	37.5	19.5	3.69	16.85
MMES5-008A	1.8	0.0018	0.054	1.12	9.29	10	122.5	0.64	0.14	9.96	0.39	21.2	12	2.11	12.45
MMES5-008B	1.2	0.0012	0.084	1.81	12.7	20	193.5	0.87	0.2	2.78	0.49	31.2	18.5	3.38	17.05
MMES5-009	2.1	0.0021	0.074	2.05	14.55	20	211	0.96	0.22	3.07	0.38	34.5	19.7	4.16	19.4
MMES5-010	1.7	0.0017	0.04	1.6	19.2	10	128.5	0.84	0.18	1.2	0.34	29.9	18.5	2.65	13.45
MMES5-011	1.6	0.0016	0.043	1.83	17.25	10	183.5	0.95	0.21	1.62	0.44	33.6	18.6	3.12	16.05
MMES5-012	1	0.001	0.057	1.59	12.75	20	203	0.75	0.16	6.64	0.37	25.2	14.2	2.55	13.75
MMES5-013	1.7	0.0017	0.1	1.31	11.9	10	150.5	0.78	0.14	9.54	0.37	25	12.7	2.03	15.45
MMES5-014	2.3	0.0023	0.102	1.22	12.45	10	120.5	0.7	0.13	9.97	0.4	22.1	12.8	1.9	13.35
MMES5-015	2.9	0.0029	0.099	1.55	13.2	10	132	0.77	0.17	7.77	0.5	24.5	15.3	2.3	14.85
MMES5-016	0.6	0.0006	0.094	2.03	13.25	20	180	0.94	0.21	5.36	0.67	32.9	18.6	3.19	16.4
MMES5-017	2.2	0.0022	0.084	1.5	11	20	151	0.75	0.14	10.4	0.64	25.2	12.4	2.48	15.5
MMES5-018	2.2	0.0022	0.12	1.94	14.75	10	187	0.93	0.18	7.18	0.66	30.9	17.2	3.29	16.75
MMES5-019	0.9	0.0009	0.086	1.59	12.65	20	155	0.85	0.17	7.99	0.51	31.5	12.9	2.77	15.4
MMES5-020	6.6	0.0066	0.096	1.49	22.6	10	125.5	0.8	0.14	7.91	0.46	29.9	13.1	2.22	13.9
MMES5-021	3.4	0.0034	0.096	2.11	36.6	20	185	1.04	0.23	3.02	0.58	36.6	17.6	3.51	18.85
MMES5-022	5.7	0.0057	0.103	2.04	47.2	20	182	0.99	0.2	5.83	0.68	33.5	16.2	3.07	17.9
MMES5-023	9.9	0.0099	0.112	1.62	33	10	143.5	0.84	0.16	9.21	0.54	31.1	13.3	2.34	15.65
MMES5-024	7.8	0.0078	0.094	2.04	53.3	20	163	1.1	0.2	5.76	0.53	37.2	17	3.15	19.55
MMES5-025	5	0.005	0.109	1.96	40.6	20	205	1.05	0.21	4.42	0.63	40.5	16.3	3.27	18.3
MMES5-026	8.6	0.0086	0.111	2	38.2	20	423	1.05	0.2	5.51	0.57	36.3	16.2	3.1	17.95
MMES5-027	11.6	0.0116	0.124	1.71	39.3	20	168.5	0.83	0.18	6.84	0.53	33.5	14.7	2.69	18.2
MMES5-028	3.3	0.0033	0.087	1.95	23.2	10	211	0.91	0.24	1.68	0.48	40.3	16.1	3.01	16.6
MMES7-001	14.9	0.0149	0.172	2.08	18.3	10	169	1.25	0.23	0.54	0.47	49.1	24.9	2.77	19.55
MMES7-002	2.4	0.0024	0.103	2.04	12.7	10	163.5	1.19	0.27	0.38	0.43	35.6	23.4	2.8	17.9
MMES7-003	10.1	0.0101	0.093	2.07	13.6	10	181	1.21	0.24	0.42	0.52	37	22.7	3.03	20.9
MMES7-004	17.2	0.0172	0.322	2.35	14.85	10	183	1.48	0.27	0.54	0.48	37.3	25	3.27	22.4

Sample_ID	Au_ppb	Au_ppm	Ag_ppm	Al_%	As_ppm	B_ppm	Ba_ppm	Be_ppm	Bi_ppm	Ca_%	Cd_ppm	Ce_ppm	Cr_ppm	Cs_ppm	Cu_ppm
MMES7-005	3	0.003	0.126	1.27	16.15	10	106	0.8	0.17	2.08	0.83	30	22.4	2.05	15.35
MMES7-006	9.1	0.0091	0.103	1.73	24.6	10	195	1.04	0.2	2.53	0.76	31.2	24	4.19	20.5
MMES7-007	52.7	0.0527	0.254	1.55	25.5	10	317	0.94	0.17	5.42	0.67	27.4	20.1	3.88	19.5
MMES7-008	36.4	0.0364	0.228	1.6	30	10	411	0.97	0.18	3.89	0.71	29.4	21.1	4.41	19.4
MMES7-009	2.1	0.0021	0.059	2.1	17.95	20	290	1.17	0.24	1	0.8	39.4	23.5	3.9	18.45
MMES7-010	3.7	0.0037	0.095	1.73	19.9	20	234	0.86	0.18	5.05	0.78	30.3	18.4	3.36	18.7
MMES7-011	7.7	0.0077	0.069	1.34	11.2	10	155	0.77	0.16	2.15	0.97	22.8	16.3	2.79	13.15
MMES7-012	2.7	0.0027	0.159	1.91	16.2	10	384	1.04	0.19	3.55	1.17	30.3	19.2	3.58	17.4
MMES7-013	6.6	0.0066	0.214	2.23	19.15	10	292	1.26	0.23	1.88	1.3	36.3	23.1	4.3	19.75
MMES7-014	6	0.006	0.124	2.13	13.7	10	212	1.08	0.25	0.88	1.18	35.5	21	3.82	17.05
MMES7-015	4.1	0.0041	0.086	2.01	10.65	10	196.5	1.08	0.21	0.64	1.02	36.9	19.8	3.6	16.05
MMES7-016	18.9	0.0189	0.132	1.94	15.3	10	158.5	1.03	0.2	2.43	0.79	31	20.5	2.82	16.35
MMES7-017	4.8	0.0048	0.125	2.06	12.85	10	185	1.2	0.24	1.72	0.71	38.1	20.7	3.28	18.6
MMES7-018	6.2	0.0062	0.107	2.16	13.9	10	197.5	1.25	0.23	0.8	0.59	39.9	23.8	3.3	16.9
MMES7-019	4.9	0.0049	0.128	2.06	12.65	10	203	1.26	0.23	0.97	0.7	40.4	21.8	3.02	17.4
MMES7-020	3	0.003	0.078	1.86	13.1	10	176.5	1.02	0.23	0.59	0.62	37.8	19.1	2.77	15.35
MMES7-021	5.2	0.0052	0.085	1.77	12	10	173	0.93	0.19	4.54	0.59	30.9	16	2.74	16.65
MMES7-022	2.5	0.0025	0.088	1.78	12.8	10	159.5	0.91	0.2	3.85	0.53	29.6	17	2.53	16.15
MMES7-023	2.4	0.0024	0.087	1.86	10.95	10	194	0.95	0.19	4.73	0.51	32.3	16.6	2.88	17.25
MMES7-024	0.9	0.0009	0.067	1.76	15.25	10	155.5	0.85	0.22	2.1	0.58	32.4	17.2	2.5	14.2
MMES7-025	0.5	0.0005	0.061	1.28	17.9	10	98.1	0.71	0.16	5.06	0.46	25.5	14	1.97	12.4
MMES7-026	1	0.001	0.052	1.48	17.65	20	125.5	0.7	0.17	5.22	0.41	28.8	15.2	2.33	13.1
MMES7-027	1.7	0.0017	0.056	1.34	21.5	10	108.5	0.67	0.15	5.36	0.47	24	13.1	2.04	12.35
MMES7-028	2.1	0.0021	0.084	1.66	19.05	10	140.5	0.72	0.17	5.39	0.49	26.6	15.3	2.62	15.45
MMES7-029	2.1	0.0021	0.069	1.62	17.85	20	141.5	0.8	0.17	6.77	0.46	27.3	14.4	2.72	15.25
MMES7-030	1.9	0.0019	0.099	1.51	16.45	10	155.5	0.78	0.17	7.67	0.43	27.6	13.1	2.54	14.3
MMES7-031	2	0.002	0.094	1.92	14.65	20	187	0.92	0.2	6.33	0.55	33	15.5	3.16	17.5
MMES7-032	1.3	0.0013	0.098	1.84	13.85	20	175.5	0.87	0.18	6.24	0.56	31.3	15.4	2.84	16.5

Sample_ID	Au_ppb	Au_ppm	Ag_ppm	Al_%	As_ppm	B_ppm	Ba_ppm	Be_ppm	Bi_ppm	Ca_%	Cd_ppm	Ce_ppm	Cr_ppm	Cs_ppm	Cu_ppm
SSES1-001	2	0.002	0.056	1.88	8.73	10	291	0.97	0.27	1.15	0.36	47.4	12.4	1.45	13.05
SSES1-002	2.3	0.0023	0.065	1.99	7.05	10	312	1.09	0.23	2.63	0.3	44.2	13.4	1.86	13
SSES1-003	1.3	0.0013	0.065	1.83	6.1	20	434	1.13	0.23	4.46	0.35	47.6	11	1.9	11.85
SSES1-004	1	0.001	0.061	1.72	7.91	20	177.5	1	0.2	3.05	0.43	38.8	14.2	1.66	12.75
SSES1-005	1.6	0.0016	0.065	1.9	8.01	10	218	1.03	0.25	1.09	0.49	44.7	15.4	2.27	15.3
SSES1-006	1.6	0.0016	0.074	1.71	17.2	10	299	0.93	0.23	1.03	0.5	38.1	16	2.86	17.55
SSES1-007	1.9	0.0019	0.05	1.35	14.05	10	163.5	0.61	0.16	2.89	0.53	24.1	14.8	2.3	11.3
SSES1-008	9.6	0.0096	0.057	1.14	26.2	10	112	0.54	0.15	6.75	0.54	15.8	11.9	1.85	13.3
SSES1-009	2.2	0.0022	0.076	1.32	20.1	10	139	0.62	0.16	1.77	0.67	28.8	15.6	2.06	14.9
SSES1-010	2.7	0.0027	0.06	1.17	15.5	10	114	0.62	0.14	5.53	0.43	21.2	11.1	1.87	11.8
SSES1-011	1	0.001	0.089	1.68	22.9	10	180	0.84	0.19	5.55	0.51	31.4	15	2.71	14.45
SSES1-012	25.2	0.0252	0.161	1.73	58.4	10	524	0.78	0.22	1.17	0.67	35.6	17.9	2.99	15.5
SSES1-013	305	0.305	0.481	1.77	216	10	208	0.81	0.22	0.95	0.8	41.8	17	2.91	20.6
SSES1-014A	8.4	0.0084	0.096	1.04	47.9	-10	114	0.67	0.18	0.27	0.66	30.2	11.9	1.61	16.45
SSES1-014B	93.7	0.0937	0.246	1.37	122	-10	109.5	0.85	0.16	0.42	0.57	36.1	13.9	1.76	16.2
SSES1-015	9.2	0.0092	0.084	1.2	44.4	-10	141.5	0.64	0.18	0.28	0.55	32.5	12.2	1.92	15.6
SSES1-016	13.3	0.0133	0.113	1	67.2	-10	121.5	0.61	0.18	0.72	0.63	31.8	10.9	1.86	16.65
SSES1-017	15.7	0.0157	0.113	1.52	41.2	10	161.5	0.81	0.24	0.45	0.62	40.9	14.6	2.37	19.65
SSES1-018	2.5	0.0025	0.112	1.77	17.35	10	181.5	0.97	0.22	0.98	0.58	42.2	16.6	3.04	19.65
SSES1-019	1.1	0.0011	0.11	1.8	13.2	10	194.5	1	0.26	0.86	0.56	40.8	17.2	3.1	20.6
SSES1-020	0.9	0.0009	0.083	1.9	12.2	10	192.5	0.98	0.21	2.14	0.55	36.4	17.2	3.34	19.85
SSES1-021	1.1	0.0011	0.095	1.97	10.4	10	214	0.96	0.25	0.96	0.54	42.5	18	3.34	19.75
SSES1-022	0.4	0.0004	0.077	2.06	10.55	20	220	1.02	0.24	1.09	0.5	42.6	17.6	3.51	20.4
SSES2-001	1.1	0.0011	0.057	1.83	8.01	10	314	1.15	0.19	3.59	0.39	46.8	10.5	1.47	12
SSES2-002	1	0.001	0.066	1.87	9.65	10	213	1.06	0.25	0.91	0.41	47.1	14.5	2.25	15.3
SSES2-003	1	0.001	0.071	1.94	8.57	10	258	1.02	0.27	1.02	0.39	45.2	14.4	2.24	15.65
SSES2-004	0.2	0.0002	0.069	1.87	9.71	10	235	1.11	0.21	1.05	0.44	48.1	15	2.34	16.35
SSES2-005	1	0.001	0.077	1.78	23.5	10	257	1.03	0.23	0.72	0.6	49.5	14.7	2.44	19.75

Sample_ID	Au_ppb	Au_ppm	Ag_ppm	Al_%	As_ppm	B_ppm	Ba_ppm	Be_ppm	Bi_ppm	Ca_%	Cd_ppm	Ce_ppm	Cr_ppm	Cs_ppm	Cu_ppm
SSES2-006	2.1	0.0021	0.071	1.76	22.3	10	690	0.93	0.19	2.5	0.51	34.1	16.1	2.8	15
SSES2-007	22.1	0.0221	0.099	1.55	20.3	10	203	0.76	0.18	3.35	0.63	27.5	14.8	2.69	15.45
SSES2-008	1.5	0.0015	0.056	1.38	13.4	20	139	0.74	0.19	4.42	0.56	22.4	13	2.39	12.35
SSES2-009	1.9	0.0019	0.048	0.77	11.55	10	73.3	0.41	0.12	2.77	0.44	13.95	8.5	1.47	9.26
SSES2-010	1	0.001	0.075	1.59	17.55	10	176.5	0.79	0.18	4.8	0.51	28.3	14	2.98	15.2
SSES2-011	1.8	0.0018	0.073	1.63	19.05	10	171	0.87	0.2	4.18	0.62	28.6	15.6	3.11	16.2
SSES2-012	1.4	0.0014	0.059	1.67	21.6	10	163.5	0.85	0.19	3.86	0.4	34.1	14.5	2.91	14.5
SSES2-013	23.2	0.0232	0.116	1.61	67.9	20	169	0.84	0.19	3.48	0.49	34.1	14.9	2.94	14.9
SSES2-014A	139	0.139	0.524	1.84	136	10	197	0.9	0.23	1.12	0.85	41.2	17.2	3.14	18.3
SSES2-014B	385	0.385	0.46	1.71	311	10	185.5	0.87	0.2	0.9	0.88	42.9	16.7	2.92	19.45
SSES2-015	101	0.101	0.257	1.17	175	10	119.5	0.7	0.16	0.44	0.9	37.7	12.7	1.94	21.4
SSES2-016	20.8	0.0208	0.104	1.22	98.7	-10	125	0.65	0.15	0.31	0.6	32.2	12.2	1.63	13.95
SSES2-017	8.4	0.0084	0.099	1.38	47.5	10	137	0.74	0.21	0.36	0.48	34.2	14.2	2.09	16
SSES2-018	13.7	0.0137	0.126	1.61	59.7	10	155.5	0.91	0.19	1.04	0.58	39.9	15.1	2.51	18.35
SSES2-019	2.5	0.0025	0.142	1.75	17.3	10	191	0.93	0.26	2.98	0.52	35.1	15	2.98	19.3
SSES2-020	0.6	0.0006	0.081	1.78	12.35	10	198.5	1	0.23	1.11	0.55	39.5	16.6	3.06	19.05
SSES2-021	0.2	0.0002	0.046	1.8	11.4	20	188	0.88	0.22	1.15	0.48	40.2	17	3.19	17.65
SSES2-022	0.9	0.0009	0.106	2	11.1	20	207	1.11	0.26	1.41	0.5	40.3	17.1	3.51	21

Sample_ID	Fe_%	Ga_ppm	Ge_ppm	Hg_ppm	Hf_ppm	In_ppm	K_%	La_ppm	Li_ppm	Mg_%	Mn_ppm	Mo_ppm	Na_%	Nb_ppm	Ni_ppm
CSES4-001	1.54	4.15	0.07	0.06	0.08	0.027	0.42	13.1	12.6	0.46	562	1.15	0.01	1.14	15.2
CSES4-002	1.78	5.09	0.08	0.04	0.16	0.03	0.38	20.9	14.8	0.44	419	1.07	0.02	1.14	17.3
CSES4-003	1.73	5.41	0.07	0.02	0.09	0.024	0.49	20.8	17.3	0.52	457	1.12	0.02	1.14	18.3
CSES4-004	1.5	5.12	0.09	0.04	0.14	0.03	0.41	15.4	22.1	0.58	447	0.99	0.03	1.24	13.8
CSES4-005	1.61	5.4	0.09	0.03	0.17	0.026	0.36	16.3	20	0.56	429	0.83	0.02	1.3	13.7
CSES4-006	1.81	5.5	0.09	0.03	0.24	0.026	0.4	18.8	21.3	0.49	495	0.69	0.02	1.43	15
CSES4-007	1.42	4.32	0.07	0.03	0.14	0.02	0.43	14.1	16.5	0.6	341	0.73	0.03	1.31	13.4
CSES4-008	1.92	5.73	0.1	0.03	0.25	0.029	0.45	15.9	20.5	0.61	448	0.95	0.02	1.48	15.2
CSES4-009	0.83	2.45	0.05	0.04	0.08	0.016	0.22	7.2	9.3	0.44	224	0.51	0.02	0.69	9.4
CSES4-010	1.31	3.9	0.07	0.05	0.09	0.02	0.37	11.6	15.1	0.52	357	1.01	0.02	1.12	11.7
CSES4-011A	1.24	3.45	0.05	0.1	0.1	0.016	0.33	9.4	11.7	0.35	307	1.28	0.02	0.86	13.5
CSES4-011B	1.75	4.72	0.06	0.06	0.1	0.024	0.41	13.3	15.7	0.47	435	1.05	0.03	1.17	23
CSES4-012	2.12	6.73	0.11	0.03	0.26	0.033	0.51	21.7	23.8	0.61	680	0.99	0.03	1.39	16.9
CSES4-013	1.7	5.7	0.08	0.02	0.13	0.028	0.51	16.8	19.4	0.6	442	0.84	0.03	1.59	15.5
CSES6-001	1.77	4.3	0.07	0.14	0.09	0.028	0.39	16.1	15.2	0.46	378	2.22	0.02	0.96	29.5
CSES6-002	1.93	5.1	0.08	0.02	0.12	0.03	0.5	19.5	18.7	0.57	525	1.23	0.02	1.24	20.7
CSES6-003	1.85	4.89	0.09	0.03	0.09	0.026	0.48	15.3	21	0.76	433	1.39	0.02	1.27	25.3
CSES6-004	2	5.69	0.09	0.03	0.13	0.027	0.41	18.1	25.7	0.75	529	1.18	0.03	1.53	16.4
CSES6-005	1.91	5.56	0.1	0.04	0.1	0.028	0.52	17.9	25.2	0.87	556	1.01	0.03	1.35	15.4
CSES6-006	1.58	4.36	0.08	0.03	0.1	0.025	0.42	14.1	20.6	0.82	470	0.76	0.04	1.31	11.9
CSES6-007	1.63	4.8	0.08	0.07	0.07	0.026	0.49	15.3	22.2	0.76	490	1.24	0.03	1.39	14.8
CSES6-008	1.93	5.36	0.07	0.02	0.09	0.027	0.5	16.7	25.5	0.98	446	0.97	0.03	1.33	16.1
CSES6-009	1.96	5.17	0.09	0.04	0.12	0.027	0.48	16.3	21.3	0.67	496	0.92	0.02	1.57	15.5
CSES6-010	1.87	5.36	0.08	0.02	0.2	0.026	0.4	17.3	20.3	0.49	534	0.79	0.01	1.34	13.5
CSES6-011	1.72	4.98	0.09	0.02	0.08	0.024	0.44	16.5	19.2	0.6	461	0.64	0.02	1.21	12.4
CSES6-012	1.49	4.27	0.08	0.02	0.1	0.019	0.43	13.5	15.5	0.6	346	0.59	0.02	1.15	11.8
CSES6-013	1.62	4.73	0.07	0.03	0.08	0.025	0.43	15.6	16.4	0.6	367	0.63	0.02	1.32	12.9
CSES6-014A	1.55	4.33	0.06	0.04	0.1	0.021	0.38	14.7	14.6	0.56	346	0.6	0.02	1.17	11.9

Sample_ID	Fe_%	Ga_ppm	Ge_ppm	Hg_ppm	Hf_ppm	In_ppm	K_%	La_ppm	Li_ppm	Mg_%	Mn_ppm	Mo_ppm	Na_%	Nb_ppm	Ni_ppm
CSES6-014B	1.85	5.21	0.09	0.01	0.11	0.026	0.47	17.7	17.5	0.55	468	0.6	0.02	1.25	12.1
CSES6-015	1.46	4.38	0.06	0.04	0.1	0.02	0.35	13.4	15.5	0.56	287	0.59	0.02	1.24	12.4
CSES6-016	1.35	4.1	0.06	0.04	0.07	0.017	0.37	12.6	13.9	0.5	306	0.56	0.02	1.07	11.9
CSES6-017	1.19	3.47	-0.05	0.02	0.07	0.02	0.35	11.5	12.4	0.48	253	0.55	0.02	1.05	10.9
CSES6-018	1.54	4.68	0.07	0.03	0.12	0.021	0.4	15.3	18.9	0.57	372	0.65	0.02	1.5	11.8
CSES6-019	1.29	3.67	0.06	0.03	0.05	0.021	0.38	13.3	14.2	0.5	277	0.59	0.02	1.22	11.9
CSES6-020	1.23	3.68	0.06	0.05	0.1	0.019	0.33	11.8	13.2	0.46	258	0.64	0.02	0.98	10.8
CSES6-021	1.6	4.69	0.06	0.04	0.09	0.026	0.45	15	16	0.55	409	0.76	0.02	1.32	12.6
CSES6-022	1.67	5.01	0.07	0.02	0.09	0.027	0.45	15.4	17.6	0.61	395	0.7	0.02	1.43	13.1
CSES6-023	1.67	4.94	0.07	0.05	0.07	0.029	0.42	16	18	0.64	328	0.73	0.02	1.58	13.8
CSES6-024	1.76	5.13	0.07	0.03	0.08	0.028	0.43	16.2	18.9	0.63	362	0.68	0.02	1.41	13.6
CSES6-025	2.16	6.19	0.1	0.02	0.09	0.033	0.64	21.8	22.2	0.75	558	0.87	0.02	1.54	15.5
CSES6-026	1.68	4.5	0.07	0.01	0.09	0.023	0.46	16.3	15.3	0.52	505	0.68	0.02	1.19	12.5
CSES6-027	1.65	4.51	0.07	0.02	0.08	0.029	0.46	16.6	16.3	0.53	480	0.71	0.02	1.27	12.7
CSES6-028	1.72	4.5	0.06	0.01	0.12	0.026	0.43	16.3	14.8	0.52	516	0.71	0.02	1.23	12.4
CSES8-001	2.01	5.87	0.13	0.02	0.12	0.03	0.49	18.3	19.2	0.55	430	1.61	0.02	1.48	23.4
CSES8-002	2.1	6.02	0.13	0.03	0.19	0.028	0.58	20.1	20.1	0.46	487	1.57	0.01	1.49	22.1
CSES8-003	1.97	5.38	0.14	0.02	0.23	0.027	0.37	24.6	16.7	0.38	537	1.76	0.04	1.39	21.7
CSES8-004	2.3	6.58	0.13	0.06	0.21	0.033	0.53	21.8	21.6	0.43	550	2.27	0.01	1.55	29.5
CSES8-005	1.52	3.43	0.09	0.02	0.11	0.023	0.34	15.2	10.9	0.33	468	1.98	0.01	0.94	24.2
CSES8-006	1.84	4.94	0.11	0.02	0.14	0.025	0.47	16.4	17.9	0.75	419	1.7	0.02	1.19	27.1
CSES8-007	1.39	3.6	0.11	0.1	0.07	0.016	0.31	12.1	12.7	0.7	275	1.64	0.02	0.96	30.6
CSES8-008	1.6	4.15	0.1	0.07	0.09	0.021	0.43	13.3	15.7	0.73	306	2.11	0.02	1.06	27.7
CSES8-009	1.1	2.33	0.09	0.69	0.04	0.015	0.23	8.8	8.9	0.58	229	3.28	0.01	0.5	25.3
CSES8-010	1.91	5.9	0.13	0.05	0.11	0.029	0.53	15.3	23.8	0.85	492	1.6	0.03	1.37	25.1
CSES8-011	1.74	5.38	0.11	0.06	0.16	0.028	0.45	17	17.7	0.59	500	1.11	0.01	1.27	23.5
CSES8-012	1.55	4.71	0.1	0.03	0.15	0.022	0.42	14.2	15.5	0.49	431	0.78	0.01	1.27	14.1
CSES8-013	1.94	6.25	0.13	0.03	0.24	0.026	0.47	17.6	21.8	0.63	610	0.88	0.02	1.41	16.3

Sample_ID	Fe_%	Ga_ppm	Ge_ppm	Hg_ppm	Hf_ppm	In_ppm	K_%	La_ppm	Li_ppm	Mg_%	Mn_ppm	Mo_ppm	Na_%	Nb_ppm	Ni_ppm
CSES8-014A	2.05	6.83	0.14	0.03	0.16	0.031	0.47	19.6	22.9	0.65	651	0.9	0.02	1.43	17.3
CSES8-014B	2.04	6.54	0.13	0.03	0.13	0.029	0.52	18.6	21.3	0.7	489	0.93	0.02	1.36	19.2
CSES8-015	1.8	5.98	0.12	0.04	0.14	0.029	0.45	17.7	22.1	0.68	505	0.94	0.02	1.4	16.8
CSES8-016	1.89	6.12	0.11	0.03	0.18	0.026	0.4	17.1	20.2	0.54	510	0.89	0.01	1.14	16.1
CSES8-017	1.64	5.6	0.12	0.03	0.13	0.025	0.39	16.1	18.4	0.59	390	1.02	0.02	1.33	16.3
CSES8-018	1.72	5.41	0.12	0.03	0.12	0.026	0.49	15.8	16.4	0.54	424	1.04	0.02	1.47	18.1
CSES8-019	1.97	6.28	0.12	0.03	0.18	0.029	0.47	19.3	19.4	0.61	468	1	0.02	1.61	19.2
CSES8-020	1.81	5.68	0.12	0.03	0.14	0.026	0.44	15.9	17.2	0.6	407	0.91	0.02	1.44	17.1
CSES8-021	1.3	4.28	0.1	0.04	0.09	0.019	0.35	11.3	13.8	0.51	276	0.68	0.02	1.06	14.3
CSES8-022	2	6.07	0.11	0.01	0.13	0.028	0.53	19.9	19.1	0.6	459	0.92	0.02	1.47	18.4
CSES8-023	1.77	4.93	0.1	0.02	0.17	0.026	0.47	15.8	14.9	0.49	394	1.37	0.01	1.38	18.4
CSES8-024	1.37	3.96	0.09	0.06	0.08	0.019	0.41	11.7	11.7	0.45	255	0.98	0.01	1.03	17.2
CSES8-025	1.52	4.43	0.1	0.03	0.1	0.022	0.41	12.9	12.8	0.47	304	0.78	0.01	1.09	15.4
CSES8-026	1.26	3.84	0.09	0.04	0.09	0.017	0.36	14.2	11.9	0.44	270	0.66	0.01	0.91	13.7
CSES8-027	0.64	2.12	0.09	0.04	0.08	0.011	0.16	9.4	6.7	0.24	138	0.51	0.02	0.49	8.7
CSES8-028	1.41	5	0.12	0.05	0.1	0.02	0.39	16	15.8	0.48	291	0.69	0.02	1.13	14.7
CSES8-029	1.38	4.99	0.12	0.04	0.1	0.027	0.36	15.7	16.7	0.51	296	0.7	0.03	1.32	15.5
CSES8-030	1.34	3.67	0.06	0.04	0.09	0.022	0.35	13.7	13.7	0.52	322	0.59	0.02	0.93	12.3
CSES8-031	1.79	4.97	0.06	0.03	0.11	0.027	0.53	15.3	18.4	0.64	421	0.63	0.02	1.41	13.2
CSES8-032	1.84	5.4	0.08	0.03	0.09	0.03	0.5	17.3	20.5	0.68	403	0.65	0.03	1.43	14.3
MMES3-001	1.52	5.14	0.07	0.05	0.14	0.025	0.35	16.7	18.9	0.48	310	0.74	0.03	1.6	15.7
MMES3-002	1.87	6.04	0.08	0.05	0.41	0.026	0.36	25	20.3	0.4	457	2.69	0.02	0.88	24
MMES3-003	1.88	6.35	0.08	0.06	0.13	0.031	0.5	19.7	19.6	0.6	395	1.13	0.03	1.29	19.7
MMES3-004	1.32	4	0.08	0.05	0.09	0.019	0.33	13.3	15.8	0.7	340	0.92	0.03	1.07	14.3
MMES3-005	1.45	4.37	0.07	0.05	0.12	0.024	0.3	12.8	15.4	0.43	365	1.11	0.02	1.15	15.8
MMES3-006	1.59	4.93	0.08	0.05	0.12	0.024	0.39	14.8	19	0.6	410	1.02	0.03	1.29	15
MMES3-007	1.61	5.44	0.08	0.04	0.14	0.025	0.4	16.2	21.2	0.68	356	0.92	0.03	1.41	14.3
MMES3-008	1.42	4.94	0.1	0.03	0.15	0.023	0.38	14.5	20.4	0.67	347	0.92	0.03	1.29	13.7

Sample_ID	Fe_%	Ga_ppm	Ge_ppm	Hg_ppm	Hf_ppm	In_ppm	K_%	La_ppm	Li_ppm	Mg_%	Mn_ppm	Mo_ppm	Na_%	Nb_ppm	Ni_ppm
MMES3-009	0.98	3	0.05	0.07	0.08	0.013	0.22	9.3	11	0.41	255	0.73	0.03	0.83	10.9
MMES3-010	0.95	3.18	0.07	0.07	0.12	0.019	0.22	9.1	11.8	0.62	211	0.89	0.03	1.02	11
MMES3-011	1.12	3.26	0.11	0.07	0.1	0.016	0.3	8.7	12.3	0.37	300	1.85	0.02	0.66	13.6
MMES3-012A	1.83	5.87	0.16	0.04	0.17	0.029	0.44	17.1	20.5	0.53	556	1.1	0.02	1.38	15.6
MMES3-012B	1.47	4.89	0.14	0.02	0.12	0.024	0.44	15.7	17.6	0.52	438	0.98	0.03	1.28	14.7
MMES3-013	1.21	3.83	0.13	0.04	0.1	0.021	0.28	12.4	13.8	0.45	278	0.78	0.03	0.98	11.6
MMES3-014	1.54	4.53	0.13	0.05	0.09	0.024	0.4	16.1	14.4	0.44	375	0.91	0.02	1.21	14.6
MMES3-015	1.79	5.24	0.14	0.03	0.16	0.03	0.41	21.8	18.8	0.46	463	0.86	0.02	1.04	15.7
MMES3-016	1.83	5.74	0.15	0.02	0.17	0.03	0.42	21.9	19.9	0.45	502	0.88	0.02	0.94	17.1
MMES3-017	1.5	4.79	0.13	0.04	0.1	0.02	0.38	17.8	17.5	0.46	360	0.84	0.02	1.07	14.7
MMES3-018	1.41	4.42	0.12	0.04	0.12	0.021	0.36	13.7	16.1	0.51	301	0.81	0.02	1.14	13.6
MMES3-019	1.79	5.89	0.16	0.04	0.11	0.032	0.51	19.3	21	0.63	398	0.86	0.03	1.38	16.5
MMES3-020	1.43	3.94	0.14	0.06	0.13	0.022	0.34	17.6	13.3	0.33	316	1.56	0.02	0.92	16.3
MMES3-021	1.45	4.3	0.13	0.05	0.11	0.02	0.35	16.1	14.4	0.4	326	0.94	0.02	1.04	15
MMES3-022	1.8	5.43	0.15	0.02	0.18	0.03	0.41	21.8	18.7	0.49	488	0.88	0.02	1.21	15.6
MMES3-023	1.61	5.09	0.15	0.03	0.13	0.027	0.42	19.3	17.8	0.46	460	0.83	0.02	1.24	15.4
MMES4-014	1.25	3.84	0.14	0.03	0.13	0.017	0.4	14.1	13.5	0.43	319	0.79	0.03	1.01	13.8
MMES4-015	1.41	4.43	0.15	0.04	0.1	0.026	0.35	15.5	14.4	0.4	280	0.71	0.02	1.07	14.2
MMES4-016	1.52	4.72	0.15	0.03	0.13	0.026	0.37	18	15.2	0.4	344	0.66	0.02	1.07	15.8
MMES4-017	1.68	5.15	0.17	0.04	0.16	0.026	0.32	26.2	17.3	0.38	499	0.83	0.01	1.12	16.5
MMES4-018	1.81	5.96	0.16	0.04	0.22	0.028	0.4	22.7	21.6	0.49	532	1.08	0.02	1.32	17.8
MMES4-019	1.71	5.22	0.14	0.03	0.12	0.023	0.42	16.3	18.4	0.5	420	0.9	0.02	1.36	14.8
MMES4-020	1.71	5.52	0.15	0.04	0.12	0.027	0.53	20.4	19.4	0.51	412	1.1	0.05	1.39	15.8
MMES4-021	1.47	4.79	0.13	0.04	0.11	0.028	0.37	15.4	17.3	0.48	337	0.86	0.03	1.28	14.2
MMES4-022	1.87	6.43	0.16	0.02	0.21	0.035	0.46	20.3	22.2	0.58	425	0.81	0.03	1.58	16.5
MMES4-023	1.77	5.32	0.16	0.02	0.15	0.028	0.45	20	18.4	0.52	547	0.83	0.02	1.24	14.5
MMES5-001	1.82	5.81	0.09	0.04	0.22	0.03	0.44	17.4	18.5	0.53	436	1.31	0.02	1.48	22
MMES5-002	1.7	5.48	0.08	0.04	0.12	0.026	0.48	17.3	18.2	0.57	413	1.45	0.02	1.34	24.5

Sample_ID	Fe_%	Ga_ppm	Ge_ppm	Hg_ppm	Hf_ppm	In_ppm	K_%	La_ppm	Li_ppm	Mg_%	Mn_ppm	Mo_ppm	Na_%	Nb_ppm	Ni_ppm
MMES5-003	1.44	3.67	0.06	0.02	0.11	0.019	0.34	17.2	11.2	0.35	464	1.85	0.01	1.08	27.9
MMES5-004	1.65	5.59	0.08	0.03	0.14	0.027	0.53	17.3	22.7	0.63	567	0.81	0.03	1.44	15
MMES5-005	1.74	6.01	0.09	0.03	0.14	0.03	0.48	17.8	26.4	0.83	513	1.01	0.03	1.52	16.2
MMES5-006	1.77	5.93	0.09	0.03	0.18	0.029	0.49	16.9	24.5	0.6	560	0.79	0.03	1.4	15.6
MMES5-007	1.81	6.39	0.1	0.03	0.2	0.031	0.49	18.2	25.9	0.66	533	0.77	0.03	1.73	15
MMES5-008A	1.01	3.37	0.06	0.07	0.08	0.017	0.22	10.1	13.3	0.67	249	0.73	0.02	1.27	11.5
MMES5-008B	1.65	5.48	0.09	0.03	0.14	0.024	0.42	15.1	21.4	0.79	447	0.95	0.03	1.53	15.4
MMES5-009	1.81	6.4	0.08	0.05	0.16	0.031	0.51	17.6	25.5	0.89	432	1.07	0.03	1.67	17.8
MMES5-010	1.48	5.08	0.09	0.06	0.17	0.024	0.31	14.6	15.9	0.5	373	0.71	0.02	1.3	16
MMES5-011	1.63	5.73	0.08	0.05	0.22	0.03	0.4	17.3	19.1	0.48	416	0.81	0.02	1.83	15.3
MMES5-012	1.32	4.47	0.07	0.04	0.14	0.019	0.38	12.7	16.1	0.62	318	0.61	0.03	1.34	12.3
MMES5-013	1.12	4.02	0.06	0.05	0.12	0.02	0.31	11.8	13.3	0.51	244	0.56	0.02	1.21	12.5
MMES5-014	1.06	3.63	0.05	0.05	0.11	0.017	0.25	10.8	11.4	0.43	244	0.59	0.02	1.02	12.4
MMES5-015	1.34	4.53	0.05	0.05	0.12	0.024	0.31	13.3	14.5	0.46	276	0.65	0.02	1.21	13.9
MMES5-016	1.69	5.93	0.08	0.04	0.13	0.027	0.47	17.3	19.5	0.57	443	0.78	0.03	1.63	16.1
MMES5-017	1.17	4.51	0.06	0.04	0.17	0.021	0.37	12.5	14.8	0.48	296	0.69	0.03	1.21	12.5
MMES5-018	1.59	5.69	0.08	0.03	0.14	0.027	0.39	16.3	19.3	0.56	398	0.83	0.03	1.45	15.1
MMES5-019	1.33	4.66	0.06	0.04	0.17	0.021	0.34	14.8	17.2	0.53	343	0.73	0.03	1.36	13
MMES5-020	1.25	4.28	0.05	0.03	0.12	0.019	0.27	14.8	13.8	0.43	274	0.74	0.03	1.2	12.7
MMES5-021	1.79	6.38	0.09	0.04	0.13	0.031	0.47	18.7	22	0.63	454	0.97	0.03	1.5	16.7
MMES5-022	1.67	5.81	0.09	0.04	0.12	0.024	0.49	16.1	19.1	0.59	415	0.82	0.03	1.48	15.8
MMES5-023	1.29	4.74	0.06	0.05	0.13	0.021	0.29	14.5	15.7	0.46	271	0.89	0.03	1.2	14
MMES5-024	1.68	6.03	0.09	0.12	0.15	0.031	0.46	19.4	19.4	0.58	327	1.11	0.03	1.46	16.9
MMES5-025	1.67	5.71	0.09	0.03	0.11	0.028	0.42	20.8	22.1	0.6	406	1.02	0.03	1.36	15.3
MMES5-026	1.65	5.72	0.09	0.04	0.11	0.025	0.43	18	21.2	0.62	367	1	0.03	1.3	15.9
MMES5-027	1.43	5.07	0.07	0.07	0.13	0.024	0.38	16.9	17.3	0.53	295	1.04	0.03	1.26	14.5
MMES5-028	1.8	5.75	0.1	0.01	0.25	0.031	0.45	18.5	21.4	0.62	458	0.86	0.03	1.45	14.5
MMES7-001	2.03	6.12	0.1	0.02	0.2	0.028	0.51	22.1	22.7	0.48	409	1.38	0.01	1.36	26.2

Sample_ID	Fe_%	Ga_ppm	Ge_ppm	Hg_ppm	Hf_ppm	In_ppm	K_%	La_ppm	Li_ppm	Mg_%	Mn_ppm	Mo_ppm	Na_%	Nb_ppm	Ni_ppm
MMES7-002	2.01	6.27	0.09	0.01	0.26	0.031	0.46	20.7	22.6	0.41	428	1.2	0.02	1.36	21.3
MMES7-003	2.03	6.29	0.11	0.01	0.23	0.031	0.46	21.4	23.5	0.39	521	1.44	0.02	1.48	22.5
MMES7-004	2.1	6.61	0.1	0.06	0.27	0.033	0.51	23.1	23.1	0.44	479	1.39	0.02	1.44	26
MMES7-005	1.42	3.83	0.07	0.03	0.13	0.024	0.32	17.3	13.3	0.34	426	1.91	0.01	1.03	26
MMES7-006	1.81	5.08	0.1	0.04	0.11	0.032	0.49	17.7	19.6	0.72	449	2.25	0.03	1.27	31.8
MMES7-007	1.58	4.49	0.08	0.09	0.08	0.032	0.42	15	17	0.66	330	2.89	0.03	1.13	28.3
MMES7-008	1.6	4.72	0.08	0.07	0.1	0.028	0.41	14.7	16.7	0.57	330	1.85	0.03	1.13	30.6
MMES7-009	2.01	5.91	0.09	0.03	0.33	0.032	0.56	18.5	24.9	0.65	571	1.15	0.03	1.32	21.8
MMES7-010	1.67	4.8	0.07	0.03	0.13	0.03	0.5	15.4	20.3	0.63	507	1.13	0.03	1.41	21.2
MMES7-011	1.23	3.78	0.06	0.04	0.12	0.024	0.34	11	13.9	0.38	344	0.73	0.02	1.19	12.5
MMES7-012	1.65	5.43	0.08	0.03	0.15	0.033	0.41	15.6	18.5	0.57	525	0.83	0.02	1.41	17.9
MMES7-013	1.88	6.6	0.11	0.05	0.19	0.033	0.46	19.8	23.6	0.55	683	1.14	0.02	1.7	19.7
MMES7-014	1.82	6.26	0.1	0.02	0.23	0.028	0.4	19.2	22.3	0.57	554	0.8	0.02	1.67	17.1
MMES7-015	1.77	6.03	0.1	0.02	0.2	0.026	0.39	17.8	20.8	0.55	543	0.75	0.02	1.24	16.8
MMES7-016	1.68	5.29	0.08	0.05	0.14	0.028	0.48	15.5	17	0.49	412	0.79	0.02	1.46	18.8
MMES7-017	1.83	6.32	0.08	0.02	0.17	0.034	0.47	18.9	19.8	0.58	454	0.8	0.03	1.63	20.1
MMES7-018	1.95	6.36	0.08	0.01	0.26	0.029	0.39	22.8	22.1	0.54	497	0.84	0.02	1.26	20.6
MMES7-019	1.91	6.01	0.11	0.03	0.23	0.031	0.44	22.9	20	0.54	491	0.8	0.02	1.51	20.1
MMES7-020	1.75	5.67	0.07	0.02	0.25	0.026	0.45	20.8	17.7	0.44	504	0.94	0.02	1.51	19.4
MMES7-021	1.55	5.42	0.06	0.03	0.13	0.026	0.41	15	16.5	0.55	385	0.83	0.02	1.48	17.2
MMES7-022	1.58	5.35	0.06	0.03	0.14	0.026	0.4	14.4	16.1	0.56	335	0.99	0.02	1.5	17.8
MMES7-023	1.63	5.71	0.08	0.02	0.13	0.025	0.44	15.5	18.5	0.56	373	0.83	0.02	1.56	17
MMES7-024	1.6	5	0.08	0.01	0.11	0.022	0.48	15.8	15.9	0.51	393	0.95	0.02	1.39	16.5
MMES7-025	1.32	3.66	0.05	0.02	0.11	0.016	0.33	13.7	10.3	0.37	239	0.67	0.01	0.97	14.7
MMES7-026	1.4	4.26	0.06	0.03	0.1	0.024	0.41	14.8	13	0.46	293	0.88	0.02	1.22	15.9
MMES7-027	1.25	3.83	0.06	0.03	0.14	0.02	0.34	12.3	10.8	0.38	220	0.65	0.01	0.95	14.1
MMES7-028	1.44	4.83	0.06	0.02	0.1	0.022	0.41	13.7	14.8	0.52	284	0.74	0.02	1.22	15
MMES7-029	1.4	4.8	0.06	0.04	0.1	0.022	0.41	14.3	15.8	0.55	287	0.76	0.02	1.22	14.9

Sample_ID	Fe_%	Ga_ppm	Ge_ppm	Hg_ppm	Hf_ppm	In_ppm	K_%	La_ppm	Li_ppm	Mg_%	Mn_ppm	Mo_ppm	Na_%	Nb_ppm	Ni_ppm
MMES7-030	1.32	4.59	0.07	0.03	0.12	0.022	0.4	14.1	15.7	0.53	310	0.61	0.02	1.45	13.7
MMES7-031	1.6	5.64	0.08	0.03	0.14	0.024	0.48	17.1	20.3	0.63	379	0.74	0.02	1.48	15.2
MMES7-032	1.52	5.33	0.08	0.02	0.12	0.024	0.47	16.9	18.1	0.57	375	0.73	0.03	1.52	15
SSES1-001	1.85	5.41	0.14	0.05	0.2	0.032	0.35	23.7	9	0.46	605	0.69	0.02	0.42	10.1
SSES1-002	1.84	5.89	0.13	0.02	0.24	0.03	0.32	21.4	12.3	0.57	503	0.65	0.03	0.63	11.7
SSES1-003	1.41	5.29	0.14	0.05	0.12	0.023	0.38	24.5	13	0.67	343	0.52	0.03	0.74	11.4
SSES1-004	1.61	5.36	0.13	0.06	0.14	0.029	0.38	19.3	14.3	0.64	454	0.85	0.02	0.9	12.3
SSES1-005	1.8	6.18	0.15	0.01	0.23	0.033	0.43	21.8	15.9	0.7	502	0.79	0.02	0.84	13.4
SSES1-006	1.77	5.42	0.16	0.01	0.24	0.027	0.45	17.9	19	0.56	534	0.84	0.03	1.11	13.6
SSES1-007	1.32	4.11	0.13	0.03	0.13	0.023	0.36	10.9	14	0.37	499	1.74	0.02	0.94	13.5
SSES1-008	1.11	3.14	0.12	0.07	0.11	0.022	0.3	8	10.2	0.3	277	1.28	0.02	0.61	13.7
SSES1-009	1.44	3.73	0.13	0.02	0.1	0.02	0.36	14.4	13.3	0.39	478	1.29	0.02	0.8	17
SSES1-010	1.05	3.44	0.11	0.04	0.08	0.018	0.32	10.1	12	0.35	276	0.58	0.02	0.76	12
SSES1-011	1.54	4.9	0.15	0.03	0.12	0.028	0.42	15.6	19	0.54	447	0.86	0.03	1.16	14.1
SSES1-012	1.74	5.26	0.17	0.05	0.19	0.03	0.41	15.8	19.9	0.49	532	1.27	0.03	1.2	14.8
SSES1-013	1.71	5.37	0.08	0.1	0.17	0.037	0.38	20.5	17.8	0.49	509	1.18	0.03	1.23	17.3
SSES1-014A	1.23	3.39	0.07	0.03	0.27	0.024	0.21	17.5	10.3	0.21	346	1.15	0.02	0.76	13.4
SSES1-014B	1.26	4.25	0.08	0.09	0.19	0.024	0.24	25	13.5	0.24	328	0.94	0.01	0.62	16.8
SSES1-015	1.28	3.76	0.07	0.03	0.29	0.023	0.25	17.2	13.1	0.24	400	0.75	0.02	0.9	11.9
SSES1-016	1.11	3.31	0.05	0.04	0.25	0.018	0.2	16.1	11.1	0.2	382	0.9	0.02	0.82	12.1
SSES1-017	1.53	4.71	0.07	0.03	0.32	0.026	0.34	19.4	15.9	0.33	537	0.93	0.02	1.14	15
SSES1-018	1.69	5.77	0.1	0.02	0.21	0.03	0.43	21.4	19.6	0.55	458	0.85	0.02	1.21	17.5
SSES1-019	1.77	5.72	0.11	0.03	0.29	0.031	0.47	20	21.9	0.61	505	0.92	0.03	1.07	17.5
SSES1-020	1.76	5.85	0.1	0.04	0.17	0.028	0.49	18.7	22.4	0.66	445	0.84	0.03	1.5	18.3
SSES1-021	1.88	6.12	0.11	0.02	0.34	0.034	0.49	19.7	23.6	0.64	522	0.86	0.03	1.18	17.1
SSES1-022	1.95	6.16	0.1	0.02	0.34	0.029	0.51	19.8	24.2	0.68	548	0.84	0.03	1.16	17.3
SSES2-001	1.52	5.58	0.06	0.05	0.14	0.032	0.28	23.7	9.3	0.57	432	0.74	0.02	0.6	10.2
SSES2-002	1.79	5.91	0.07	0.04	0.27	0.034	0.33	23.1	13.2	0.54	505	0.74	0.02	0.7	13.2

Sample_ID	Fe_%	Ga_ppm	Ge_ppm	Hg_ppm	Hf_ppm	In_ppm	K_%	La_ppm	Li_ppm	Mg_%	Mn_ppm	Mo_ppm	Na_%	Nb_ppm	Ni_ppm
SSES2-003	1.77	5.91	0.07	0.06	0.23	0.033	0.41	21.9	15.2	0.57	494	0.77	0.02	1.06	13.1
SSES2-004	1.75	5.98	0.07	0.02	0.22	0.03	0.43	23.7	14.9	0.57	500	0.75	0.02	0.9	14.3
SSES2-005	1.87	5.6	0.07	0.03	0.24	0.032	0.43	23.4	15.3	0.47	595	0.93	0.03	1.19	15.7
SSES2-006	1.67	5.02	0.08	0.03	0.2	0.029	0.43	15.9	17.9	0.55	497	1.06	0.03	1.45	14.6
SSES2-007	1.39	4.67	0.09	0.07	0.12	0.023	0.37	12.5	15.8	0.38	445	1.21	0.02	1.27	17.9
SSES2-008	1.2	4.02	0.06	0.05	0.12	0.023	0.41	10.3	14.9	0.41	406	1.09	0.03	1.15	12.7
SSES2-009	0.77	2.18	0.05	0.02	0.08	0.018	0.23	6.6	7.3	0.23	238	0.78	0.02	0.66	9.1
SSES2-010	1.45	4.7	0.09	0.03	0.11	0.022	0.41	13.9	18.4	0.53	401	0.85	0.03	1.2	14.6
SSES2-011	1.48	4.99	0.09	0.03	0.12	0.028	0.39	13.6	18.5	0.47	433	0.93	0.03	1.29	16.4
SSES2-012	1.49	4.97	0.09	0.02	0.12	0.026	0.42	16.5	17.7	0.5	386	0.68	0.03	1.39	14.4
SSES2-013	1.51	4.93	0.07	0.03	0.11	0.026	0.42	17.1	19.2	0.54	444	0.9	0.03	1.36	14.3
SSES2-014A	1.71	5.71	0.1	0.05	0.26	0.03	0.45	20.8	20.5	0.53	567	1.27	0.03	1.54	17.4
SSES2-014B	1.68	5.19	0.08	0.08	0.14	0.033	0.38	20	18.2	0.45	588	1.47	0.03	1.42	19.9
SSES2-015	1.18	3.8	0.09	0.05	0.16	0.022	0.28	22.3	12.1	0.24	435	1.31	0.01	0.95	18.2
SSES2-016	1.22	3.63	0.05	0.03	0.23	0.019	0.26	16.3	12.8	0.25	429	0.82	0.01	0.67	13.1
SSES2-017	1.39	4.24	0.06	0.03	0.25	0.021	0.31	17.1	14.1	0.31	411	0.91	0.02	1.02	14.7
SSES2-018	1.53	4.92	0.09	0.02	0.19	0.024	0.35	18.9	16.7	0.37	456	0.93	0.02	1.1	18.2
SSES2-019	1.63	5.28	0.09	0.04	0.16	0.028	0.45	16.4	20.6	0.63	436	0.8	0.03	1.47	15.7
SSES2-020	1.75	5.44	0.09	0.02	0.25	0.027	0.43	19.1	21.1	0.6	519	0.9	0.03	1.09	17.1
SSES2-021	1.76	5.61	0.1	0.03	0.27	0.029	0.46	20	21.6	0.59	489	0.94	0.03	1.61	17.2
SSES2-022	1.79	6.02	0.11	0.03	0.23	0.035	0.48	18.7	23.8	0.66	463	0.87	0.03	1.52	17.7

Sample_ID	P_ppm	Pb_ppm	Rb_ppm	Re_ppm	S_%	Sb_ppm	Sc_ppm	Se_ppm	Sn_ppm	Sr_ppm	Ta_ppm	Te_ppm	Th_ppm	Ti_%	Tl_ppm
CSES4-001	690	13.35	21.9	-.001	0.03	6.9	2.2	0.6	0.7	88.9	-0.01	0.05	1.6	0.03	0.58
CSES4-002	690	14.2	24.9	.001	0.03	2.24	3.8	1.1	0.8	42.5	-0.01	0.01	3.9	0.027	0.78
CSES4-003	670	13.3	28.8	.001	0.03	1.685	3.1	1.3	0.9	39.3	-0.01	-0.01	2.5	0.04	0.72
CSES4-004	540	10.45	31.7	-.001	0.04	1.47	2.7	0.7	0.7	59.8	-0.01	0.02	2	0.053	0.71
CSES4-005	410	12.6	30.3	-.001	0.03	1.175	3.3	0.9	0.8	30.5	-0.01	0.01	3.8	0.049	0.52
CSES4-006	300	12.6	31.2	-.001	0.02	1.005	3.9	1.1	0.9	28.3	-0.01	-0.01	4.6	0.058	0.58
CSES4-007	500	9.26	27.2	-.001	0.04	0.808	2.3	1	0.7	73.5	-0.01	-0.01	1.4	0.044	0.42
CSES4-008	320	13.7	33.2	-.001	0.02	0.946	3.9	0.6	0.9	32.7	-0.01	-0.01	4.7	0.059	0.56
CSES4-009	400	5.66	14.8	-.001	0.04	1.135	1.3	1	0.4	98.6	-0.01	-0.01	0.6	0.019	0.59
CSES4-010	430	9.62	23.2	-.001	0.03	1.555	2.3	0.7	0.6	65.9	-0.01	-0.01	2	0.038	0.73
CSES4-011A	400	9.41	19.3	-.001	0.03	2.67	2.1	1.3	0.5	48.7	-0.01	-0.01	1.3	0.024	0.71
CSES4-011B	690	11.6	25.5	-.001	0.04	2	2.5	1	0.8	74.2	-0.01	0.01	1.8	0.032	1.09
CSES4-012	560	16.3	38.4	-.001	0.02	1.69	4.3	1.1	1	37	-0.01	-0.01	5.3	0.07	0.84
CSES4-013	610	12.05	32.6	-.001	0.04	1.245	3.1	0.7	0.9	60.8	-0.01	-0.01	2.1	0.052	0.65
CSES6-001	960	10.3	23.2	-.001	0.04	4.78	2.3	0.8	0.7	50.1	-0.01	0.03	1.2	0.032	1.22
CSES6-002	700	11.45	29.2	-.001	0.02	1.75	3.2	1.1	0.8	36.5	-0.01	0.02	2.6	0.053	0.75
CSES6-003	810	11.45	28.4	-.001	0.03	1.325	3	1.3	0.8	64.6	-0.01	0.01	2.5	0.051	0.9
CSES6-004	640	12.2	31.6	-.001	0.03	1.12	3.2	1.1	0.9	52.9	-0.01	0.02	2.7	0.066	0.48
CSES6-005	710	11.1	33.9	-.001	0.03	1.055	3.1	1	0.9	82.1	-0.01	0.02	2.3	0.066	0.51
CSES6-006	640	9.51	25.6	-.001	0.04	0.947	2.4	0.7	0.8	135	-0.01	0.01	2	0.054	0.6
CSES6-007	730	10.15	29.8	-.001	0.04	1.885	2.7	1.4	0.8	104	-0.01	0.03	1.5	0.051	0.78
CSES6-008	630	10.9	31.5	-.001	0.04	1.18	3.4	0.7	0.9	94	-0.01	0.02	2.6	0.061	0.8
CSES6-009	610	12.6	30.2	-.001	0.04	1.415	3.2	0.8	0.9	39.4	-0.01	0.04	2.5	0.055	1.26
CSES6-010	450	12.95	31.6	-.001	0.01	0.889	3.6	0.6	0.9	27	-0.01	0.02	4.2	0.057	0.67
CSES6-011	540	11.15	29.5	-.001	0.02	0.703	2.8	1.1	0.7	35	-0.01	0.02	2.1	0.054	0.45
CSES6-012	550	9.85	24.5	-.001	0.02	0.866	2.1	0.4	0.7	46.3	-0.01	-0.01	1.3	0.04	0.53
CSES6-013	550	10.35	26.3	-.001	0.03	0.94	2.4	0.9	0.8	53.5	-0.01	0.05	1.5	0.044	0.6
CSES6-014A	520	10.65	21.6	-.001	0.02	0.889	2.2	0.8	0.7	42.3	-0.01	0.03	1.8	0.04	0.47

Sample_ID	P_ppm	Pb_ppm	Rb_ppm	Re_ppm	S_%	Sb_ppm	Sc_ppm	Se_ppm	Sn_ppm	Sr_ppm	Ta_ppm	Te_ppm	Th_ppm	Ti_%	Tl_ppm
CSES6-014B	370	11.55	28.6	-.001	0.01	0.845	3.2	1	0.8	33.3	-0.01	0.01	3.1	0.054	0.48
CSES6-015	580	8.93	22.6	-.001	0.03	0.976	2.1	0.8	0.7	68.9	-0.01	0.03	1.2	0.037	0.38
CSES6-016	620	8.49	20.8	-.001	0.04	1.03	1.7	0.5	0.7	73.6	-0.01	0.01	1	0.033	0.42
CSES6-017	620	7.6	17.4	.001	0.04	0.958	1.4	0.6	0.6	94.6	-0.01	0.01	0.9	0.031	0.36
CSES6-018	600	10.5	24.5	-.001	0.03	1.185	2.1	1.2	0.8	76.2	-0.01	0.03	1.3	0.043	0.61
CSES6-019	520	8.13	20.7	-.001	0.03	0.925	1.7	0.7	0.6	102	-0.01	0.02	1	0.03	0.41
CSES6-020	600	7.66	19.1	-.001	0.03	1.445	1.5	-0.1	0.6	98	-0.01	0.02	0.9	0.03	0.42
CSES6-021	530	11.15	27.4	.001	0.02	1.61	2.3	1.2	0.7	75.2	-0.01	0.04	1.6	0.044	0.9
CSES6-022	570	10.4	27.5	-.001	0.02	1.395	2.5	0.9	0.8	78.8	-0.01	0.03	1.7	0.047	0.54
CSES6-023	580	9.95	25.9	-.001	0.03	1.735	2.5	0.8	0.8	108.5	-0.01	0.01	1.7	0.044	0.45
CSES6-024	610	10.85	28.8	-.001	0.03	1.255	2.6	0.9	0.9	96.9	-0.01	0.02	2.1	0.049	0.42
CSES6-025	780	14	38.6	.001	0.02	1.345	3.5	1.2	1	65	-0.01	0.02	3	0.065	0.48
CSES6-026	570	10.8	26.6	-.001	0.02	1.105	2.5	0.7	0.7	42.4	-0.01	-0.01	2.2	0.047	0.43
CSES6-027	590	10.5	26.2	-.001	0.02	1.14	2.5	0.8	0.8	52.2	-0.01	0.03	1.9	0.045	0.45
CSES6-028	560	11	27	-.001	0.02	1.285	2.9	0.7	0.7	39.1	-0.01	0.01	3.2	0.047	0.45
CSES8-001	720	14.7	32.4	.001	0.02	1.665	3.7	1.2	0.9	46.4	-0.01	0.05	3.5	0.049	0.31
CSES8-002	560	14.35	33.9	-.001	0.01	1.49	4	0.4	0.9	26.6	-0.01	0.03	4.7	0.054	0.34
CSES8-003	450	16.35	37.7	-.001	0.01	1.65	4	1.2	0.9	29.2	-0.01	0.05	6.5	0.065	0.35
CSES8-004	760	16.65	36.5	-.001	0.02	3.08	5.2	1.5	1	33.3	-0.01	0.03	4.5	0.049	0.53
CSES8-005	980	14.1	18.6	-.001	0.02	2.22	2.5	1	0.6	29	-0.01	0.02	2.2	0.032	0.31
CSES8-006	850	11.05	29.4	-.001	0.02	1.535	3.3	1.4	0.8	49.5	-0.01	0.03	2.4	0.047	0.61
CSES8-007	900	9.12	20.1	-.001	0.03	1.65	1.8	1.4	0.6	78.7	-0.01	0.03	1	0.032	0.84
CSES8-008	650	9.23	24.4	-.001	0.02	5.07	2.5	1.8	0.7	64.3	-0.01	0.03	1.5	0.037	1.46
CSES8-009	660	7.35	12.7	-.001	0.03	8.04	1.4	0.8	0.4	81.2	-0.01	0.05	0.7	0.017	1
CSES8-010	680	14.15	35.8	-.001	0.03	1.78	3.9	1.1	1	61.5	-0.01	0.04	3.1	0.055	1.18
CSES8-011	510	14.65	33.6	-.001	0.01	1.335	4	1.3	0.9	24.6	-0.01	0.03	4.2	0.043	0.53
CSES8-012	360	12.25	27.8	-.001	0.01	1.23	3.3	0.7	0.8	26.7	-0.01	0.02	3.7	0.044	0.45
CSES8-013	530	13.3	35.3	-.001	0.02	1.115	3.8	0.7	0.9	32.3	-0.01	0.04	3.4	0.06	0.56

Sample_ID	P_ppm	Pb_ppm	Rb_ppm	Re_ppm	S_%	Sb_ppm	Sc_ppm	Se_ppm	Sn_ppm	Sr_ppm	Ta_ppm	Te_ppm	Th_ppm	Ti_%	Tl_ppm
CSES8-014A	610	14.3	36.9	-.001	0.02	1.315	4.1	0.8	1	34	-0.01	0.03	4.2	0.067	0.53
CSES8-014B	500	13.8	34.8	-.001	0.02	0.983	3.8	1.2	1	34	-0.01	0.04	3.2	0.06	0.46
CSES8-015	670	11.65	34	-.001	0.02	1.485	3.2	0.9	0.9	56.3	-0.01	0.04	2.5	0.058	0.51
CSES8-016	340	12.6	31.7	-.001	0.01	1.42	3.7	0.8	0.9	30.4	-0.01	0.03	4.2	0.058	0.47
CSES8-017	550	10.85	30.2	-.001	0.02	1.4	2.8	1	0.8	49	-0.01	0.03	1.8	0.048	0.38
CSES8-018	530	11.15	29.5	-.001	0.02	1.905	3	0.7	0.8	46.3	-0.01	0.03	2.3	0.049	0.41
CSES8-019	500	13.4	35.1	-.001	0.01	1.43	3.8	0.8	1	38.9	-0.01	0.02	3.4	0.054	0.39
CSES8-020	650	11.6	30	.001	0.03	1.245	2.6	1	0.9	45.9	-0.01	0.05	1.6	0.048	0.33
CSES8-021	590	8.82	21.9	-.001	0.03	1.14	1.9	0.7	0.7	74.4	-0.01	0.03	1	0.033	0.27
CSES8-022	620	13	33.1	-.001	0.02	0.892	3.6	0.6	0.9	36.5	-0.01	0.03	3.3	0.055	0.34
CSES8-023	440	12.15	25.6	-.001	0.02	0.753	3.2	0.9	0.8	34.4	-0.01	0.03	3.2	0.04	0.5
CSES8-024	480	9.31	20.9	-.001	0.02	1.2	1.9	0.8	0.6	50.6	-0.01	0.03	1.2	0.027	0.49
CSES8-025	500	9.84	23.6	-.001	0.02	1.025	2.2	0.7	0.6	54.3	-0.01	0.02	1.4	0.032	0.35
CSES8-026	500	8.38	21.7	-.001	0.02	0.936	1.9	0.8	0.6	76.9	-0.01	0.03	1.1	0.027	0.29
CSES8-027	410	6.07	9.6	-.001	0.03	0.664	1.2	0.3	0.3	101.5	-0.01	0.01	0.8	0.013	0.15
CSES8-028	660	11.65	24.4	-.001	0.04	1.175	2.3	0.5	0.8	58.5	-0.01	-0.01	1.2	0.035	0.33
CSES8-029	580	11.15	25.3	-.001	0.04	1.18	2.4	0.7	0.8	71.5	-0.01	-0.01	1.4	0.039	0.3
CSES8-030	560	9.23	20.1	-.001	0.03	2.77	1.7	1.1	0.6	91.2	-0.01	0.01	1	0.033	0.63
CSES8-031	610	12.5	28.2	-.001	0.03	1.06	2.7	1	0.8	66.6	-0.01	0.03	2	0.052	0.41
CSES8-032	690	11.15	29.7	-.001	0.03	0.975	2.8	1.1	0.9	73.8	-0.01	0.03	1.8	0.054	0.38
MMES3-001	500	11	26.2	-.001	0.02	1.31	2.7	0.7	0.8	62.9	-0.01	0.02	2.6	0.043	0.36
MMES3-002	210	13.55	30.4	.001	0.01	2.73	4.2	0.8	0.9	23.7	-0.01	0.02	6.5	0.04	0.44
MMES3-003	960	13.3	32.4	.001	0.04	2.11	3.1	0.9	0.9	43.1	-0.01	0.01	1.8	0.044	0.8
MMES3-004	620	9.98	22.9	-.001	0.03	1.35	2.2	0.9	0.7	71.7	-0.01	0.03	1.8	0.04	0.62
MMES3-005	420	12.75	22.7	-.001	0.03	1.385	2.5	0.6	0.7	31.4	-0.01	-0.01	2.2	0.039	0.42
MMES3-006	530	11.7	28.6	.001	0.04	1.175	2.7	0.8	0.8	55.3	-0.01	0.01	2.2	0.047	0.44
MMES3-007	470	10.8	32	-.001	0.04	1.03	2.9	0.9	0.8	68.2	-0.01	0.01	2.2	0.053	0.44
MMES3-008	550	9.37	30	-.001	0.05	1.025	2.4	1	0.7	91.4	0.01	0.03	1.6	0.046	0.47

Sample_ID	P_ppm	Pb_ppm	Rb_ppm	Re_ppm	S_%	Sb_ppm	Sc_ppm	Se_ppm	Sn_ppm	Sr_ppm	Ta_ppm	Te_ppm	Th_ppm	Ti_%	Tl_ppm
MMES3-009	390	7.08	17	-.001	0.05	1.55	1.4	1	0.5	70.8	-0.01	0.02	0.9	0.023	0.92
MMES3-010	460	7.43	17.3	.001	0.04	1.4	1.4	1	0.5	107	-0.01	0.01	0.9	0.026	0.61
MMES3-011	530	9.54	18.1	.001	0.04	4.88	1.8	1.2	0.6	72.5	-0.01	0.01	1.2	0.018	2.05
MMES3-012A	520	15.45	32.3	-.001	0.03	1.9	3.8	1.1	0.9	36.9	-0.01	0.05	3.6	0.049	0.89
MMES3-012B	570	10.3	26.7	-.001	0.03	1.525	2.8	1.1	0.7	61.4	-0.01	0.02	2.1	0.041	0.92
MMES3-013	680	8.06	20.4	.001	0.04	1.445	1.9	0.7	0.6	77.2	-0.01	0.04	1.1	0.031	0.56
MMES3-014	530	12.8	23.1	-.001	0.03	2.02	2.7	0.7	0.8	41.6	-0.01	0.02	2.2	0.031	0.61
MMES3-015	320	13.9	28.4	.001	0.02	1.41	3.5	0.9	0.8	29	-0.01	0.02	4.5	0.044	0.56
MMES3-016	330	13.85	29.2	-.001	0.02	1.275	4	1.2	0.9	24.1	-0.01	0.02	5.1	0.041	0.55
MMES3-017	580	11.2	23.9	.001	0.02	2.27	2.5	1.2	0.8	62.6	-0.01	0.04	1.9	0.038	0.49
MMES3-018	620	9.76	23.2	-.001	0.03	2.84	2.4	0.4	0.7	92	-0.01	-0.01	1.5	0.034	0.56
MMES3-019	720	11.3	30.4	.001	0.03	2.45	3.3	0.8	0.9	67.4	-0.01	0.03	2.2	0.046	0.55
MMES3-020	430	10.3	18.3	-.001	0.03	2.88	2.3	0.7	0.6	41.5	-0.01	0.01	1.9	0.028	0.75
MMES3-021	420	10.25	20	.001	0.03	2.01	2.7	1	0.7	49.4	-0.01	0.05	2.1	0.037	0.6
MMES3-022	460	13	30.2	.001	0.02	1.695	3.7	1	0.9	36.1	-0.01	0.05	4.1	0.05	0.55
MMES3-023	510	12.05	27.4	-.001	0.02	2.07	3	0.9	0.8	50	-0.01	0.01	2.6	0.042	0.57
MMES4-014	600	9.03	20.8	.001	0.04	1.14	1.8	1.1	0.6	135	-0.01	0.01	1	0.031	0.55
MMES4-015	420	9.82	23.2	-.001	0.03	1.095	2.5	1.1	0.7	48	-0.01	0.02	1.8	0.033	0.47
MMES4-016	350	11.45	24	.001	0.02	1.79	3	0.8	0.7	29	-0.01	0.01	2.9	0.033	0.67
MMES4-017	460	13.25	28.7	-.001	0.01	2.57	3.8	0.8	0.8	26.8	-0.01	0.03	5.4	0.041	0.67
MMES4-018	400	13.55	29.4	-.001	0.01	4.04	4.2	1	1	33.3	-0.01	0.03	5.3	0.05	0.55
MMES4-019	530	12.8	26.7	.001	0.03	2.33	3	1.3	0.8	57.8	-0.01	0.05	2.5	0.045	0.51
MMES4-020	420	11.85	27.4	.001	0.03	3.87	3.3	0.8	0.8	52.3	-0.01	0.02	2.7	0.046	0.57
MMES4-021	510	9.65	23.3	.001	0.03	2.45	2.6	0.6	0.7	72.6	-0.01	0.03	1.7	0.043	0.65
MMES4-022	440	13.4	36.7	-.001	0.02	1.62	4.2	0.8	1	43.4	-0.01	0.03	4.8	0.058	0.5
MMES4-023	590	12.65	30.5	.001	0.02	1.47	3.4	0.9	0.8	33.1	-0.01	0.01	3.7	0.052	0.48
MMES5-001	440	13.8	30.3	.001	0.02	2.2	3.9	1.1	0.9	34	-0.01	0.01	4.6	0.05	0.65
MMES5-002	740	11.3	29	-.001	0.03	2.91	3.1	1.1	0.8	47.3	-0.01	0.03	2.2	0.045	0.93

Sample_ID	P_ppm	Pb_ppm	Rb_ppm	Re_ppm	S_%	Sb_ppm	Sc_ppm	Se_ppm	Sn_ppm	Sr_ppm	Ta_ppm	Te_ppm	Th_ppm	Ti_%	Tl_ppm
MMES5-003	980	14.7	19	-.001	0.03	2.23	2.6	1.3	0.6	31.1	-0.01	0.02	2.3	0.026	0.4
MMES5-004	600	10.95	38	-.001	0.03	0.956	2.9	0.7	0.8	46.9	-0.01	0.04	2.1	0.06	0.39
MMES5-005	690	11.95	36.7	-.001	0.04	1.205	3.3	0.9	0.9	78.7	-0.01	0.03	2.6	0.061	0.48
MMES5-006	320	11.6	37.4	-.001	0.02	1.14	3.9	0.6	0.8	37.2	-0.01	0.01	4.1	0.066	0.43
MMES5-007	360	12.45	39.1	-.001	0.02	0.903	4.1	0.6	0.9	42.4	-0.01	0.02	4.2	0.067	0.44
MMES5-008A	540	8.6	17.7	.001	0.04	1.08	1.6	0.5	0.6	86.2	-0.01	0.03	1	0.03	0.76
MMES5-008B	530	12.9	30.6	-.001	0.04	1.32	3.4	0.7	0.8	42.4	-0.01	0.03	3.2	0.053	0.8
MMES5-009	610	13	37.1	-.001	0.04	1.335	3.6	1.1	0.9	56.3	-0.01	0.03	2.7	0.059	1.11
MMES5-010	270	12.8	24.6	-.001	0.02	1.15	3.2	0.6	0.7	20.3	-0.01	0.01	3.5	0.037	0.93
MMES5-011	360	13.7	31.2	.001	0.03	1.1	3.6	0.6	0.9	33.2	-0.01	0.02	3.9	0.046	0.95
MMES5-012	570	9.97	24	.001	0.04	0.924	2.3	0.6	0.7	54.1	-0.01	-0.01	1.5	0.041	0.67
MMES5-013	590	8.35	20.1	.001	0.04	0.907	1.7	0.8	0.6	77.9	-0.01	0.03	1	0.03	0.44
MMES5-014	550	7.92	18	-.001	0.04	1.145	1.5	0.7	0.7	53.9	-0.01	0.01	1	0.026	0.38
MMES5-015	550	9.24	21.8	.001	0.03	1.205	2.1	0.9	0.7	52.8	-0.01	0.01	1.4	0.033	0.42
MMES5-016	570	12.7	32.6	.001	0.04	1.08	3.2	0.7	0.9	54.5	-0.01	0.02	2.7	0.047	0.63
MMES5-017	630	8.79	23.4	.001	0.05	1.205	1.8	0.9	0.6	80.8	-0.01	-0.01	1	0.035	0.42
MMES5-018	550	11.05	29.7	.001	0.03	1.43	2.8	1.1	0.8	60.7	-0.01	0.02	1.8	0.044	0.53
MMES5-019	570	9.79	26.8	-.001	0.03	1.08	2.1	0.9	0.7	82.7	-0.01	0.01	1.5	0.039	0.4
MMES5-020	580	9.83	21	-.001	0.03	1.16	2	0.9	0.7	78.6	-0.01	0.01	1.5	0.033	0.39
MMES5-021	610	14.45	36	.001	0.03	2.36	3.4	1	0.9	56	-0.01	0.03	2.7	0.05	0.58
MMES5-022	650	12.2	32.7	-.001	0.04	2.31	2.7	0.6	0.9	65.8	-0.01	0.01	1.5	0.045	0.53
MMES5-023	700	9.43	23.1	-.001	0.04	1.745	1.8	1	0.7	86.7	-0.01	0.02	1	0.035	0.46
MMES5-024	620	11.55	32.6	.001	0.04	3.18	2.6	1.2	0.8	88.2	-0.01	0.01	1.4	0.042	0.64
MMES5-025	610	12.15	32.1	.001	0.03	2.46	3	1.4	0.8	81	-0.01	0.02	2.1	0.052	0.52
MMES5-026	630	11.3	31.6	-.001	0.05	2.99	2.6	1.2	0.8	81.7	-0.01	0.03	1.4	0.045	0.46
MMES5-027	620	10.45	27.6	-.001	0.06	3.19	2.3	1.2	0.8	92.7	-0.01	0.02	1.3	0.038	0.49
MMES5-028	530	13.35	32.7	-.001	0.02	2.03	3.7	1	0.9	49.1	-0.01	0.04	5.4	0.063	0.39
MMES7-001	560	13.9	38.3	-.001	0.02	2.08	4.2	1.4	0.9	26.4	-0.01	0.03	4.3	0.052	0.43

Sample_ID	P_ppm	Pb_ppm	Rb_ppm	Re_ppm	S_%	Sb_ppm	Sc_ppm	Se_ppm	Sn_ppm	Sr_ppm	Ta_ppm	Te_ppm	Th_ppm	Ti_%	Tl_ppm
MMES7-002	550	13.25	41.9	-.001	0.01	1.345	4	0.9	0.9	29	-0.01	-0.01	4.8	0.061	0.36
MMES7-003	570	14.95	38.3	-.001	0.02	2.51	4.4	1	1	29.4	-0.01	-0.01	4.6	0.065	0.38
MMES7-004	550	15.6	35.8	-.001	0.02	2.42	4.4	1.4	1	28.3	-0.01	0.01	4.5	0.053	1.01
MMES7-005	830	12.25	20.4	-.001	0.02	2.03	2.6	1.2	0.6	33.6	-0.01	-0.01	1.8	0.033	0.38
MMES7-006	840	11.75	32.7	-.001	0.03	3.92	3.3	2.4	0.8	47.4	-0.01	-0.01	2.4	0.049	1.01
MMES7-007	730	9.67	27.1	-.001	0.03	8.39	2.6	1.3	0.7	62.1	-0.01	0.07	1.5	0.04	1.73
MMES7-008	560	10.3	27.6	-.001	0.03	11.15	3.1	1.3	0.8	43.6	-0.01	0.01	1.9	0.037	2.02
MMES7-009	360	12.65	38	-.001	0.02	3.53	4.5	1.3	0.9	35.7	-0.01	-0.01	5.6	0.074	0.77
MMES7-010	520	10.65	30.1	-.001	0.03	2.4	3	1.4	0.8	55.4	-0.01	-0.01	1.9	0.051	1.08
MMES7-011	370	11.1	23.5	-.001	0.03	1.675	2.4	1	0.7	26.8	-0.01	-0.01	1.9	0.034	0.59
MMES7-012	650	11.7	31.1	-.001	0.03	3.42	2.9	0.7	0.8	38.4	-0.01	-0.01	1.8	0.045	1
MMES7-013	520	16	36.4	-.001	0.03	4.71	4.1	1.2	1	31.3	-0.01	0.01	3.5	0.061	1.19
MMES7-014	530	14.45	34.5	-.001	0.02	1.915	3.8	0.7	0.9	31.2	-0.01	-0.01	3.9	0.059	0.81
MMES7-015	410	12.8	34.8	.001	0.02	1.445	3.7	0.9	0.9	32.3	-0.01	-0.01	3.9	0.06	0.68
MMES7-016	550	12.1	29.2	-.001	0.03	1.625	3.1	0.9	0.8	34.6	-0.01	-0.01	2.5	0.046	0.76
MMES7-017	410	12.95	35.3	-.001	0.02	1.4	3.9	1.2	1	37.9	-0.01	-0.01	3.3	0.053	0.48
MMES7-018	330	13.8	35.2	-.001	0.01	1.205	4.3	1.1	0.9	29.1	-0.01	0.01	5.4	0.059	0.53
MMES7-019	430	13.8	36.3	-.001	0.02	1.265	4	1	0.9	29.1	-0.01	-0.01	4.7	0.056	0.46
MMES7-020	310	13.55	30.5	-.001	0.02	1.845	3.7	1	0.9	26.6	-0.01	0.04	4.8	0.045	0.54
MMES7-021	520	10.6	28.5	-.001	0.03	1.46	2.6	0.7	0.8	52.5	-0.01	0.05	1.7	0.041	0.37
MMES7-022	490	11	26.1	.001	0.03	1.115	2.6	0.9	0.8	42.7	-0.01	0.02	1.9	0.039	0.35
MMES7-023	620	10.95	29.9	-.001	0.03	1.025	2.8	0.9	0.9	55.5	-0.01	0.01	2.1	0.047	0.33
MMES7-024	470	11.85	26.9	.001	0.03	1.05	2.8	0.7	0.7	31.6	-0.01	0.02	2.5	0.042	0.45
MMES7-025	610	8.76	19	-.001	0.03	1.03	1.8	0.7	0.6	50.9	-0.01	0.02	1.3	0.019	0.33
MMES7-026	510	9.75	21.8	-.001	0.03	0.99	2.1	1.1	0.7	81.4	-0.01	0.02	1.4	0.03	0.35
MMES7-027	540	9.33	19.5	-.001	0.03	0.874	1.9	0.5	0.6	50.3	-0.01	0.01	1.3	0.022	0.33
MMES7-028	580	10.4	25.4	-.001	0.04	0.934	2.3	0.8	0.7	58.1	-0.01	0.02	1.3	0.032	0.36
MMES7-029	600	10.1	25.5	-.001	0.04	0.921	2.2	0.9	0.7	76.1	-0.01	0.02	1.3	0.035	0.34

Sample_ID	P_ppm	Pb_ppm	Rb_ppm	Re_ppm	S_%	Sb_ppm	Sc_ppm	Se_ppm	Sn_ppm	Sr_ppm	Ta_ppm	Te_ppm	Th_ppm	Ti_%	Tl_ppm
MMES7-030	540	9.05	24.6	.001	0.03	1.025	2.3	0.9	0.7	105	-0.01	0.02	1.5	0.038	0.29
MMES7-031	590	10.5	32	-.001	0.03	1.05	2.9	1	0.8	87.4	-0.01	0.03	1.8	0.049	0.29
MMES7-032	610	10.95	28.9	.001	0.04	0.976	2.6	0.8	0.8	64.8	-0.01	0.04	1.8	0.046	0.42
SSES1-001	480	21.7	20.2	.001	0.02	0.517	4.6	0.9	0.9	73.6	-0.01	0.01	8.1	0.014	0.29
SSES1-002	510	16.4	23.9	-.001	0.03	0.645	4.1	0.7	0.9	93.4	-0.01	0.03	6.5	0.02	0.28
SSES1-003	520	14.95	26	-.001	0.03	0.957	2.9	0.5	0.8	153.5	-0.01	-0.01	4.9	0.018	0.29
SSES1-004	830	14.1	22.8	.001	0.04	0.754	3.7	0.6	0.9	101.5	-0.01	-0.01	4.2	0.024	0.29
SSES1-005	650	16.55	29.6	-.001	0.02	0.825	4.3	0.7	0.9	45.4	-0.01	-0.01	6.7	0.033	0.35
SSES1-006	430	16	31.1	.001	0.02	1.49	4	1.1	0.9	43.1	-0.01	-0.01	5.4	0.049	0.41
SSES1-007	410	10.75	22.5	.001	0.02	4.07	3	0.6	0.7	30.7	-0.01	0.02	3.3	0.03	0.46
SSES1-008	740	12.3	16.1	-.001	0.04	2.58	1.7	0.5	0.6	54.6	-0.01	0.03	1.1	0.018	0.55
SSES1-009	670	11.2	20.5	-.001	0.03	1.81	2.4	1.3	0.6	28	-0.01	0.03	1.8	0.031	0.48
SSES1-010	500	8.34	18.8	-.001	0.03	1.15	1.8	0.6	0.6	47.6	-0.01	-0.01	1	0.022	0.36
SSES1-011	550	11.2	27.2	.001	0.04	1.435	3.1	0.8	0.8	54.1	-0.01	0.01	2.3	0.043	0.49
SSES1-012	470	16.4	30.5	.001	0.04	5.2	3.9	0.6	0.8	32.5	-0.01	0.03	4.2	0.045	0.64
SSES1-013	430	16.25	28.6	-.001	0.02	8.08	3.9	1.2	0.8	37.5	-0.01	0.04	4.6	0.046	0.92
SSES1-014A	200	15.65	19.1	-.001	0.01	4.45	2.8	0.7	0.6	29.7	-0.01	0.04	4.6	0.029	0.43
SSES1-014B	200	10.8	20.2	-.001	0.01	10.2	3.6	1.3	0.7	26	-0.01	0.05	3.9	0.019	0.55
SSES1-015	260	11.45	23.1	-.001	0.01	3.53	2.9	0.7	0.6	26.6	-0.01	0.03	4.9	0.041	0.39
SSES1-016	270	15.4	19.9	.001	0.01	4.45	2.6	1.2	0.7	30.6	-0.01	0.05	4.4	0.032	0.4
SSES1-017	320	17.2	28.4	-.001	0.01	3.25	3.5	0.8	0.8	30.5	-0.01	0.03	5.5	0.041	0.49
SSES1-018	630	14.65	31.6	.001	0.01	1.695	4	0.9	0.9	41.4	-0.01	0.05	5.2	0.051	0.38
SSES1-019	560	15.65	35.4	.001	0.01	1.405	4.2	0.9	0.9	47.4	-0.01	0.02	6.3	0.06	0.32
SSES1-020	570	14.45	34.4	-.001	0.02	1.445	4.1	0.7	0.9	57.5	-0.01	0.01	4.6	0.058	0.36
SSES1-021	440	16.35	37.1	.001	0.02	1.345	4.3	1	0.9	44.1	-0.01	0.02	6.1	0.067	0.32
SSES1-022	470	16.1	36	.001	0.02	1.39	4.5	0.8	0.9	46.8	-0.01	0.03	6.3	0.068	0.36
SSES2-001	740	15.65	20	.001	0.03	0.526	3.4	0.4	0.9	93.8	-0.01	0.02	4.9	0.012	0.21
SSES2-002	610	18.65	27	.001	0.02	0.788	4.3	0.7	1	52.3	-0.01	-0.01	7.3	0.026	0.27

Sample_ID	P_ppm	Pb_ppm	Rb_ppm	Re_ppm	S_%	Sb_ppm	Sc_ppm	Se_ppm	Sn_ppm	Sr_ppm	Ta_ppm	Te_ppm	Th_ppm	Ti_%	Tl_ppm
SSES2-003	580	21.1	27.8	.001	0.03	0.865	4.1	0.7	1	73.3	-0.01	0.01	6	0.03	0.27
SSES2-004	520	14.4	31.5	.001	0.02	0.922	4.1	1.3	0.9	58.8	-0.01	0.03	6	0.033	0.25
SSES2-005	560	17.2	29.8	-.001	0.03	1.44	4	0.6	0.9	43.1	-0.01	0.03	6.2	0.03	0.32
SSES2-006	490	12.8	28.3	-.001	0.03	2.35	3.6	0.8	0.7	38.7	-0.01	0.03	3.8	0.044	0.65
SSES2-007	500	13.35	26.1	.001	0.03	3.28	3.1	0.5	0.9	37.9	-0.01	0.03	2.5	0.036	0.45
SSES2-008	530	13	22.1	-.001	0.04	2.04	2.5	0.4	0.6	63.1	-0.01	0.03	1.9	0.033	0.31
SSES2-009	470	10.05	12.8	.001	0.02	1.865	1.7	0.3	0.4	28.2	-0.01	0.03	2	0.018	0.21
SSES2-010	590	10.35	27.2	-.001	0.03	1.19	2.9	0.3	0.7	63.4	-0.01	0.03	2.3	0.043	0.41
SSES2-011	520	12.7	27.6	-.001	0.04	1.315	3.2	0.9	0.8	51.7	-0.01	0.02	2.3	0.04	0.39
SSES2-012	370	11.6	28.6	-.001	0.03	1.31	3.2	0.7	0.7	47.8	-0.01	-0.01	2.8	0.046	0.5
SSES2-013	470	11.35	28.8	-.001	0.03	3.81	3.1	1.3	0.7	57.8	-0.01	0.03	2.5	0.046	0.54
SSES2-014A	510	15.5	31.5	.001	0.02	6.73	4.1	1.1	0.9	38.2	-0.01	0.04	5.1	0.053	1
SSES2-014B	440	14.4	29.6	.001	0.02	8.16	3.6	1.2	0.8	39.1	-0.01	0.05	3.5	0.043	2.52
SSES2-015	280	12.4	20.9	-.001	0.01	12	3.2	1.1	0.6	25.3	-0.01	0.03	3.7	0.026	0.87
SSES2-016	220	10.75	19	-.001	-0.01	6.22	2.9	0.5	0.5	18.5	-0.01	0.02	4.3	0.03	0.57
SSES2-017	360	14.95	24.3	-.001	0.01	3.62	3.1	0.6	0.7	29.7	-0.01	0.03	4.9	0.036	0.48
SSES2-018	420	13.35	27.6	.001	0.01	4.31	3.6	0.6	0.8	42.1	-0.01	0.04	4.6	0.041	0.59
SSES2-019	680	17.75	30.2	.001	0.03	1.53	3.5	1.2	0.8	71.2	-0.01	0.04	4.1	0.056	0.35
SSES2-020	530	15.5	32.5	.001	0.02	1.29	4	1.1	0.8	49.4	-0.01	0.02	5.7	0.061	0.34
SSES2-021	360	14.15	32.7	-.001	0.02	1.39	4	1.1	0.9	70.3	-0.01	0.03	5	0.061	0.33
SSES2-022	610	17.25	35.4	-.001	0.02	1.455	4.1	1.2	0.9	54.9	-0.01	0.03	5.2	0.063	0.35

Sample_ID	U_ppm	V_ppm	W_ppm	Y_ppm	Zn_ppm	Zr_ppm
CSES4-001	0.88	21	0.85	10.6	77.5	3.7
CSES4-002	0.63	24	0.49	14.2	73.4	5.7
CSES4-003	0.63	25	0.53	15.1	79.8	4.4
CSES4-004	0.59	24	0.56	13	68.9	4.4
CSES4-005	0.66	25	0.62	13.2	66.7	6
CSES4-006	0.59	30	0.46	15.2	73.8	8.5
CSES4-007	0.62	23	0.45	11	58.8	4.2
CSES4-008	0.64	29	0.46	13.4	79.3	9.4
CSES4-009	0.74	15	0.5	7.82	38.4	2.2
CSES4-010	0.73	22	0.59	9.1	56	2.9
CSES4-011A	0.62	19	0.65	8.99	63.1	2.7
CSES4-011B	1	29	0.72	11.4	102.5	3
CSES4-012	0.75	34	0.47	17.3	100.5	9.9
CSES4-013	0.72	27	0.44	13.2	73.1	5.3
CSES6-001	0.88	27	0.96	12.5	90.1	4.2
CSES6-002	0.61	28	0.56	14.3	84	5
CSES6-003	0.91	29	0.58	11.8	95.6	3.7
CSES6-004	0.72	31	0.49	14	90.8	5.1
CSES6-005	0.78	32	0.61	13.6	90.5	4.4
CSES6-006	0.89	29	0.71	10.9	68.1	3.3
CSES6-007	0.75	27	0.81	11.8	73.8	4.5
CSES6-008	0.81	32	0.63	12	74.8	4.2
CSES6-009	0.65	30	0.75	11.8	71.3	4.8
CSES6-010	0.57	27	0.55	13.5	78.6	8.8
CSES6-011	0.55	26	0.52	12.4	70.7	3.6
CSES6-012	0.57	22	0.56	10.5	60	3.5
CSES6-013	0.6	25	0.52	11.8	63.5	3.5
CSES6-014A	0.66	23	0.47	11.2	61	3.7

Sample_ID	U_ppm	V_ppm	W_ppm	Y_ppm	Zn_ppm	Zr_ppm
CSES6-014B	0.58	26	0.45	14.3	68.8	4.9
CSES6-015	0.75	24	0.57	10.3	52.9	3.6
CSES6-016	0.63	21	0.57	8.82	51.8	3.1
CSES6-017	0.68	19	0.65	8.62	45.1	3.3
CSES6-018	0.82	24	0.51	10.4	61.5	5
CSES6-019	0.6	20	0.58	9.94	53.3	2.5
CSES6-020	0.64	20	0.53	8.47	46.7	3.5
CSES6-021	0.57	26	0.52	11	65.8	3.9
CSES6-022	0.6	26	0.48	11.4	67.2	3.7
CSES6-023	0.62	27	0.58	12	63	3.6
CSES6-024	0.69	28	0.57	11.7	67.6	3.5
CSES6-025	0.7	32	0.45	15.7	83.4	4.8
CSES6-026	0.57	25	0.56	12.2	67.3	4.2
CSES6-027	0.55	25	0.47	12.2	64	4.1
CSES6-028	0.52	25	0.54	11.6	71	5.2
CSES8-001	0.59	29	0.67	14.6	85.3	4.5
CSES8-002	0.67	31	0.63	16.1	83.3	7.3
CSES8-003	1.18	32	0.68	17.1	74.4	9.2
CSES8-004	1.19	31	0.9	22.9	104.5	6.8
CSES8-005	0.74	24	0.68	12.4	107	3
CSES8-006	0.79	29	0.51	13.1	96	3
CSES8-007	0.84	24	0.59	10.6	80.7	2
CSES8-008	0.84	25	0.56	11.6	88.8	3
CSES8-009	0.93	17	0.88	9.64	70.9	1.6
CSES8-010	0.97	30	0.64	12	100.5	4.5
CSES8-011	0.57	26	0.56	16.3	127.5	6.1
CSES8-012	0.48	23	0.61	13.4	72.5	5.8
CSES8-013	0.66	29	0.53	14.2	88.3	5.6

Sample_ID	U_ppm	V_ppm	W_ppm	Y_ppm	Zn_ppm	Zr_ppm
CSES8-014A	0.69	30	0.5	16.6	93.3	6.3
CSES8-014B	0.7	29	0.5	15.2	92.4	4.3
CSES8-015	0.65	29	0.54	13.9	76.4	4.2
CSES8-016	0.59	27	0.46	15.3	75.7	7.6
CSES8-017	0.6	25	0.52	12.9	67.4	4.5
CSES8-018	0.52	24	0.55	12.8	72.9	4.8
CSES8-019	0.6	28	0.5	15.9	76.6	5.5
CSES8-020	0.63	27	0.57	13.2	72.1	4.5
CSES8-021	0.5	19	0.6	8.66	51.2	3
CSES8-022	0.6	30	0.54	15.5	74	4.8
CSES8-023	0.49	25	0.55	12.6	67.9	5.6
CSES8-024	0.48	19	0.55	9.98	59.4	3.1
CSES8-025	0.58	21	0.53	9.68	66	3.3
CSES8-026	0.53	19	0.54	9.31	63.1	2.7
CSES8-027	0.46	12	0.44	7.18	30.4	2.7
CSES8-028	0.61	23	0.52	10.1	62.4	3.3
CSES8-029	0.62	23	0.47	10.4	58.4	3.9
CSES8-030	0.61	24	0.62	9.27	59.2	3.3
CSES8-031	0.57	26	0.45	10.1	70.8	4.1
CSES8-032	0.67	27	0.45	11.9	71.7	3.9
MMES3-001	0.59	25	0.55	12.3	55.7	4.7
MMES3-002	0.56	27	0.54	21.3	72.2	15.9
MMES3-003	0.66	27	0.6	14.8	98.7	3.8
MMES3-004	0.67	22	0.6	11.2	66.8	3
MMES3-005	0.64	23	0.64	11.6	63.3	4.2
MMES3-006	0.79	27	0.71	11.6	70.8	3.6
MMES3-007	0.73	27	0.55	13.6	62.6	3.7
MMES3-008	0.73	24	0.58	11.4	57.7	4.6

Sample_ID	U_ppm	V_ppm	W_ppm	Y_ppm	Zn_ppm	Zr_ppm
MMES3-009	0.66	16	0.62	8.6	42.6	2.6
MMES3-010	0.66	18	0.7	7.68	40.4	3.1
MMES3-011	0.83	22	1.09	8.55	60.1	3.5
MMES3-012A	0.66	28	0.63	13.8	81.8	6.5
MMES3-012B	0.71	24	0.63	12.9	60.8	5
MMES3-013	0.96	22	0.66	10.4	52.4	3.7
MMES3-014	0.51	24	0.61	12.8	62.4	4.2
MMES3-015	0.58	29	0.58	17.1	65.1	6.9
MMES3-016	0.57	27	0.57	17.8	66.1	9.4
MMES3-017	0.61	25	0.59	12.7	57	4.2
MMES3-018	0.72	26	0.62	9.8	56.4	3.7
MMES3-019	0.71	29	0.49	13.5	65.8	4.3
MMES3-020	0.47	27	0.62	14.1	47.3	4.7
MMES3-021	0.51	27	0.51	12.1	54.9	4.1
MMES3-022	0.56	30	0.52	17.4	63.7	7.5
MMES3-023	0.58	27	0.57	15.4	62.8	4.9
MMES4-014	0.6	20	0.63	11.7	49.1	3.7
MMES4-015	0.55	22	0.53	12.9	53.5	4.2
MMES4-016	0.5	25	0.59	15.2	53.7	5.3
MMES4-017	0.55	34	0.8	23.2	57.4	7.9
MMES4-018	0.58	31	0.62	19.5	68.2	10.2
MMES4-019	0.58	29	0.56	13.4	65.1	5
MMES4-020	0.6	32	0.54	14.9	63.4	5.1
MMES4-021	0.6	28	0.5	10.7	52.9	4.5
MMES4-022	0.6	29	0.51	14.8	64	10.1
MMES4-023	0.58	28	0.67	15.5	67.7	6.1
MMES5-001	0.68	27	0.48	13	88.2	7.7
MMES5-002	0.71	26	0.5	12.7	93.7	4.2

Sample_ID	U_ppm	V_ppm	W_ppm	Y_ppm	Zn_ppm	Zr_ppm
MMES5-003	0.68	22	0.62	13.7	105.5	3.9
MMES5-004	0.7	27	0.4	11.9	85.6	4.3
MMES5-005	0.85	31	0.54	13.1	82	4.1
MMES5-006	0.57	28	0.38	12	73.6	7.4
MMES5-007	0.63	28	0.37	13.2	75.7	8.3
MMES5-008A	0.7	20	0.69	8.02	45.9	2.9
MMES5-008B	0.66	28	0.62	10.7	76.5	5.4
MMES5-009	0.8	31	0.55	12.4	78.9	4.9
MMES5-010	0.56	24	0.6	12.8	66.8	5.6
MMES5-011	0.65	26	0.61	14	73.1	9.4
MMES5-012	0.64	23	0.54	10.1	59	4.6
MMES5-013	0.67	20	0.53	8.83	47	3.9
MMES5-014	0.75	20	0.55	8.38	46.4	3.4
MMES5-015	0.85	23	0.48	9.8	53	3.7
MMES5-016	0.81	27	0.48	12.5	76.2	4.5
MMES5-017	0.8	20	0.49	9.45	51.8	5
MMES5-018	0.89	26	0.44	12.8	74.6	4.1
MMES5-019	0.83	22	0.55	11.9	57.6	4.6
MMES5-020	0.8	21	0.52	11.5	59.5	4.3
MMES5-021	0.76	29	0.51	14	87.5	4.6
MMES5-022	0.7	28	0.56	12.3	75.9	3
MMES5-023	0.86	24	0.58	11	53.9	4
MMES5-024	0.77	30	0.57	13.7	66	4.1
MMES5-025	0.81	31	0.54	15.9	68.4	3.8
MMES5-026	0.8	29	0.55	13.8	65.7	3.5
MMES5-027	0.78	25	0.51	11.7	57.1	4.1
MMES5-028	0.6	28	0.45	14.3	72.5	10.7
MMES7-001	0.67	33	0.49	18.9	93.2	6.9

Sample_ID	U_ppm	V_ppm	W_ppm	Y_ppm	Zn_ppm	Zr_ppm
MMES7-002	1.05	32	0.53	17	85.8	8.1
MMES7-003	1.06	32	0.53	17.4	92.6	8.9
MMES7-004	1.09	32	0.61	22.3	100	8.2
MMES7-005	0.79	24	0.52	14.9	98.9	3.9
MMES7-006	0.84	31	0.49	14.9	122.5	3.7
MMES7-007	0.81	27	0.46	13	99.5	2.8
MMES7-008	0.9	26	0.44	13.6	94.8	3.3
MMES7-009	0.65	32	0.37	13.7	102	12
MMES7-010	0.69	28	0.49	12.6	87.8	4.1
MMES7-011	0.63	20	0.47	9.5	69.3	4
MMES7-012	0.66	27	0.6	14.3	90.2	3.8
MMES7-013	0.65	31	0.64	18.5	103	6.4
MMES7-014	0.68	29	0.49	17.6	87.8	7.8
MMES7-015	0.61	28	0.42	16.2	82.6	7.2
MMES7-016	0.56	25	0.45	15.2	85.5	5
MMES7-017	0.55	28	0.43	16.4	80.9	6.9
MMES7-018	0.59	31	0.37	20.6	80.1	10.1
MMES7-019	0.56	29	0.44	18.4	78.4	8
MMES7-020	0.59	26	0.5	16.8	72.6	9.4
MMES7-021	0.55	23	0.45	11.5	65.2	5.1
MMES7-022	0.54	24	0.41	11.2	67.4	4.6
MMES7-023	0.6	25	0.47	11.3	68.1	4.8
MMES7-024	0.53	24	0.41	12.4	73.9	4.4
MMES7-025	0.63	17	0.48	9.11	79.5	3.2
MMES7-026	0.54	22	0.53	9.66	78.8	3.2
MMES7-027	0.59	18	0.48	8.17	63.8	3.6
MMES7-028	0.57	21	0.49	8.88	68.5	3.1
MMES7-029	0.63	22	0.44	9.1	69.7	3

Sample_ID	U_ppm	V_ppm	W_ppm	Y_ppm	Zn_ppm	Zr_ppm
MMES7-030	0.6	22	0.44	9.46	57.9	3.9
MMES7-031	0.59	24	0.32	11.9	67.6	4.9
MMES7-032	0.61	23	0.37	11.4	67.9	4.3
SSES1-001	1.5	31	0.43	13.4	61.2	7.6
SSES1-002	1.16	25	0.33	12.8	58.5	8.4
SSES1-003	1.69	20	0.32	14.4	52.8	4.6
SSES1-004	1.04	24	0.38	12.8	64.5	5
SSES1-005	1	26	0.38	15.1	71.9	9.8
SSES1-006	0.6	25	0.46	12.9	73.5	10.9
SSES1-007	0.84	21	0.56	10.5	86.7	4.9
SSES1-008	1.09	19	0.81	7.82	76.8	3.8
SSES1-009	0.64	22	0.66	12.1	74.7	3.4
SSES1-010	0.6	18	0.61	8.61	53.4	2.8
SSES1-011	0.84	25	0.55	12.4	76.1	3.8
SSES1-012	0.73	29	0.6	13.1	88.8	7.4
SSES1-013	0.62	34	0.59	13.6	76.8	7.9
SSES1-014A	0.72	22	0.68	14	57.8	11
SSES1-014B	0.64	26	0.62	20.8	51.1	8
SSES1-015	0.65	23	0.62	11.4	48.9	12.2
SSES1-016	0.65	21	0.71	11.3	48.9	10.3
SSES1-017	0.6	25	0.66	13.1	60.5	13.2
SSES1-018	0.62	25	0.47	14.9	71.4	8.5
SSES1-019	0.69	27	0.42	14	77	12.7
SSES1-020	0.64	26	0.4	13.5	77.1	7.3
SSES1-021	0.62	29	0.41	14.2	82.1	14
SSES1-022	0.65	29	0.39	14.3	79	14.4
SSES2-001	1.6	23	0.31	13.3	57.7	4
SSES2-002	0.98	26	0.36	13.9	65.4	9.4

Sample_ID	U_ppm	V_ppm	W_ppm	Y_ppm	Zn_ppm	Zr_ppm
SSES2-003	1.02	24	0.33	13.2	64.9	8
SSES2-004	0.96	25	0.36	15.3	67.1	8.8
SSES2-005	0.85	26	0.5	14.7	70.6	9.3
SSES2-006	0.63	24	0.47	11.8	74.2	7.7
SSES2-007	0.94	22	0.56	10.3	94	4.3
SSES2-008	0.63	19	0.53	7.99	64.4	4.1
SSES2-009	0.53	12	0.47	6.09	46.4	3
SSES2-010	0.86	26	0.57	10.5	72.2	4.1
SSES2-011	0.94	27	0.6	11	78.2	4.3
SSES2-012	0.58	25	0.45	11.7	58.7	4.4
SSES2-013	0.6	27	0.55	11.5	67.3	4
SSES2-014A	0.65	31	0.71	14.7	79.3	10.2
SSES2-014B	0.67	33	0.84	14.5	81	5.7
SSES2-015	0.5	25	0.94	20.4	54.7	7.1
SSES2-016	0.56	22	0.66	13.3	48.9	9.8
SSES2-017	0.54	23	0.56	11.6	55	10.3
SSES2-018	0.65	25	0.65	13.6	62.5	7.9
SSES2-019	0.61	25	0.47	11.1	71.4	6.8
SSES2-020	0.61	27	0.44	13.2	74.6	11.6
SSES2-021	0.58	27	0.41	13.9	71.5	10.7
SSES2-022	0.66	27	0.42	13.3	77.4	9.2